

PETROPHYSICAL INTERPRETATION OF THE OXFORDIAN SMACKOVER
FORMATION GRAINSTONE UNIT IN LITTLE CEDAR CREEK FIELD,
CONECUH COUNTY, SOUTHWESTERN ALABAMA

A Thesis

by

LORA CHRISTINA BREEDEN

Submitted to the Office of Graduate Studies of
Texas A&M University
in partial fulfillment of the requirements for the degree of

MASTER OF SCIENCE

Chair of Committee,	Michael C. Pope
Co-Chair of Committee,	Ernest Mancini
Committee Member,	Walter B. Ayers
Head of Department,	John R. Giardino

August 2013

Major Subject: Geology

Copyright 2013 Lora Christina Breeden

ABSTRACT

A petrophysical study of the upper grainstone/packstone reservoir of the Oxfordian Smackover Formation in Little Cedar Creek Field was conducted, integrating core description, thin section analysis, log interpretation and cathodoluminescence to characterize controls on oil production in the upper reservoir. Little Cedar Creek Field produces approximately 2.4 million barrels (bbls) of oil annually and is currently in secondary recovery. By analyzing petrophysical characteristics such as porosity and pore type and correlating them to facies changes, better predictions can be made to optimize secondary recovery.

The diagenetic history of the ooid-peloid grainstone records six separate events. Early marine phreatic dogtooth sparry rim cement helped create the framework that allowed it to maintain a good portion of its depositional porosity as it underwent subsequent compaction, dissolution and cementation events. The most common porosity types are vuggy, oomoldic and intercrystalline.

The Smackover Formation ooid-peloid grainstone/packstone unit consists of multiple alternating ooid-peloid grainstone and peloid packstone/wackestone facies with varying porosity types. The most common types are oomoldic and vuggy with a range of preserved intergranular porosity. Porosity in the grainstone facies averages 17% and 5.6% in the packstone/wackestone facies. The number of facies changes within the upper reservoir does not play a significant role in controlling well production. Facies changes are too thin to be identifiable utilizing well logs alone, although neutron and density well

logs do trace a close relationship between log values and core plug analysis values of porosity. Core reports indicate that porosity and permeability correlate strongly with pore size and facies. Areas with thicker accumulations of grainstone facies have higher porosity and permeability values and have higher oil production. Isopach maps of the cumulative grainstone facies indicate thick build-ups parallel to strike for the formation, consistent with a shoal environment. The strongest predictor of well production is the cumulative thickness of grainstone facies within the grainstone/packstone unit of the Smackover Formation. The grainstone is thickest in the southwest part of the field and pinches out updip in the northwest. Secondary recovery gas injection would be most effective if applied in the southwestern portion of the field because it could effectively sweep the oil updip towards the stratigraphic trap.

DEDICATION

In memory of Dr. Wayne M. Ahr

ACKNOWLEDGEMENTS

First and foremost I would like acknowledge Dr. Wayne Ahr. Dr. Ahr has been the most inspiring man I have ever met. Not only an incredible academic professor and mentor, he imparted excitement into every aspect of life; be it carbonate porosity, or picking wild onions along the Llano River. Coming from the coast of California I had not spent much time with carbonates. Dr. Ahr assured me in one of his first emails before I arrived to Texas A&M, “Don’t worry about carbonates...I’ll be happy to introduce you to them. They’re a lot more fun than plain old sandstones!”. I know I am very lucky to have worked with him and am very grateful for the time I was able to have.

Of course many others have helped me along this journey, namely my advisor Dr. Michael Pope who graciously took on all of Dr. Ahr’s students and course load after he passed. I recognize the tremendous amount of time and effort it takes to absorb so many duties and I am grateful for the time he was able to spend mentoring me through this process. Also, Dr. Ayers, who was willing to be called into help at the last minute. He provided invaluable advice and support. Although he may not know it, his calm demeanor reassured me through some of the shaky patches the thesis saw. As well, I would like to thank Dr. Ernest Mancini who inspired the project in Little Cedar Creek Field and has been wealth of information as he has studied this field and area in depth. I also must mention Dean Lewis at the Alabama Oil and Gas Board; thankfully he is a patient man and allowed me to look at as many rock cores as I needed.

I am also fortunate to have many colleagues to confer with, however, two stand out. Firstly, John Hayes, my travel partner to and from Alabama. He put up with my antics for a week as we studied core at the core repository of the AOGB. I am thankful for his company and insight, not to mention, rocks are heavy, and John was always willing to lend a hand. Secondly, Sandra Tonietto; I often called on her expertise in petrography and although I bugged her with countless questions she always took the time to help.

In addition I would like to acknowledge Chevron and their fellowship that allowed me the time and resources to accomplish my graduate degree.

When things really got tough, I could always rely on my Mother, Father, Sister and close friend, Brandon. I am fortunate that my Mother and Father have both worked through their graduate degrees and could guide me along the way, knowing that if they survived I could too. On top of their support, I would never have been able to keep my head on straight without my sister Kristen and friend Brandon Kennedy. We science types can have a tendency to become deeply entrenched in our work and sometimes require outside sources of motivation to remain social and ultimately happy. They were persistent and remained by my side.

As in most difficult endeavors in life, we must call on the aid of others to support us through the process. Without the time and effort of those who helped, inspired, and mentored me along the way you would be in for quite a dull read ahead.

NOMENCLATURE

LCCF	Little Cedar Creek Field
NPHI	Neutron porosity log
DPHI	Density porosity log
bbls	Barrels of Oil
mcf	Thousand cubic feet

TABLE OF CONTENTS

	Page
ABSTRACT	ii
DEDICATION	iv
ACKNOWLEDGEMENTS	v
NOMENCLATURE	vii
TABLE OF CONTENTS	viii
LIST OF FIGURES	x
LIST OF TABLES	xvi
1. INTRODUCTION.....	1
1.1 Objective	2
2. GEOLOGICAL SETTING	6
2.1 Tectonics	6
2.2 Stratigraphy	7
3. METHODS.....	10
3.1 Petrography	12
3.1.1 Facies.....	13
3.1.1.1 Grain Size, Type, and Arrangement.....	13
3.1.1.2 Vertical and Lateral Variations	16
3.1.2 Porosity.....	20
3.1.2.1 Diagenesis and Paragenetic History	21
3.2 Core: Description and Plug Analysis	28
3.2.1 Facies.....	28
3.2.1.1 Vertical and Lateral Variation.....	28
3.2.2 Porosity.....	30
3.3 Log Analysis	37
3.3.1 Correlation Between Well Logs and Facies	37
3.3.2 Log Porosity Correlation to Core Reports and Thin Sections.....	38

4. DISCUSSION	45
4.1 Production	45
4.1.1 Correlation Between Oil Production and Facies Changes	48
4.1.2 Correlation Between Oil Production and Porosity Type.....	51
4.1.3 Correlation Between Oil Production and Grainstone Facies Thickness	55
4.1.4 Implications of Gas Injection for Oil Recovery	61
4.2 Modified Ahr Porosity Type	62
5. CONCLUSIONS.....	65
REFERENCES.....	67
APPENDIX A CORE DESCRIPTIONS	70
APPENDIX B POROSITY AND PERMEABILITY CROSSPLOTS	86

LIST OF FIGURES

	Page
Figure 1. Location of Little Cedar Creek Field (adapted from Geological Survey of Alabama Oil and Gas Board, 2012).....	3
Figure 2. Generalized stratigraphic column of Upper Triassic and Jurassic strata in Little Cedar Creek Field. The Smackover Formation is highlighted (adapted from Mancini et al., 2001; 2003).....	4
Figure 3. Structure map of the top of the Smackover Grainstone Unit measured from sea level.	5
Figure 4. Idealized stratigraphy of the seven units of the Smackover Formation in Little Cedar Creek Field, Conecuh County, Alabama. Scale at base of section is the Dunham Classification (1962) for carbonate rocks (M- mudstone, Cls- calcisiltstone, W- wackestone, P- packstone, Gs- grainstone, B- boundstone) and the Wentworth size classification for siliciclastics (Sh- shale, Si- siltstone, FS- fine sandstone, MS- medium sandstone, CS- coarse sandstone, Cong- conglomerate). This study focuses on the yellow highlighted oolitic grainstone/packstone unit (Modified from Mancini et al., 2008).....	9
Figure 5. Rock types in the Smackover Formation grainstone unit. The scale bar represents 1mm. Pink circles indicate ooids, green for grapestones, and white for peloids. (A) Peloid Grainstone from well 15496-B at 11,102.5 ft with moldic porosity (B) Peloid Packstone/Wackestone from well 15165 at 11,519.5 ft with primarily vuggy porosity (C) Ooid Grainstone from well 11963 at 11,866.8 ft with moldic porosity (D) Peloid Ooid Grainstone from well 15000 at 11,125.5 ft with very little vuggy porosity (E) Peloid Grapestone Grainstone from well 14,112 at 11272.6 ft with abundant vuggy porosity (F) Peloid Ooid Grapestone Grainstone from well 15263-B at 11,218.2 ft with both vuggy and moldic porosity. (See appendix for locations of thin sections on the core descriptions).....	14
Figure 6. Syntaxial overgrowth of crinoid grain in well 13472 at 11,508.5 ft. It was very rare to find grains that lacked rim cement. Scale bar represents 200 μ m (See appendix for location of thin section on the core descriptions).....	15

Figure 7. Cross-laminae in well 15000 at 11,125.5 ft in core and in thin section. Both scale bars represent 1 cm (See appendix for location of thin section on the core descriptions).....	15
Figure 8. Distribution of algal influence in upper grainstone reservoir of the Smackover Formation. Significant algal influence includes: thick mat-like microbial coating and binding of the grains, peloids and ooids, referred to as grapestones (Winland and Matthews, 1974), and wavy laminations potentially caused by microbial activity. Some algal influence includes fewer algal coatings and grapestones and minor influence includes the samples with very few grapestones or algal coatings. Large micritic masses occur in four cores.	18
Figure 9. Grapestones encompassing many grains in well 13510 at 11506.0 ft. Scale bar represents 1 mm. (See appendix for location of thin sections on the core descriptions).....	19
Figure 10. Photomicrographs of grainstone facies in the Smackover Formation grainstone unit in well 13472; scale bar represents 1 mm: (A) Top grainstone facies at 11,495.ft with mainly moldic porosity and few vugs (B) upper middle grainstone facies at 11,502.8 ft with mainly vuggy porosity (C) lower middle grainstone facies at 11,508.5 ft with mainly interparticle porosity (D) Base grainstone facies at 11,511.6 ft with small vuggy porosity and intergranular porosity (See appendix for location of thin sections on the core descriptions).....	20
Figure 11. Paragenetic Sequence: (A) dogtooth calcite cement in well 13510 at 11,506.0 ft depth (Plain light) (B) dissolution in well 14325 at 11,046.7 ft depth (plain light) (C) microsparry calcite cement in well 14112 at 11,272.6 ft depth (D) small dissolution event in well 14112 at 11,272.6 ft (30 sec) (E) blocky calcite formation in well 14325 at 11,043.8 ft depth (25 sec) crystal labeled "A" (F) gypsum formation in well 14325 at 11,043.8 ft depth (plain light) crystal labeled "B". (See appendix for location of thin sections on the core descriptions).....	25
Figure 12. Thin section photo of partially dissolved ooid grains leaving molds and internal concentric rings, Well 13510, 11,499.2 ft. Scale bar is 1 mm. (See appendix for location of thin sections on the core descriptions).	26
Figure 13. Thin layer of microsparry calcite (bright orange cathodoluminescence) lining pore space and along pore throats in Well 14325, 11,043.8 ft and 25 secs exposure. Scale bar is 500 μ m. (See appendix for location of thin sections on the core descriptions).	26

- Figure 14. Arrow indicates dissolution path through microsparry calcite Well 14325, 11,043.8 ft. There is no microsparry calcite growth into path which implies that this dissolution event occurred after microsparry calcite cementation. Scale bar is 200 μm . (See appendix for location of thin sections on the core descriptions).....27
- Figure 15. Cathodoluminescent image of blocky calcite crystal in pore space of Well 14646-B, 11,266.5 ft and 20 sec exposure showing at least two different stages of growth as indicated by two distinct zones. The scale bar is 500 μm . (See appendix for location of thin sections on the core descriptions).....27
- Figure 16. Isopach map of the upper grainstone/packstone unit of the Smackover Formation. The colored wheels indicate the number of grainstone facies in the grainstone/packstone unit in cores by the number of colors that appear in the wheels. There are one to five grainstone facies per well.33
- Figure 17. Porosity vs. permeability plot by facies from well 14646-B, illustrating that porosity and permeability are very closely related to facies. The grainstone facies consistently has higher permeability and porosity values whereas the wackestone facies has consistently low permeability and porosity values.34
- Figure 18. Porosity vs. permeability plot from various pore sizes within oomoldic porosity type reported from the core analysis reports. Although the main porosity type is oomoldic in each sample plotted, the size of the molds affects the porosity and permeability values. Larger pores correspond with higher permeability values. As pore size increases the clusters increase in size as a response to a larger range of porosities. It is likely possible that the small oomoldic and very small oomoldic porosities include primarily molds of peloids, however, the core analyses specifically reported oomoldic.35
- Figure 19. Visible porosity type superimposed on the Smackover Formation total grainstone unit isopach. Core reports did not include intergranular. Moldic porosity occurs at a unit thickness above 12 ft. While vuggy and intergranular pores are distributed throughout the field. The data control points represent wells for which there are total grainstone thickness values. ...36
- Figure 20. Logs from well 13510 with core description. Even with a reduced gamma ray scale of 40 to 100 GAPI there are no obvious deviations indicating a change associated with facies. The gamma ray log does not have the resolution to differentiate the rapid facies changes in the grainstone/packstone unit. The porosity logs generally record higher values in the grainstone facies. However, with small facies changes (such as the

top ooid grainstones in well 13510) even utilizing porosity logs as a facies indicator becomes inconsistent.	39
Figure 21. Well logs from 13472 with core description. Although the gamma ray shows more deflection than in well 13510, it does not correlate with the facies changes. The porosity logs do record higher values that initially correspond with upper grainstone facies. However, farther down section where the changes are more rapid, the log responses do not match the facies type.	40
Figure 22. Cross plot of neutron and density porosity log values in the grainstone/packstone unit of Well 11963. The two logs have similar values, varying only slightly. With the addition of a trend line it is apparent that there is a small tendency towards a higher DPHI. This is a common trend in all described wells. The higher DPHI is likely due to the influence of the less dense siliciclastic grains affecting the density readings on a limestone scale. Also, NPHI logs are more accurate at lower porosities, which would account for why the NPHI values are closer the DPHI values as porosity decreases.	41
Figure 23. Well 14155 logs with synthetic core porosity trace. The NPHI and DPHI follow core porosity with some variation. The logs commonly overestimate the porosity rather than underestimate porosity. This is likely due to the resolution rather than an effect of lithology.	42
Figure 24. Stratigraphic dip cross-section A-A' (location on Fig. 1) illustrating the difficulty of delineating facies with logs alone.	43
Figure 25. Stratigraphic strike cross-section B-B' (location on Fig. 1) illustrating not only the difficulty of using solely logs to interpret facies, but the number of facies changes throughout the field.	44
Figure 26. First three month cumulative oil production from selected wells. Production is extremely varied across the field. Production includes commingled wells.	46
Figure 27. First three month cumulative oil production from wells that only produce from the upper reservoir.	47
Figure 28. First three month cumulative oil production in wells with described facies changes that are reported to produce only from the upper reservoir. There is no clear trend between the number of facies changes and production values.	49
Figure 29. First three month cumulative oil production from wells that produce only from the upper grainstone/packstone reservoir superimposed on the	

cumulative grainstone facies isopach. Production increases to the southwest where the grainstone facies is thickest. Data control points are wells that have values from cumulative grainstone facies thickness.	50
Figure 30. First three month cumulative oil production values from wells that produce only from the upper grainstone/packstone reservoir. The shape of the production bubbles indicates the primary type of porosity. Porosity types from core reports were used in order to consistently define the perforate intervals. The data control points are wells that have values from cumulative grainstone facies thickness.	52
Figure 31. The porosity and permeability crossplot indicates similar ranges for both moldic and vuggy pores. Data points were taken from core analysis reports from a representative selection of wells in the grainstone/packstone unit. Trend lines indicate that moldic pore types are slightly more variable than vuggy pores.	53
Figure 32. The average porosity of the perforated interval ranges from 1.3% in well 15165 to 27.2 % in well 15000. The average porosity values do not indicate any trend in production.	54
Figure 33. There is a direct correlation between three year cumulative oil production and perforated grainstone facies thickness. Wells used to create this chart were described from this study with the addition of wells 13176 and 14358 from Ridgway (2010).	57
Figure 34. An even closer correlation is seen with the cumulative amount of grainstone facies and the production values from wells that produce from the upper reservoir. Wells used to create this chart were described from this study with the addition of wells 13176 and 14358 from Ridgway (2010).	58
Figure 35. Map of average grainstone unit permeability from core analysis. Areas of higher permeability are in areas of greater grainstone facies accumulation (Fig. 29).	59
Figure 36. Location of dry wells with respect to Little Cedar Creek Field. It is possible that the thick grainstone facies trend within the grainstone/packstone unit did not extend far past the last producing grainstone well (11963) due to the termination of the ooid shoals at the field boundary leading to the dry holes past the boundary.	60
Figure 37. The modified Ahr (2008) porosity classification simplifies porosity types into three main categories, depositional, diagenetic, and fracture. Rocks can further be classified by hybrid type depending on the degree of influence	

the end members have on the main porosity characteristics. All thin section samples from the upper grainstone reservoir are classified as hybrid 1-B.64

LIST OF TABLES

	Page
Table 1. Data utilized in study.	11
Table 2. Additional wells with core and log data utilized.....	12
Table 3. Summary of diagenetic events and relative timing.....	24
Table 4. Estimated porosity from thin sections and reported porosity from core analysis	32

1. INTRODUCTION

Little Cedar Creek Field (LCCF), in southwestern Alabama (Fig.1), was discovered in 1994 with the Hunt Oil Co. Cedar Creek Land and Timber Co. 30-1 #1 well; commercial production began in November 1994 (Geological Survey of Alabama Oil and Gas Board, 2009). While operating, this well produced from the upper oolitic grainstone/packstone reservoir of the Smackover Formation. Little Cedar Creek was a one well field until Midroc Operating Company took over in 2000; since then, more than 100 wells have been drilled by Midroc and other operators. On January 1, 2005, the western portion of Little Cedar Creek field was unitized, summing the production of all the wells in the nearly 6,000-acre area and distributing production based on a predetermined allocation to the multiple field operators. In 2006, Sklar Exploration Company LLC began drilling wells in LCCF. Today Midroc and Sklar are the main operators in this field. In 2007, Midroc began gas injection in two wells in the western, unitized portion of the field, within the upper grainstone reservoir (Geological Survey of Alabama Oil and Gas Board, 2009). A total of 15,675,944 Mcf of gas and 15,181,182 bbls of oil and condensate were recovered from the field as of February 2012.

The Jurassic Smackover Formation (Fig. 2) ranges from 58-117 ft (18-36 m) thick in LCCF (Mancini, 2008). There are two reservoirs separated by an impermeable layer of lime mudstone/peloidal wackestone. The lower reservoir is microbial boundstone that ranges from 0-36 ft (0-11 m) thick; the upper reservoir consists of oolitic grainstone ranging from 0-20 ft (0-6 m) thick (Mancini, 2008). Oil accumulated

in a stratigraphic trap (Fig. 3) of the Smackover Formation (Geological Survey of Alabama Oil and Gas Board, 2009). The seal of the lower microbially influenced reservoir is the overlying subtidal laminated peloidal mudstone/peloidal wackstone within the Smackover Formation (Mancini, 2006). The most likely seal for the upper grainstone reservoir is the argillaceous bed of the overlying Haynesville Formation. Although the base of the Haynesville Formation is the Buckner anhydrite, this unit is thin and discontinuous in the field area. Unlike production from other Smackover Formation fields, LCCF produces from rocks that are little dolomitized (Heydari and Baria, 2005). It is possible that oil was generated *in situ*, however, it is thought that the oil migrated from the type I kerogen of the Smackover Formation downdip, because of the thin reservoir beds and low organic carbon content of the Smackover Formation at Little Cedar Creek Field (Mancini et al., 2003; 2008).

1.1 Objective

Well logs, core description, and thin section analyses were integrated to determine the petrophysical characteristics of the upper grainstone. Qualities such as grain types and their size, porosity, and diagenetic history were described to better understand the link between oil production and petrophysical trends. This research provides insight into where gas injection would be most effective to maximize sweeping unrecovered hydrocarbon resources.

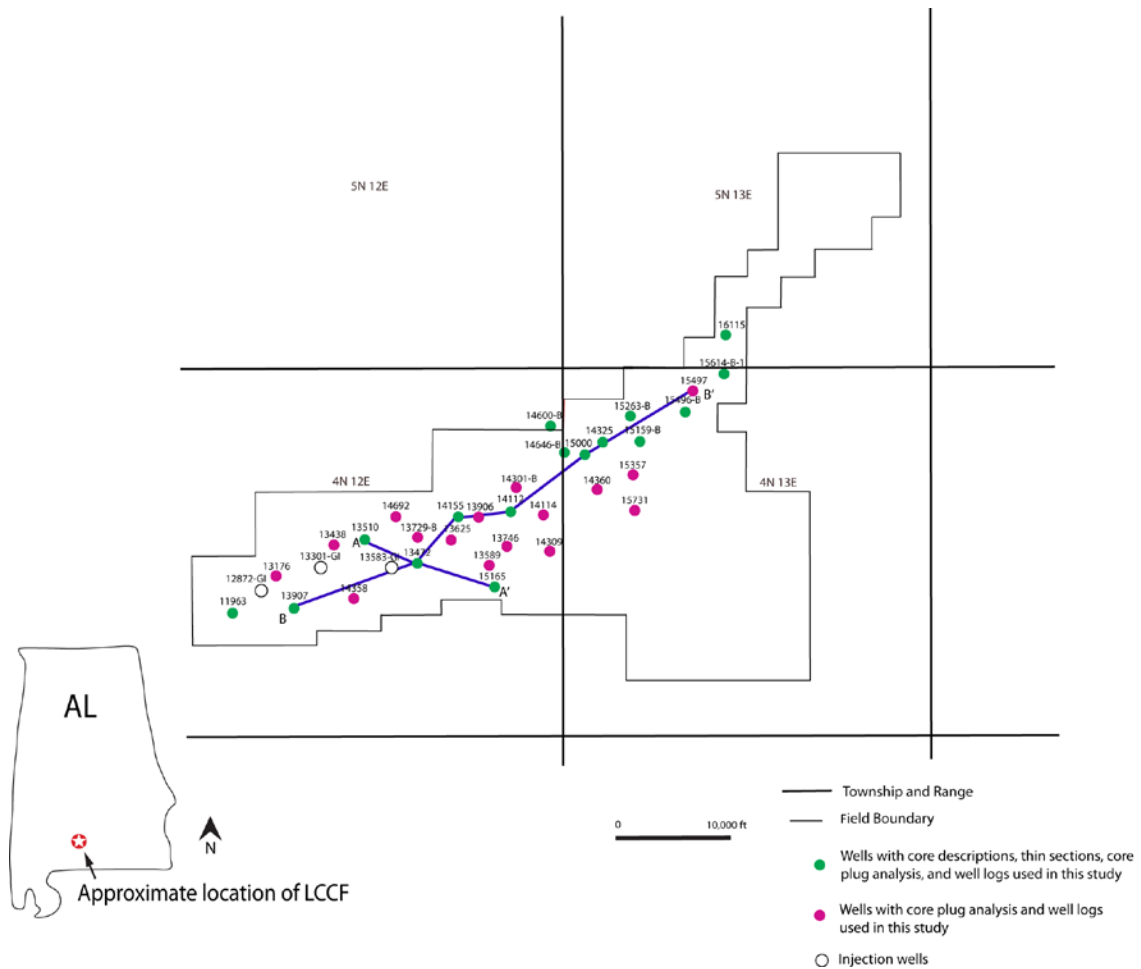


Figure 1. Location of Little Cedar Creek Field (adapted from Geological Survey of Alabama Oil and Gas Board, 2012).

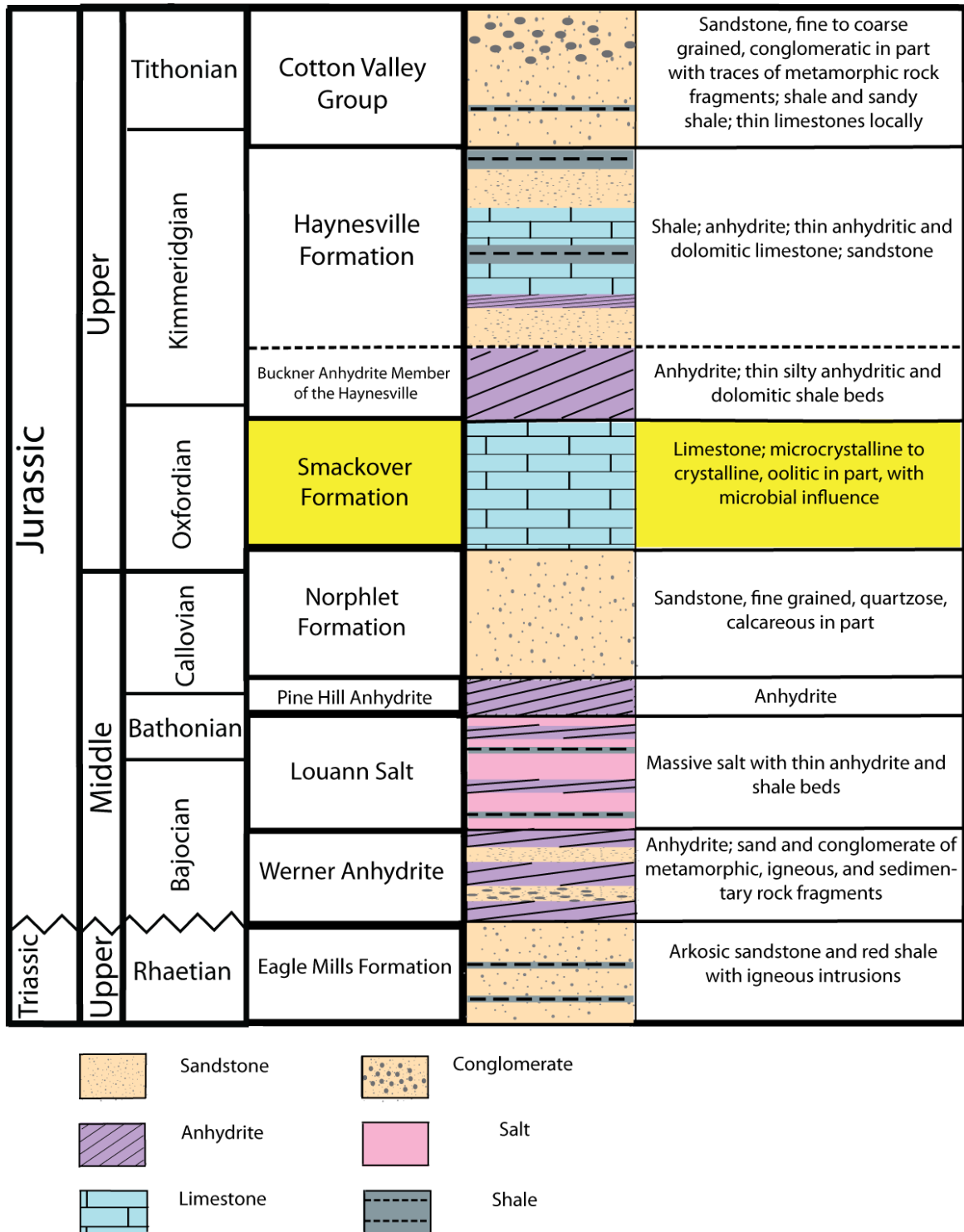


Figure 2. Generalized stratigraphic column of Upper Triassic and Jurassic strata in Little Cedar Creek Field. The Smackover Formation is highlighted (adapted from Mancini et al., 2001; 2003).

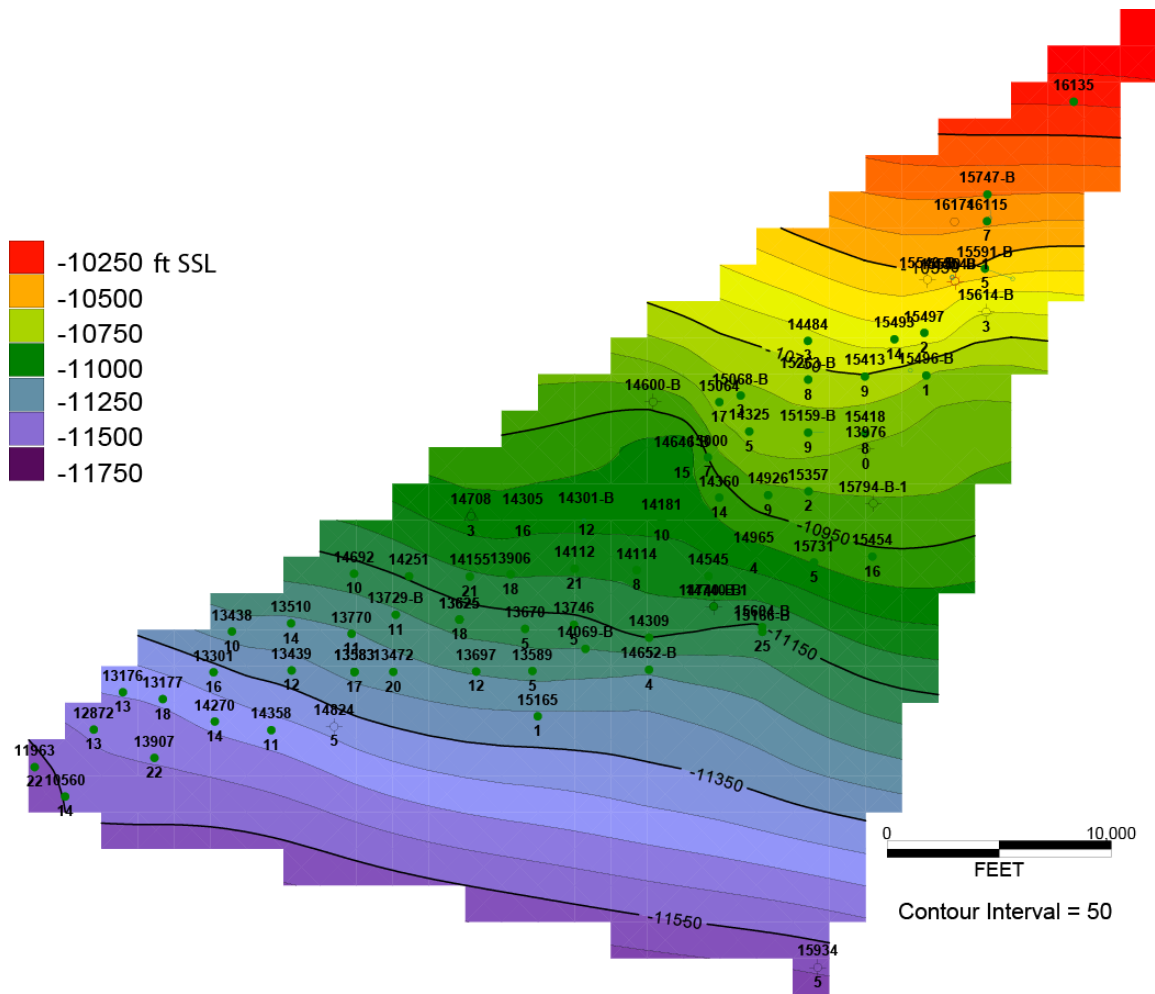


Figure 3. Structure map of the top of the Smackover Grainstone Unit measured from sea level.

2. GEOLOGICAL SETTING

2.1 Tectonics

The Jurassic Smackover Formation was deposited in a series of rift basins created by Triassic rifting of Pangaea and the subsequent creation of the Gulf of Mexico and its passive margins. Little Cedar Creek Field's geologic history is similar to that of many other basins formed during the early development of the Gulf of Mexico. The tectonic history is separated into two major events, continental rifting and continental drifting. In the first stage, Late Triassic-Middle Jurassic northwest-southeast crustal stretching and rifting of the supercontinent Pangaea separated North and South America and Africa (Scott, 2010). This separation created a series of half-graben basins separated by arches in the Gulf of Mexico, including the Conecuh Ridge (Mancini, 2001). This rifting eventually led to marine flooding in the Middle Jurassic (Scott, 2010). The second stage is dominated by drifting of the continents away from each other, the subsidence of the newly formed oceanic crust, and the counter-clockwise rotation of the Yucatan peninsula by approximately 40 degrees (Pindell, 2010). The Yucatan Peninsula ended its rotation during the Berriasian, but the Gulf of Mexico did not completely open and cease rotational spreading until the Valanginian, with the termination of northeast-southwest basement-involved extension (Pindell, 2010).

2.2 Stratigraphy

The Jurassic Norphlet Formation (Fig. 2) records the earliest deposition post-widespread rifting of the southern North American continent in the and is dominated by conglomeratic alluvial fan deposits that grade downdip into finer grained distal fan and wadi systems, as well as local lake sediments deposited in a broad, desert-plain system (Mancini et al., 1985, 1999). Farther downdip, near the paleoshoreline to the south, the Norphlet contains large-scale eolian sandstone and nearshore marine deposits that were derived from the southern Appalachians in an arid climate (Mancini et al., 1985). Thermal subsidence, from the cooling new oceanic crust, produced a major transgressive sequence above the pre-existing desert plain, causing deposition of the Norphlet Formation's thick eolian sands to backstep northward (Mancini, 2010). In some areas in the northeastern Gulf of Mexico the uppermost sands of the Norphlet have been reworked into clastic shoreface facies (Mancini, 2010). The Oxfordian Smackover Formation is a carbonate ramp deposited conformably over the Norphlet Formation during this transgression and the subsequent regression. The Smackover Formation at LCCF (Fig. 4) consists of seven lithofacies formed during a 3rd-order depositional sequence. Listed from the base the seven lithofacies are: (1) laminated peloidal wackestone; (2) bioturbated peloidal packstone; (3) microbial boundstone; (4) laminated peloidal wackestone/packstone; (5) bioturbated peloidal packstone; (6) oolitic grainstone; and (7) a siliciclastic unit containing shale to conglomerate (Heydari and Baria, 2005). The laminated peloidal wackestone (1) and the bioturbated peloidal

packstone (2) often include evidence of microbial influence such as wavy laminations and a gradual transition into the boundstone above. The microbial boundstone (3) unit formed as a series of coalescing bioherms deposited in a subtidal environment on the inner ramp (Mancini et al., 2008). The laminated peloidal wackestone/packstone (4) records the deepest-water facies on the ramp and grades upward into bioturbated peloidal packstone (5), which was deposited as sea level began to fall. Oolitic grainstone (6) was deposited in a shallow subtidal to beach environment (Heydari and Baria, 2006). The grainstone is composed of alternating peloid packstone and peloid-oid grainstone. The uppermost siliciclastic unit (7) commonly is comprised of conglomerate and locally includes red and green shale. This siliciclastic unit represents tidal flat deposition, including paleosols formed during prolonged subaerial exposure (Heydari and Baria, 2005; Mancini et al., 2008). The Smackover Formation at Little Cedar Creek field most likely formed within three miles (5 km) of the paleoshoreline (Mancini et al., 2006).

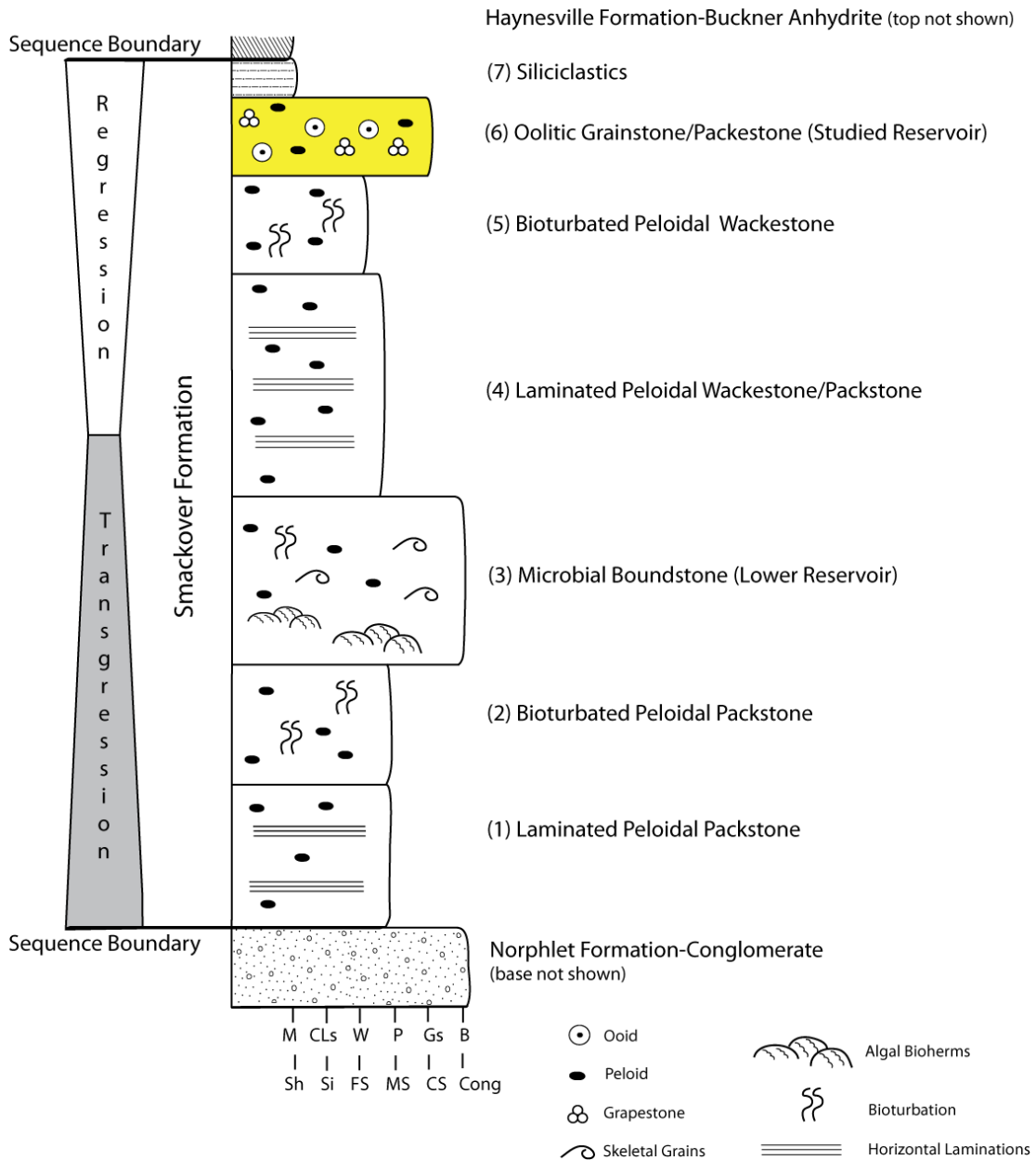


Figure 4. Idealized stratigraphy of the seven units of the Smackover Formation in Little Cedar Creek Field, Conecuh County, Alabama. Scale at base of section is the Dunham Classification (1962) for carbonate rocks (M-mudstone, CLs- calcisiltstone, W-wackestone, P- packstone, Gs-grainstone, B-boundstone) and the Wentworth size classification for siliciclastics (Sh-shale, Si-siltstone, FS-fine sandstone, MS-medium sandstone, CS- coarse sandstone, Cong-conglomerate). This study focuses on the yellow highlighted oolitic grainstone/packstone unit (Modified from Mancini et al., 2002).

3. METHODS

Cores from 15 wells in LCCF were described at the Alabama Oil and Gas Board in Tuscaloosa, Alabama, in December 2011. Thin sections were made from the grainstone facies of each well; two thin sections from each well were made from plugs sampled in reservoir-quality grainstone facies (Table 1). In well 13472, four samples were collected from each grainstone facies in the upper reservoir. The available logs from the described wells and 20 additional wells were integrated to compare calculated log porosity to measured core porosity from core analyses obtained from the operators. Only wells with sufficient data to determine grainstone unit thickness were added, limiting the number of additional wells used in this study. All wells have corresponding core analysis reports. The wireline logs from each well (Table 2) also were used to construct the isopach maps.

Table 1. Data utilized in study.

Well Permit #	Descriptions	Thin sections (depth)	Logs
11963	Grainstone Unit	11866.8 11874.2	GR, NPHI, DPHI
13472	Grainstone Unit	11495.2 11502.8 11508.2 11511.6	GR, NPHI, DPHI
13510	Grainstone Unit	11499.4 11506.0	GR, NPHI, DPHI
13907	Grainstone Unit	11802.5 11815.5	GR, NPHI, DPHI
14112	Grainstone Unit	11267.6 11272.6	GR, NPHI, DPHI
14155	Grainstone Unit	11311.2 11312.5	GR, NPHI, DPHI
14325	Grainstone Unit	11043.8 11046.7	GR, PHIE
14646-B	Grainstone Unit	11255.4 11266.5	-
15000	Grainstone Unit	11121.6 11125.5	GR, NPHI, DPHI
15159-B	Grainstone Unit	11129.2 11132.5	GR, NPHI
15165	Grainstone Unit	11502.4 11519.5	GR, NPHI, DPHI
15263-B	Full Smackover	11218.2 11223.3	-
15496-B	Grainstone Unit	11102.5 11108.5	GR, NPHI
15614-B-1	Full Smackover	-	-
16115	Grainstone Unit	10795.2	-

Table 2. Additional wells with core and log data utilized.

Permit #	Logs	Permit #	Logs
13176	GR, NPFI, DPHI	15357	GR, NPFI, DPHI
13177	GR, NPFI, DPHI	15497	GR, NPFI, DPHI
13438	GR, NPFI, DPHI	15713	GR, NPFI, DPHI
13589	GR, NPFI, DPHZ		
13625	GR, NPFI, DPHI		
13729-B	GR, NPFI, DPHI		
13746	GR, NPFI, DPHI		
13906	GR, NPFI, DPHI		
14114	GR, NPFI, DPHI		
14270	GR, NPFI, DPHI		
14301-B	GR, NPFI, DPHI		
14309	GR, NPFI, DPHI		
14358	GR, NPFI, DPHI		
14360	GR, NPFI, DPHI		
14545	GR, NPFI, DPHI		
14692	GR, NPFI, DPHI		
14708	GR, NPFI, DPHI		

3.1 Petrography

Twenty-nine thin sections from 14 wells were sampled in reservoir quality grainstone. Petrographic thin sections were described using Dunham’s Classification (1962). Descriptions include grain types and grain sizes, cements, diagenesis, and porosity estimation. Slides were impregnated with blue epoxy to highlight porosity.

3.1.1 Facies

3.1.1.1 Grain Size, Type, and Arrangement

Although interpreted as the ooid grainstone unit of the Smackover Formation (Heydari and Baria, 2005; Mancini et al., 2008), thin sections from this unit contain a significant amount of peloids, grapestones, intraclasts, and many samples also include a few siliciclastic grains. Of the 29 thin sections described from the “ooid grainstone” and classified according to the Dunham Classification (1962) two are peloid grainstone; two are peloid packstone/wackestone; seven are ooid grainstone; four are peloid-ooid grainstone; three are peloid-grapestone grainstone; and eleven are peloid-ooid-grapestone grainstone (Fig. 5). Peloids ranged in diameter from less than 0.05 mm to 1 mm and ooids were ~1 mm (Fig. 5d). Grapestones often encased two or more ooids, peloids, or intraclasts. The grapestones range in size from less than 0.5 cm to greater than 2.5 cm (Fig. 5e). Milliolid foraminifera and small skeletal fragments, mostly bivalves and gastropods, also are common. A syntaxial overgrowth around a crinoid fragment occurs in one thin section (Fig. 6). Commonly, grains are heterogeneously arranged with no preferred grain orientations. However, thin horizontal laminations occur in four wells: 13472, 13510, 15263-B, and 15496-B. Cross bedding occurs in well 15000 (Fig. 7). Grain size, type, and arrangement were wide-ranging and varied, even vertically in the same well only inches or feet apart. It was not uncommon to have two thin sections a few feet apart in a well, where one thin section is well sorted ooids and

peloids and one is poorly sorted, and composed of a combination of grapestones, peloids and ooids.

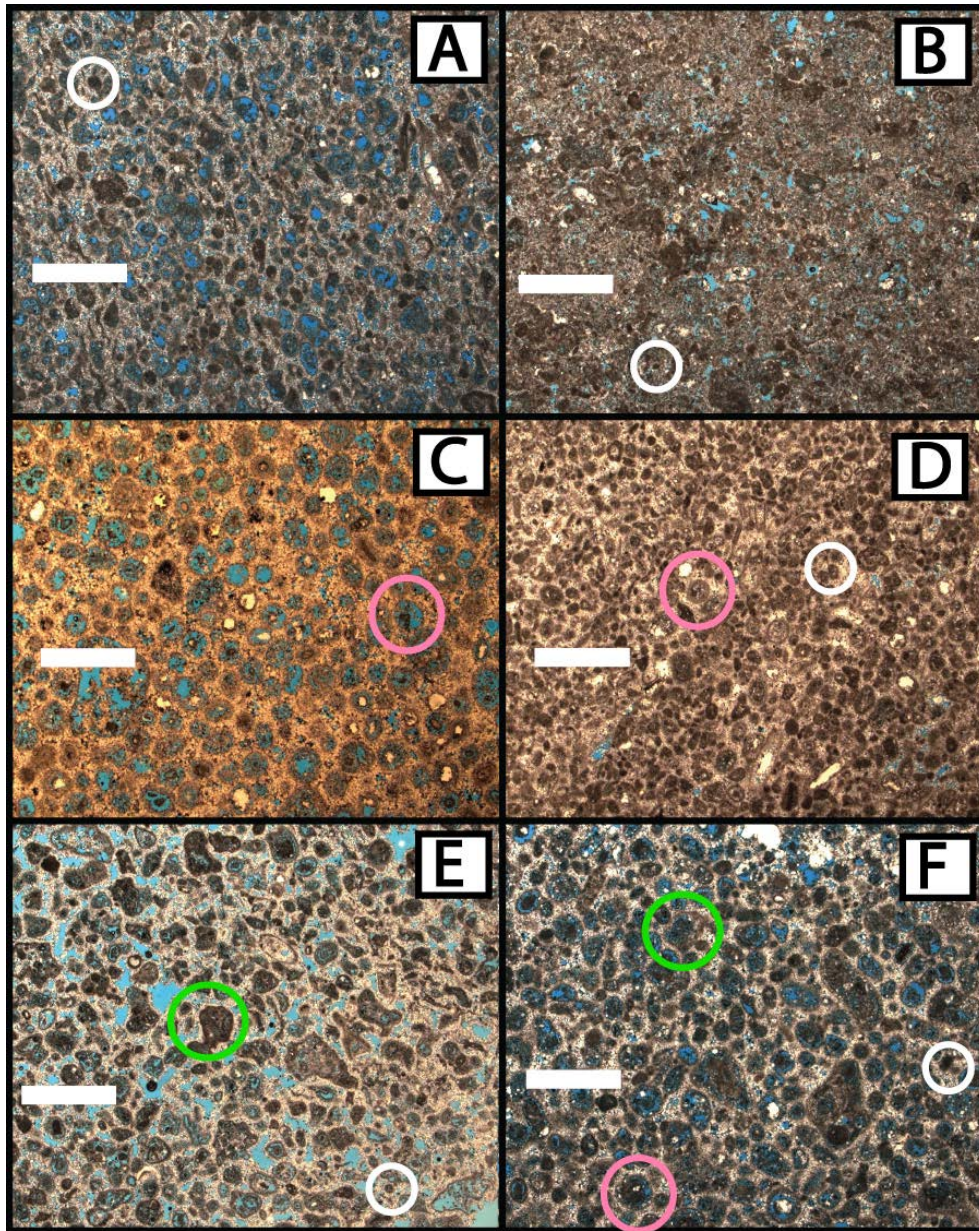


Figure 5. Rock types in the Smackover Formation grainstone unit. The scale bar represents 1mm. Pink circles indicate ooids, green for grapestones, and white for peloids. (A) Peloid Grainstone from well 15496-B at 11,102.5 ft with moldic porosity (B) Peloid Packstone/Wackestone from well 15165 at 11,519.5 ft with primarily vuggy porosity (C) Ooid Grainstone from well 11963 at 11,866.8 ft with moldic porosity (D) Peloid Ooid Grainstone from well 15000 at 11,125.5 ft with very little vuggy porosity (E) Peloid Grapestone Grainstone from well 14,112 at 11272.6 ft with abundant vuggy porosity (F) Peloid Ooid Grapestone Grainstone from well 15263-B at 11,218.2 ft with both vuggy and moldic porosity. (See appendix for locations of thin sections on the core descriptions).

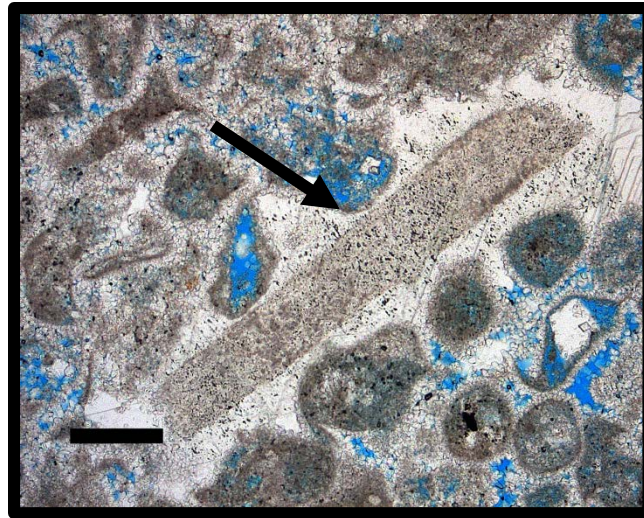


Figure 6. Syntaxial overgrowth of crinoid grain in well 13472 at 11,508.5 ft. It was very rare to find grains that lacked rim cement. Scale bar represents 200 μm (See appendix for location of thin section on the core descriptions).

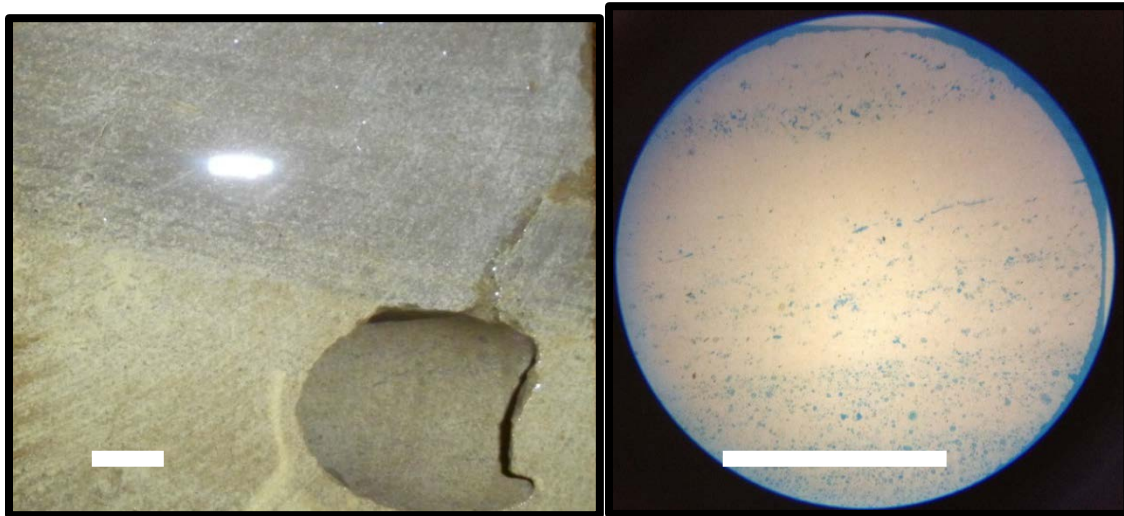


Figure 7. Cross-laminae in well 15000 at 11,125.5 ft in core and in thin section. Both scale bars represent 1 cm (See appendix for location of thin section on the core descriptions).

3.1.1.2 Vertical and Lateral Variations

Some degree of algal influence in the form of algal structures that commonly are wavy microbial laminations, microbial coatings, binding of grains, and grapestones occur in each of the thin sections (Fig. 8). Microbial coating and binding of the grains occurs in wells 13510 and 13472, and seven wells have algal coatings on grains and contain aggregated grapestones bound with algal material (Fig. 8). The remaining four wells contain small grapestones. Large (up to about 0.5mm) vugs formed by preferential dissolution within most algal grapestones. In all thin sections, the more algal influence there was, the darker the matrix. Therefore, grainstone without significant algal influence are lighter colored buff to grey. Algal influence was more pronounced in the southwestern portion of the field. For example, in well 13510 most grains are encompassed by many large grapestones, the microbial binding is so extensive that the overall color of the rock is darker than most grainstone samples (Fig. 9). In the lower two grainstone facies of well 13472 there is extensive microbial binding (Fig. 10).

Each grainstone facies in well 13472 differs clearly from the others on a continuum of decreasing algal content and increasing ooid content (Fig. 10). The sample at 11,511.6 ft features mostly microbially bound grains. This sample is nearly devoid of ooids, the ooids that are present were only distinguishable by the residual circular rim cement (Fig. 10d). The sample at 11,508.5 ft was not as pervasively influenced by microbial activity but has a wavy texture from the algal binding material. Grapestones were more discernable from other grains; however, there were few ooids, and they are

only recognizable from the residual circular rim cement (Fig. 10c). The sample at 11,502.8 ft has a clear distinction between the algally influenced grey-brownish patches and the buff, more ooid-rich, grainstone. The grapestones were bound by algal material and ranged from about 1.0 mm across to about 1.0 cm. Ooid content is estimated to be approximately 10%, still only discernable from the residual rim cement and located mainly in the buff patches (Fig. 10b). Lastly, the sample at 11,495.2 ft is buff color with fewer and smaller algal grapestones, and there is a significant increase in ooid content (about 25% ooid grains). The ooid grains are in variable stages of dissolution and recrystallization (Fig. 10a); this uppermost grainstone facies had the most visible porosity (20% estimated and 20.3% core plug analysis porosity), mainly in molds and small vugs.

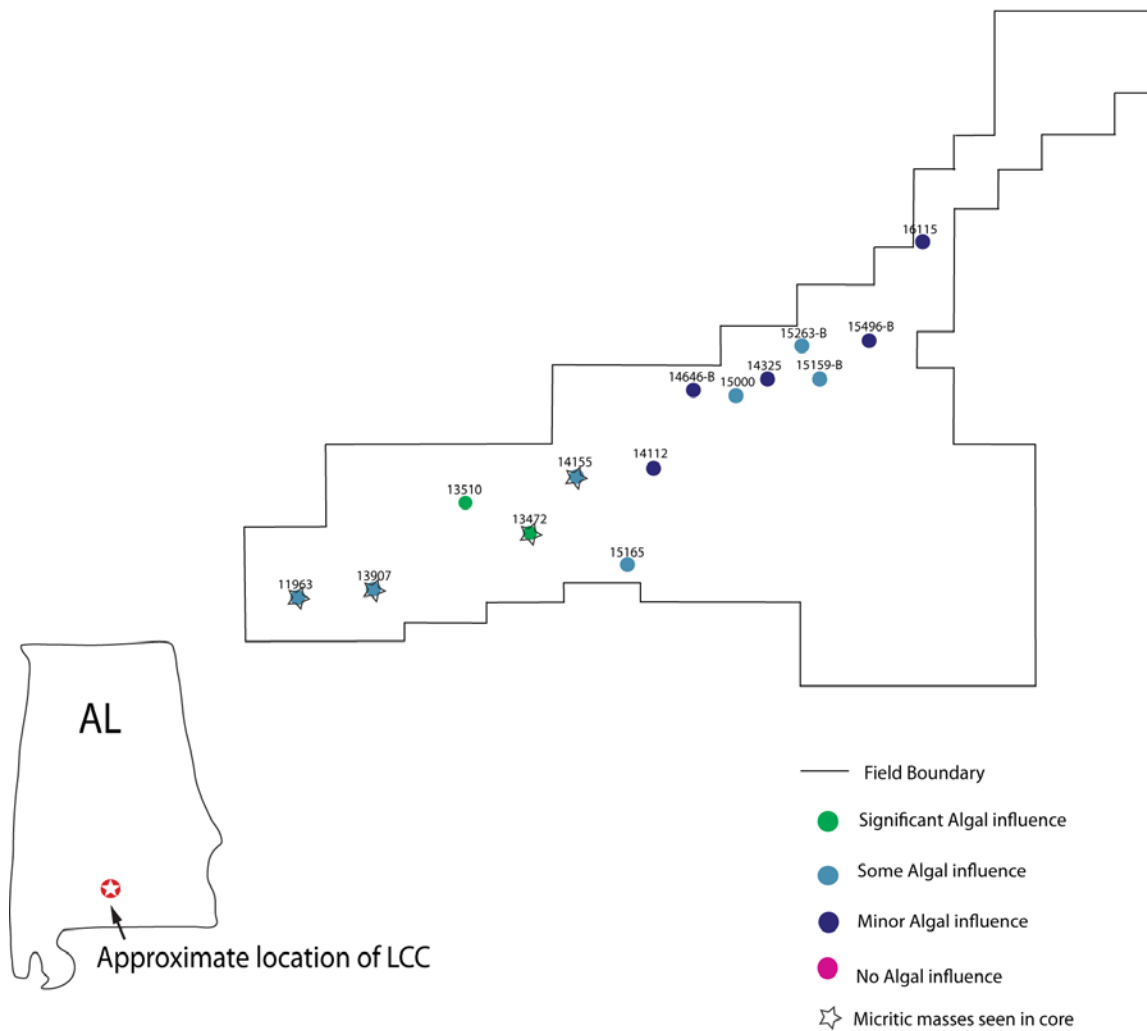


Figure 8. Distribution of algal influence in upper grainstone reservoir of the Smackover Formation. Significant algal influence includes: thick mat-like microbial coating and binding of the grains, peloids and ooids, referred to as grapestones (Winland and Matthews, 1974), and wavy laminations potentially caused by microbial activity. Some algal influence includes fewer algal coatings and grapestones and minor influence includes the samples with very few grapestones or algal coatings. Large micritic masses occur in four cores.

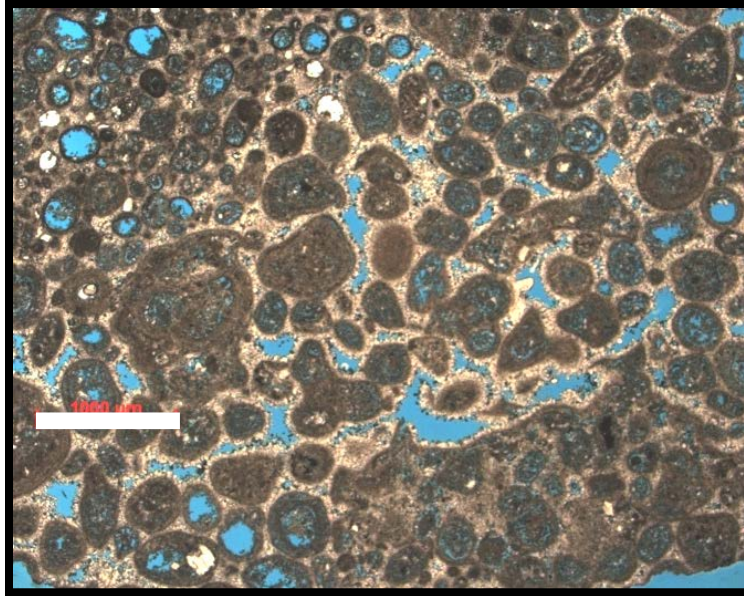


Figure 9. Grapestones encompassing many grains in well 13510 at 11506.0 ft. Scale bar represents 1 mm. (See appendix for location of thin sections on the core descriptions).

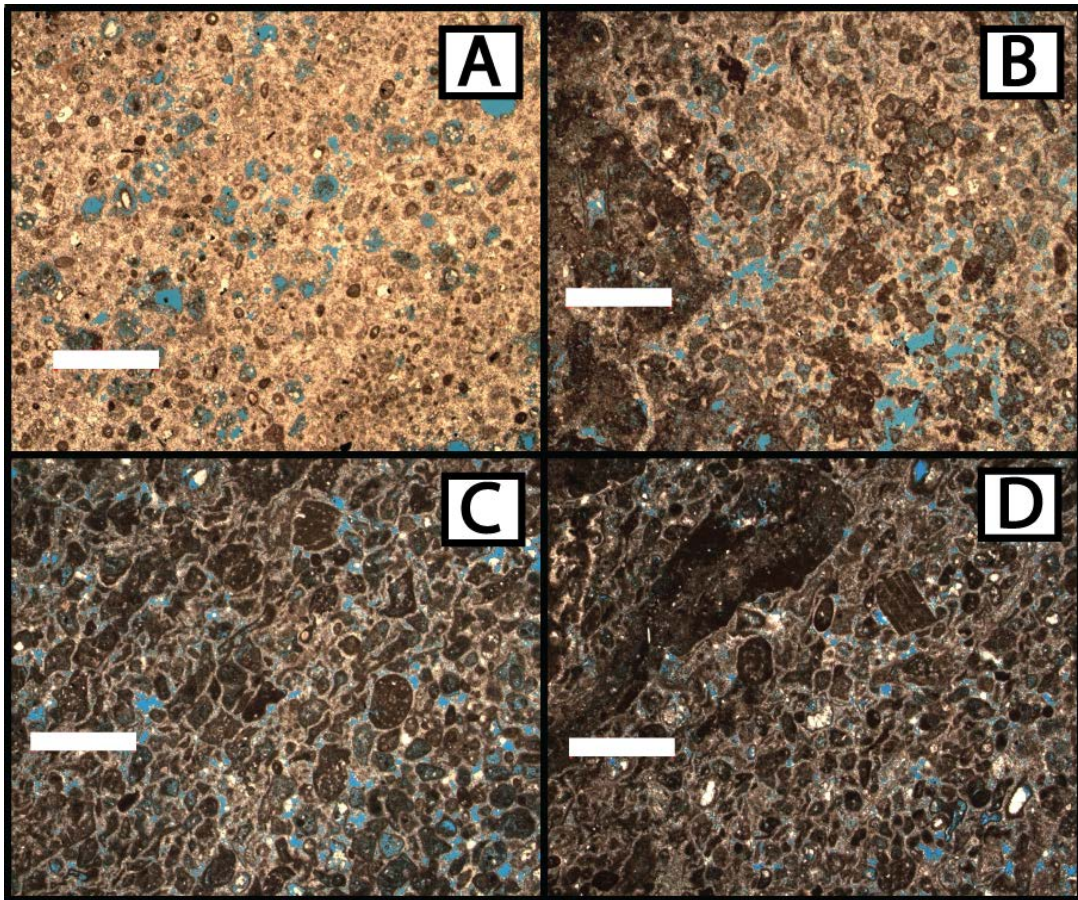


Figure 10. Photomicrographs of grainstone facies in the Smackover Formation grainstone unit in well 13472; scale bar represents 1 mm: (A) Top grainstone facies at 11,495.ft with mainly moldic porosity and few vugs (B) upper middle grainstone facies at 11,502.8 ft with mainly vuggy porosity (C) lower middle grainstone facies at 11,508.5 ft with mainly interparticle porosity (D) Base grainstone facies at 11,511.6 ft with small vuggy porosity and intergranular porosity (See appendix for location of thin sections on the core descriptions).

3.1.2 Porosity

Diagenetic porosity in the grainstone facies is primarily moldic, vuggy and enhanced interparticle. The best porosity occurs in samples with a combination of two or all three types of porosity. Many samples also retain depositional intergranular porosity.

The most common combinations were oomoldic and vuggy and oomoldic and interparticle. Of the twelve samples with these types of porosity, all had porosity values from plugs and thin section estimates above or near 20%, compared to the average grainstone porosity of 17%. Additionally, the five samples with all three pore types also had higher than average porosity. The samples with the lowest porosities are more recrystallized, have more cement in the pores, or they contained only oomoldic porosity.

3.1.2.1 Diagenesis and Paragenetic History

The paragenetic history of the Smackover Formation grainstone unit, determined by thin section petrography and cathodoluminescence, indicates there were six diagenetic events (Table 3, Fig. 11). Not all diagenetic events occur in all thin sections, and the degree of diagenesis varies among samples. Shortly after deposition, clear dogtooth sparry calcite (1) formed an isopachous rim cement that completely surrounded each grain, suggesting the rock had not yet undergone significant compaction. This cement formed in a phreatic environment. Commonly, just this rim cement remains in samples with good moldic porosity. This early rim cement created the framework for the grainstone and aided retention of depositional porosity. Although it mainly aided porosity, this rim cement decreased interparticle pore space to varying degrees. Dissolution (2), the next diagenetic event, dissolved most ooids, leaving few with recognizable internal structure. Many ooids and peloids were completely dissolved, leaving only the rim cement (Fig. 12). This dissolution event was widespread, as it

occurs in samples from every well. At Little Cedar Creek Field this dissolution event most likely occurred as undersaturated fresh water passed through the rock in the meteoric phreatic environment while the Smackover Formation was subareally exposed (Heydari and Baria, 2005).

Next, calcite precipitated (3) as a fine layer of microsparry calcite in pore throats (Fig. 13). The microsparry calcite cement closed important pore spaces and was the most destructive phase of diagenesis. This cement is brightly cathodoluminescent, indicating a Mn^{+} rich water source indicative of the meteoric environment (Meyers, 1974 and Meyers and Lohmann, 1985). Well #16115 was the only well with no visible porosity; all its pore space was occluded during the microsparry calcite cementation phase, as indicated by the lack of internal structure in any of the ooid grains.

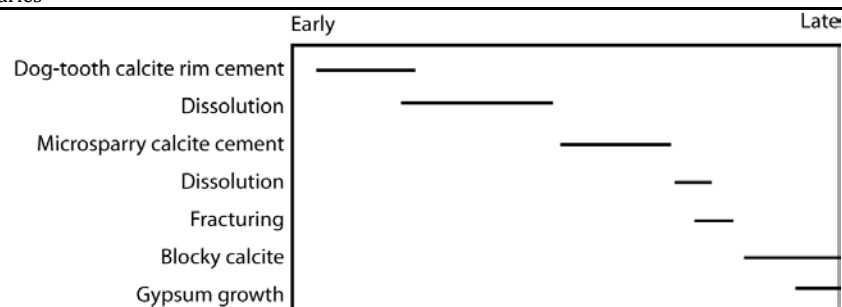
A minor dissolution (4) episode formed large vugs that cut across previous cements and dissolved some of the microsparry calcite (Fig. 14). This second dissolution event opened up larger voids and created increased pathways for fluid flow. It was not as pervasive as the first dissolution event, appearing to only enlarge previous voids rather than creating a substantial amount of new voids. In rocks that retained oomoldic porosity from the first dissolution event, the second phase of dissolution connected molds into vugs and enhanced interparticle porosity. New blocky calcite crystals (5) formed in these larger voids and smaller calcite crystals formed in the voids between grains or in molds. The large clear calcite crystals are as long as 2.5 cm in core. Cathodoluminescence of the larger crystals shows some zones (Fig. 15), that could record changes in pore water chemistry and temperature (Heydari and Moore, 1993). These large blocky calcite

crystals have bright cathodoluminescence indicating that the waters from which they were precipitated contained a significant amount of Mn⁺. Due to their large size, they do not fill pore throats, but preferentially occur in larger molds, vugs and fractures.

Lastly, gypsum (6) occurs as smaller crystals in pore spaces and large crystals that envelope and eventually replace grains and voids (Fig. 11F). The largest gypsum crystals occur primarily in the northern part of the field. Gypsum generally forms at depths above 4,000 ft (Murray, 1964) and most likely formed in a shallow burial environment at LCCF when the Haynesville anhydrite was forming in an arid environment (Ridgway, 2010). The later phases of large blocky calcite and gypsum crystal growth were not as pervasive or destructive as earlier cementation events.

Table 3. Summary of diagenetic events and relative timing

Diagenetic Event	Plain Light Characteristics	Cathodoluminescent (CL) Characteristics	Diagenetic Environment	Interpretation
(1) Dogtooth calcite rim cement	Light yellow to clear bladed calcite crystals encircling grains	Dark brown, color makes it difficult to discriminate between initial micrite cement, bladed shape	Marine Phreatic	The cement completely surrounds each grain, suggesting that it occurred early after deposition. This cement builds the framework that helps maintain depositional porosity.
(2) Dissolution		No Light	Meteoric Vadose	This dissolution was widespread and created the abundant moldic porosity.
(3) Microsparry calcite cement	Often occludes pores and pore throats. Grows between, around, and in grains. Fine clear to yellowish calcite crystals	Dull dark orange to bright orange luminescence. Brighter luminescence often surrounds grains whereas darker luminescence fills voids	Meteoric Phreatic	Most destructive cement. Bright luminescence indicates Mn >> Fe.
(4) Dissolution		No Light	Burial	Smaller dissolution opened some pore spaces that had been occluded during the microsparry calcite stage as well as creating larger vugs and molds.
(5) Blocky Calcite cement	Opaque light yellow blocky calcite crystals that form in larger voids between and in grains	Bright orange with zonations in medium and large crystals.	Burial	The zonations in the CL record changing water chemistry and temperatures in pore spaces.
(6) Gypsum crystal growth	Light yellowish to clear medium to large crystals with two distinct cleavage planes. Occurs in voids or unimpeded by grain or cement boundaries	Red orange to bright orange. Zonation and gradational changes in color	Burial	Large gypsum laths replace and obscure all other minerals and grains that they encompass, indicating that this was the last major diagenetic event.



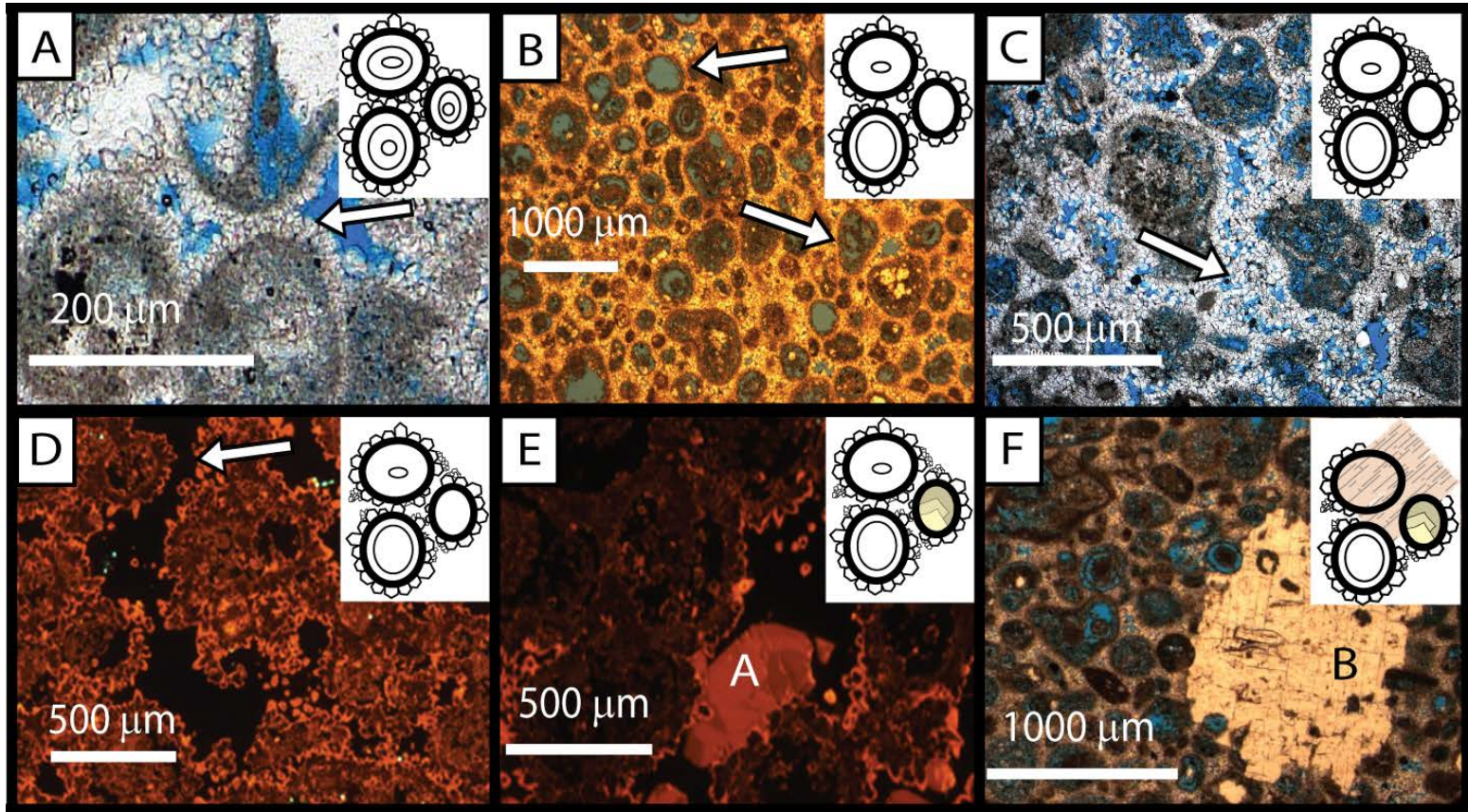


Figure 11. Paragenetic Sequence: (A) dogtooth calcite cement in well 13510 at 11,506.0 ft depth (Plain light) (B) dissolution in well 14325 at 11,046.7 ft depth (plain light) (C) microsparry calcite cement in well 14112 at 11,272.6 ft depth (D) small dissolution event in well 14112 at 11,272.6 ft (30 sec) (E) blocky calcite formation in well 14325 at 11,043.8 ft depth (25 sec) crystal labeled “A” (F) gypsum formation in well 14325 at 11,043.8 ft depth (plain light) crystal labeled “B”. (See appendix for location of thin sections on the core descriptions).

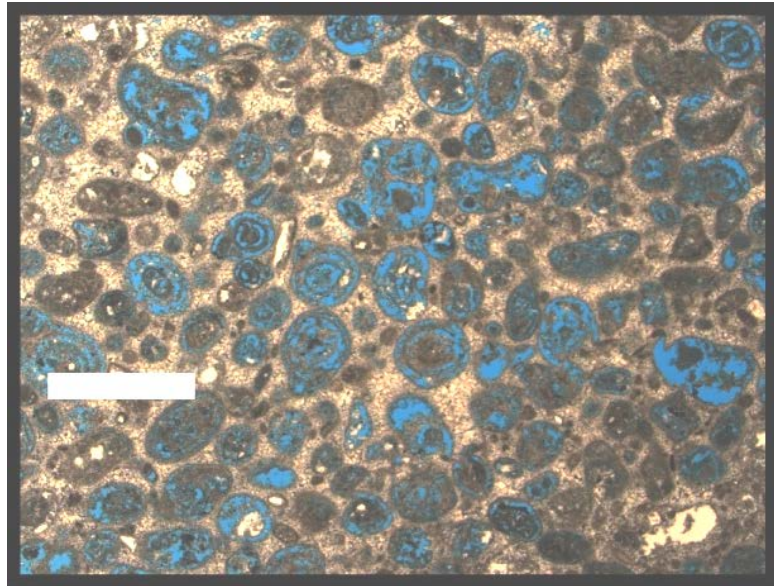


Figure 12. Thin section photo of partially dissolved ooid grains leaving molds and internal concentric rings, Well 13510, 11,499.2 ft. Scale bar is 1 mm. (See appendix for location of thin sections on the core descriptions).

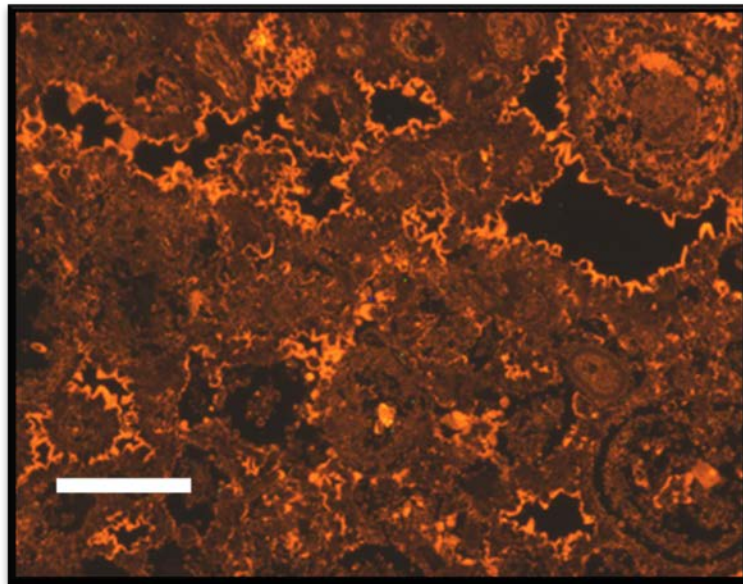


Figure 13. Thin layer of microsparry calcite (bright orange cathodoluminescence) lining pore space and along pore throats in Well 14325, 11,043.8 ft and 25 secs exposure. Scale bar is 500 μm . (See appendix for location of thin sections on the core descriptions).

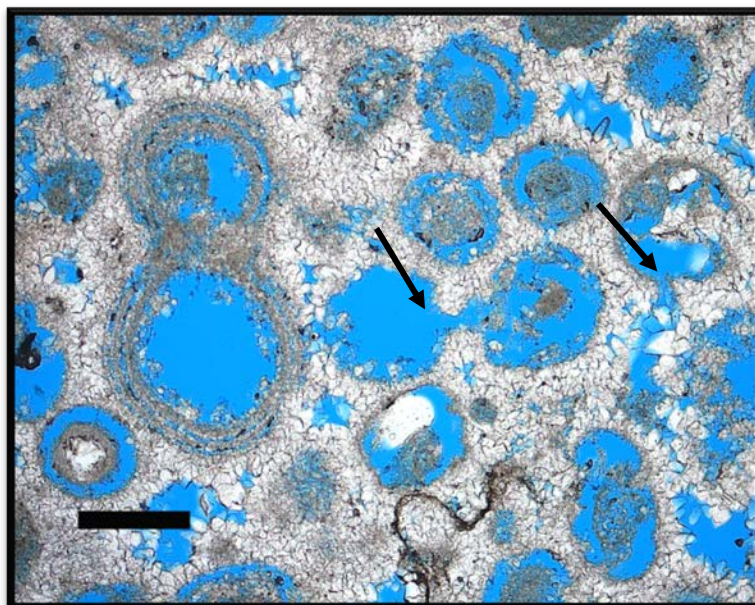


Figure 14. Arrow indicates dissolution path through microsparry calcite Well 14325, 11,043.8 ft. There is no microsparry calcite growth into path which implies that this dissolution event occurred after microsparry calcite cementation. Scale bar is 200 μm . (See appendix for location of thin sections on the core descriptions).

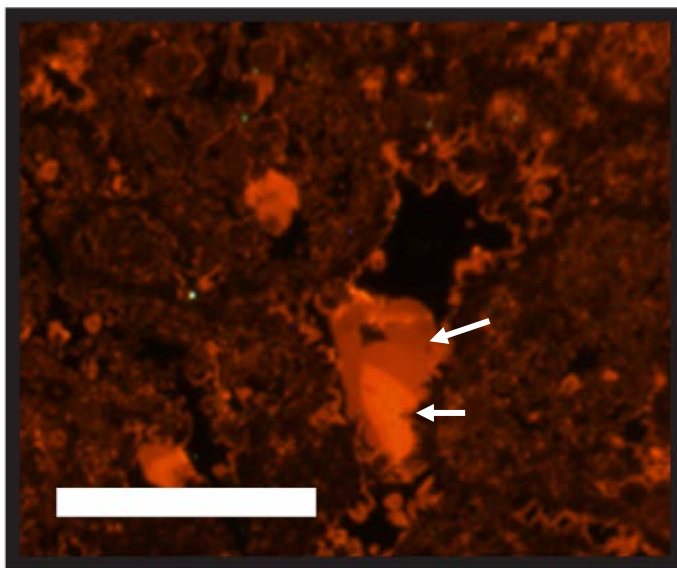


Figure 15. Cathodoluminescent image of blocky calcite crystal in pore space of Well 14646-B, 11,266.5 ft and 20 sec exposure showing at least two different stages of growth as indicated by two distinct zones. The scale bar is 500 μm . (See appendix for location of thin sections on the core descriptions).

3.2 Core: Description and Plug Analysis

Cores from fifteen wells in the Little Cedar Creek Field were described using a hand-lense and microscope at the Alabama Oil and Gas board in Tuscaloosa, Alabama, in December of 2011. Thirteen of the fifteen cores described only the grainstone unit of the Smackover Formation, identifying the different rock types within this unit. The rock types were determined by grain size and matrix/grain ratio changes of intervals greater than one inch (2.5 cm) indicated by a change in Dunham (1962) classification. A thickness of more than six inches (15 cm) indicates a ‘facies change’ and is identified on the descriptions with its separate Dunham classification as a new rock type interval (See appendix for core descriptions). Six inches was chosen because the rock type was usually not fully developed in thinner intervals due to the often gradational changes in facies. Core plug analysis reports were available for all wells.

3.2.1 Facies

3.2.1.1 Vertical and Lateral Variation

Rapid changes in lithology occur only inches apart in the cores. Transitions from ooid grainstone to peloidal packstone/wackestone range from very abrupt with obvious color changes (Appendix A- Well 15000) to gradational (Appendix A- Well 13907). It is very common for 1-3 in (2.5-7.6 cm) thick intervals of differing rock types to be

intimately interbedded. In the core descriptions, smaller (less than 6 in) gradational beds within a facies are noted in the facies profile but without separation into a new facies unit. Wells in the southwestern part of the field have more facies changes (Fig. 15). Wells 11963 and 13907 had four and five distinct grainstone facies, respectively, the most observed in the wells described. Surrounding wells averaged just over two grainstone facies in the Smackover Formation grainstone/packstone unit. The northern wells had one to two grainstone facies per well. On average, the grainstone is lighter in color and contains more ooid grains up section within the unit. Cores from wells 13907, 14155, and 15000 have small-scale cross-bedding (Fig. 6) and wells 13472 and 16115 have distinct horizontal laminations. Most wells do not have any ordered depositional texture or have light wavy laminations.

Algal influence on deposition of the upper peloid-ooid grainstone/packstone is visible in cores 11963, 13472, 13907, and 14155 (Fig. 7). All four wells are located in the southwestern part of the field. Algal influence includes large grapestones, algal coatings on grains, and irregular micrite masses averaging 0.5-1 in (1.3-2.5 cm) diameter. Algal influence diminished up section in both core and thin section. For example, in well 11963, the bottom two of four grainstone facies have large irregular micrite masses that do not occur in the upper two grainstone beds. A sample of one of the upper ooid grainstone facies did not indicate any algal influence, whereas a second thin section in one of the lower peloid-ooid grainstone records algal activity; this is a common trend in the wells. In well 13472, all samples, except the uppermost ooid

grainstone facies, had distinct algal micrite masses visible in core and thin sections.

Wells 13907 and 14155 had algal influence in all grainstone facies.

3.2.2 Porosity

Intergranular, moldic, and vuggy porosity are common visible porosity types in the cores of the peloid-oid grainstone/packstone unit of the Smackover Formation. Molds are formed by dissolution of the ooid and peloid grains, whereas the grapestones grains were dissolved to form vugs. Some vugs are associated with stylolites occurring within the peloid-oid grainstone/packstone unit. The peloidal packstone/wackestone facies has very little visible porosity. Fracture porosity formed locally, and many fractures are filled with large, blocky calcite crystals. Fractures are not a significant form of porosity in the grainstone unit of the Smackover Formation. The visual estimates of porosity from core descriptions are similar to the measured core values for porosity. Thin section estimates were quantitatively consistent with the core plug analysis, except when more than 25% porosity was estimated visually (Table 4). The grainstone facies has distinctly higher values for both porosity and permeability than the packstone/wackestone facies. The core plugs indicate the porosity averages 17% in the grainstone and 5.6% in the wackestone. There is a strong correlation between the described facies and porosity values from the core plug analysis (Fig. 16).

Crossplots from core plug analysis indicate that pore types also are significant porosity and permeability indicators (Appendix B). Moldic and vuggy porosity were the

two main types of porosity reported in the core analysis. Although the reports do not note intergranular porosity, all thin section samples with the exception of two retained significant intergranular porosity. Core plugs with vuggy pores had an average porosity of approximately 17.3 % and cores with moldic porosity averaged 16.3%. The permeabilities are varied and do not indicate higher values associated with either the moldic or vuggy porosity type. The size of the pores has a strong impact on porosity and permeability with smaller pores having worse porosity and permeability values (Fig. 17). Porosity type is not evenly distributed; wells with primarily moldic type porosity cluster in the southwestern-central part of the field. The concentration of moldic porosity occurs where unit thickness is greater than 10 ft (Fig. 18) this is likely because fresh, undersaturated waters move more easily through the ooid-rich facies.

Table 4. Estimated porosity from thin sections and reported porosity from core analysis

Well	Estimated Thin Section PHI	Core report PHI
Well 11963		
11866.8 ft	25%	19.9%
11874.2 ft (11874.5 ft Core sample depth)	15	13.7
Well 13472		
11495.2 ft (11495.1)	15-20	20.3
11502.8 ft (11502.6)	15	16.8
11508.5 ft (11508.35)	10-15	12.1
11511.6 ft (11511.55)	5	0.1
Well 13510		
11499.4 ft (11499.2)	35	22.2
11506 ft (11505.7)	25	16.1
Well 13907		
11802.5 ft (11802.15)	20-25	11.2
11815.5 ft (11815.7)	5	2.8
Well 14112		
11267.6 ft (11267.95)	35	28.1
11272.6 ft (11272.8)	30	24.4
Well 14155		
11311.2 ft (11311.1)	25	23.6
11312.5 ft (11312.75)	30	19.5
Well 14325		
11043.8 ft (11043.7)	40/15	21.9
11046.7 ft (11046.5)	35	27.7
Well 14646-B		
11255.4 ft (11255.7)	35	25.4
11266.5 ft (11266.35)	5/20	3
Well 15000		
11121.6 ft (11121.7)	35	25.4
11125.5 ft (11125.85)	5/20	19.1
Well 15159-B		
11129.2 ft	35	29.6
11132.5 ft (11132.9)	35	25.1
Well 15165		
11502.4 ft (11502.55)	1	1.4
11519.5 ft (11519.3)	10-15	13.3
Well 15263-B		
11218.2 ft	30	19.5
11223.3 ft (11223.2)	35	24.7
Well 15496-B		
11102.5 ft	30	Depths did not match
11108.5 ft	35	
Well 16115		
10795.2 ft (10795.5)	0-1	5

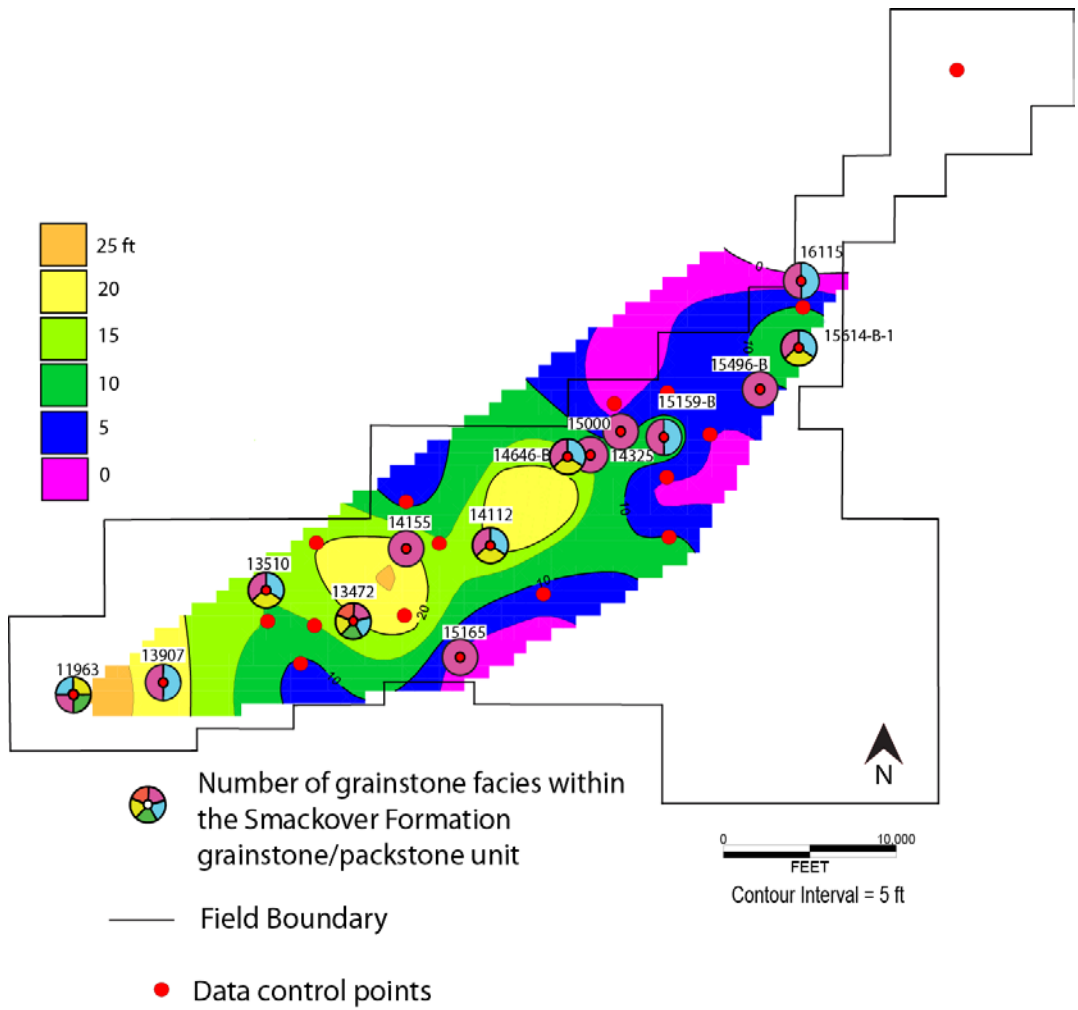


Figure 16. Isopach map of the upper grainstone/packstone unit of the Smackover Formation. The colored wheels indicate the number of grainstone facies in the grainstone/packstone unit in cores by the number of colors that appear in the wheels. There are one to five grainstone facies per well.

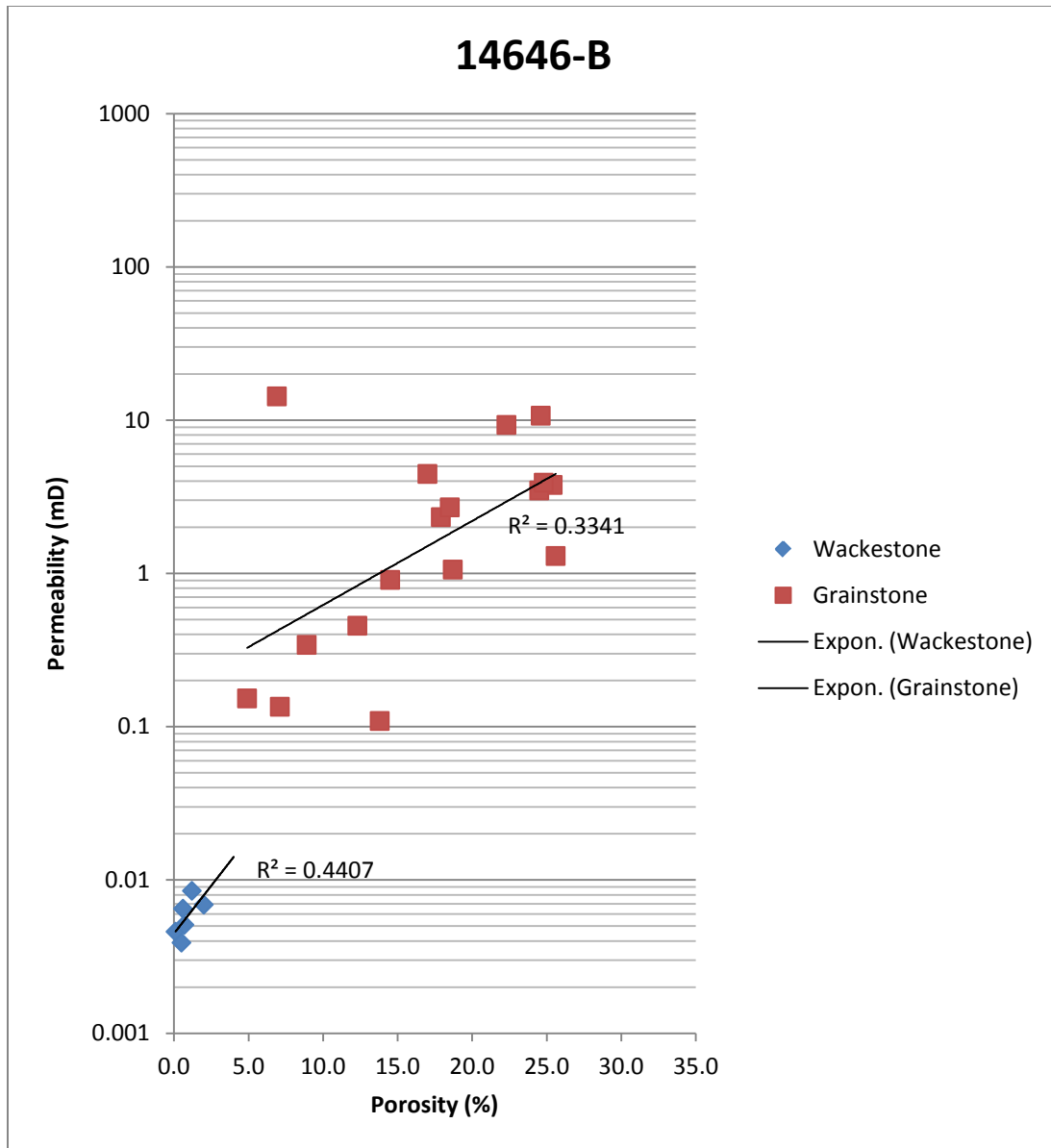


Figure 17. Porosity vs. permeability plot by facies from well 14646-B, illustrating that porosity and permeability are very closely related to facies. The grainstone facies consistently has higher permeability and porosity values whereas the wackestone facies has consistently low permeability and porosity values.

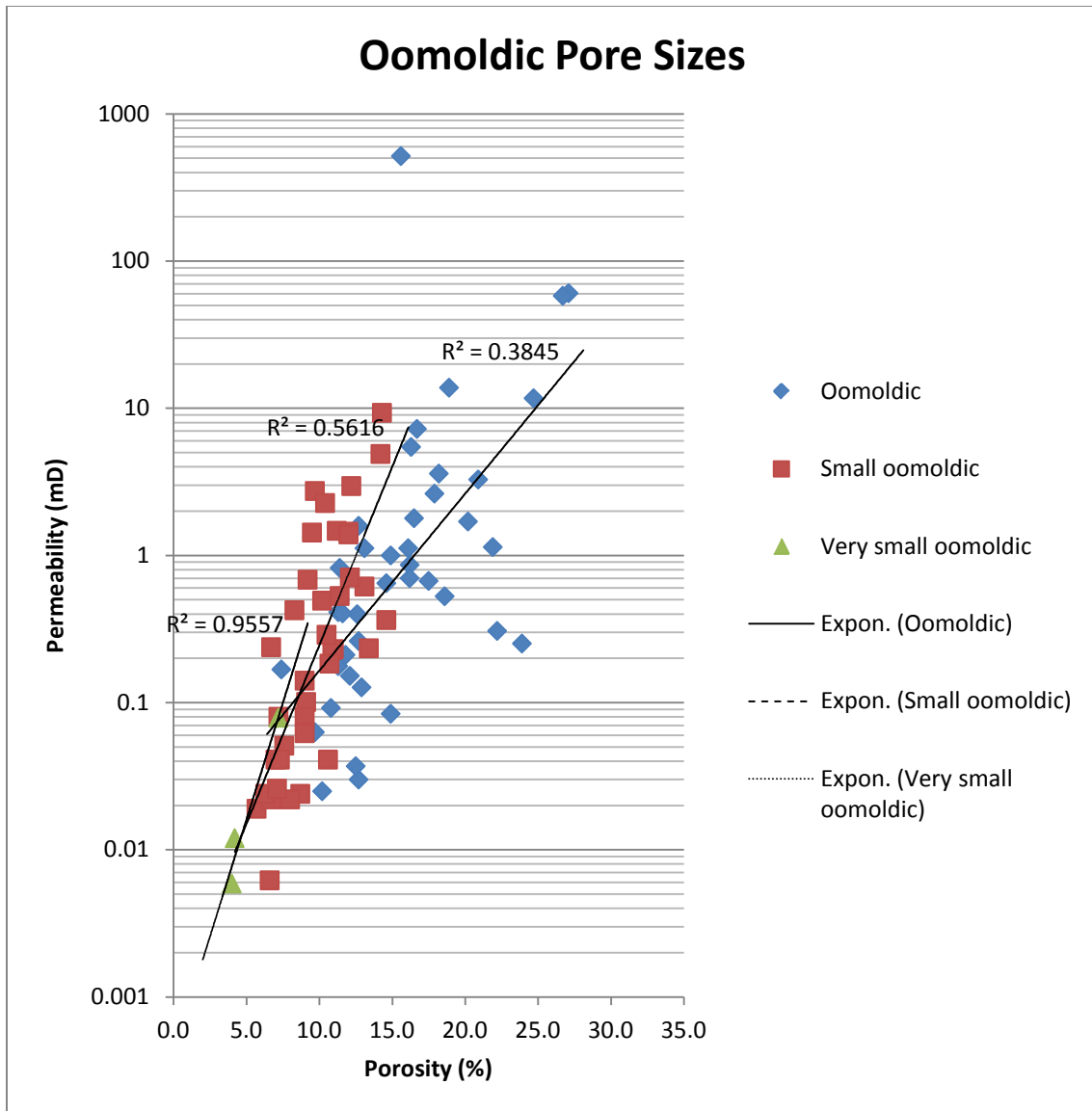


Figure 18. Porosity vs. permeability plot from various pore sizes within oomoldic porosity type reported from the core analysis reports. Although the main porosity type is oomoldic in each sample plotted, the size of the molds affects the porosity and permeability values. Larger pores correspond with higher permeability values. As pore size increases the clusters increase in size as a response to a larger range of porosities. It is likely possible that the small oomoldic and very small oomoldic porosities include primarily molds of peloids, however, the core analyses specifically reported oomoldic.

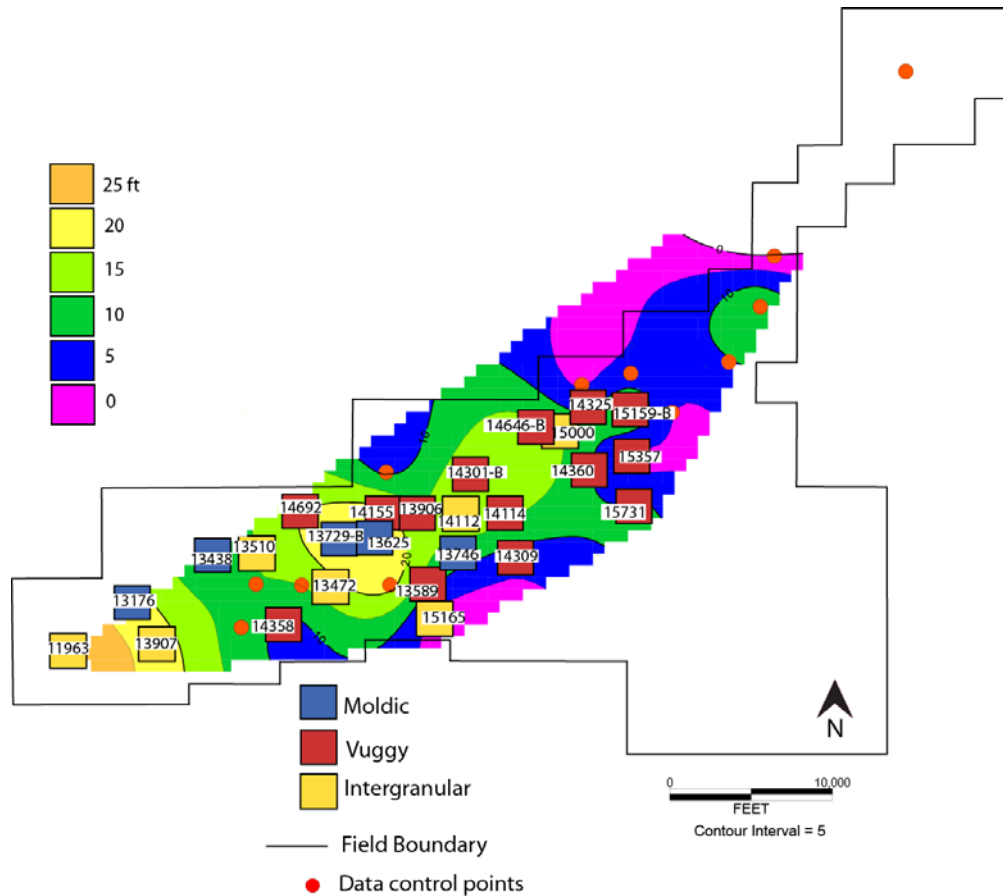


Figure 19. Visible porosity type superimposed on the Smackover Formation total grainstone unit isopach. Core reports did not include intergranular. Moldic porosity occurs at a unit thickness above 12 ft. While vuggy and intergranular pores are distributed throughout the field. The data control points represent wells for which there are total grainstone thickness values.

3.3 Log Analysis

3.3.1 Correlation Between Well Logs and Facies

Logs from all described wells were analyzed to determine if a correlation exists between the grainstone and packstone/wackestone facies and the log responses. Inspection of the logs indicates no consistent pattern for identifying facies in wells utilizing logs alone. For this analysis, well logs were correlated by matching grainstone/packstone unit tops picked on logs with the tops of the described wells. The gamma ray values change inconsistently across facies boundaries; for example, in well 13510, the gamma ray log shows little change in value in the Smackover Formation grainstone/packstone unit (Fig. 20). In well 13472 the gamma ray values are more variable (Fig. 21). There is no common pattern in the gamma ray values within grainstone facies from well to well, making a facies determination utilizing only the gamma ray curves inconclusive.

Neutron porosity (NPHI) and density porosity (DPHI) logs have a greater resolution than the gamma ray logs and show more variation in the grainstone/packstone unit. Typically the NPHI and DPHI logs track each other closely (Fig. 22). When compared to the core description, the log responses are minimal and appear to lag the facies changes by inches. Unfortunately, since many transitions between facies are gradual and are only a few inches thick as well as varying significantly between wells, it is difficult to interpret where a facies would start and end with logs alone (Fig. 20).

Other logs such as the spontaneous potential (SP) or caliper (CALI) logs also did not indicate a useful pattern in delineating facies in the grainstone unit (Figs. 20 and 21).

3.3.2 Log Porosity Correlation to Core Reports and Thin Sections

The logs were analyzed and compared to measured porosity from core analysis as well as with the estimated porosity from thin sections. Synthetic logs were created utilizing depth and core porosity data (Fig. 23). The core log was then depth shifted to better match with the porosity log values. The three porosity values often correlated closely. The core samples were taken in intervals of less than 6 in, which is also the vertical resolution of DPHI logs after processing. NPHI resolution can be even finer. However, because of the slight variations, the small and rapid facies changes would be difficult to accurately interpret and map field wide utilizing logs alone (Figs. 23 and 24)

13510

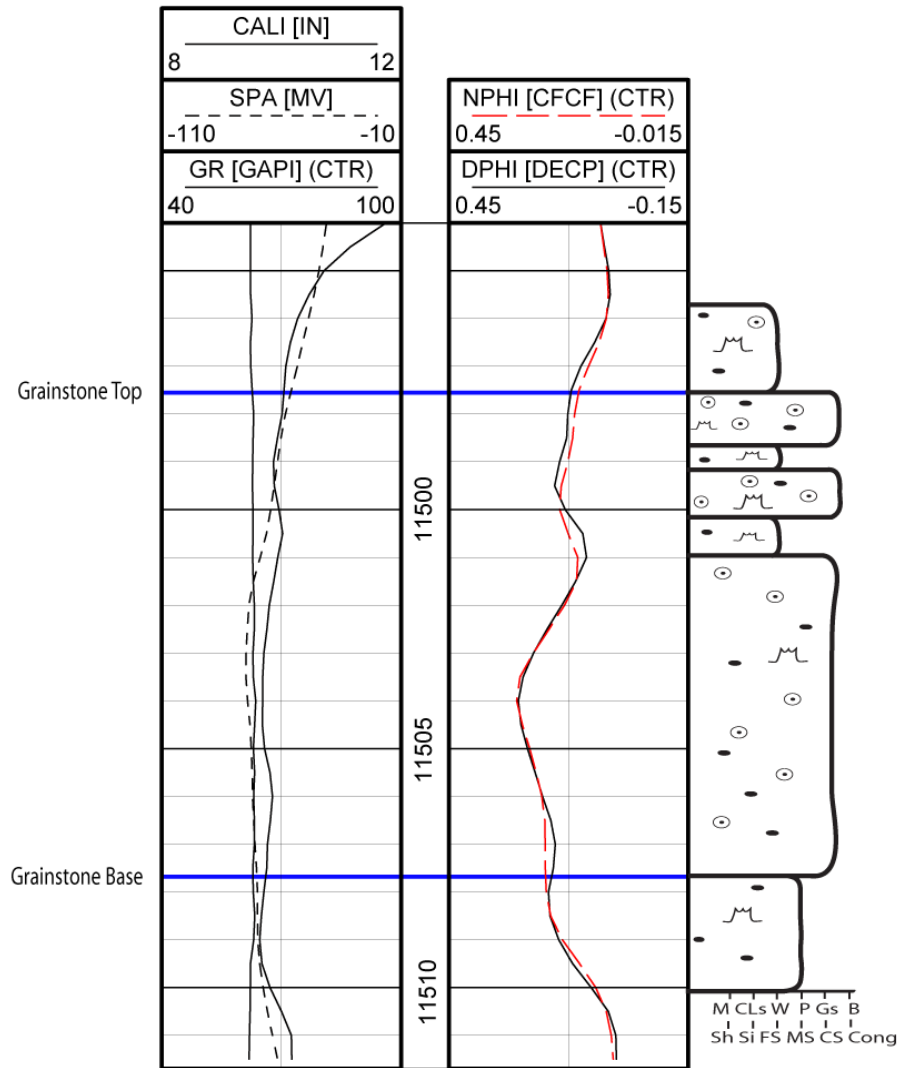


Figure 20. Logs from well 13510 with core description. Even with a reduced gamma ray scale of 40 to 100 GAPI there are no obvious deviations indicating a change associated with facies. The gamma ray log does not have the resolution to differentiate the rapid facies changes in the grainstone/packstone unit. The porosity logs generally record higher values in the grainstone facies. However, with small facies changes (such as the top ooid grainstones in well 13510) even utilizing porosity logs as a facies indicator becomes inconsistent.

13472

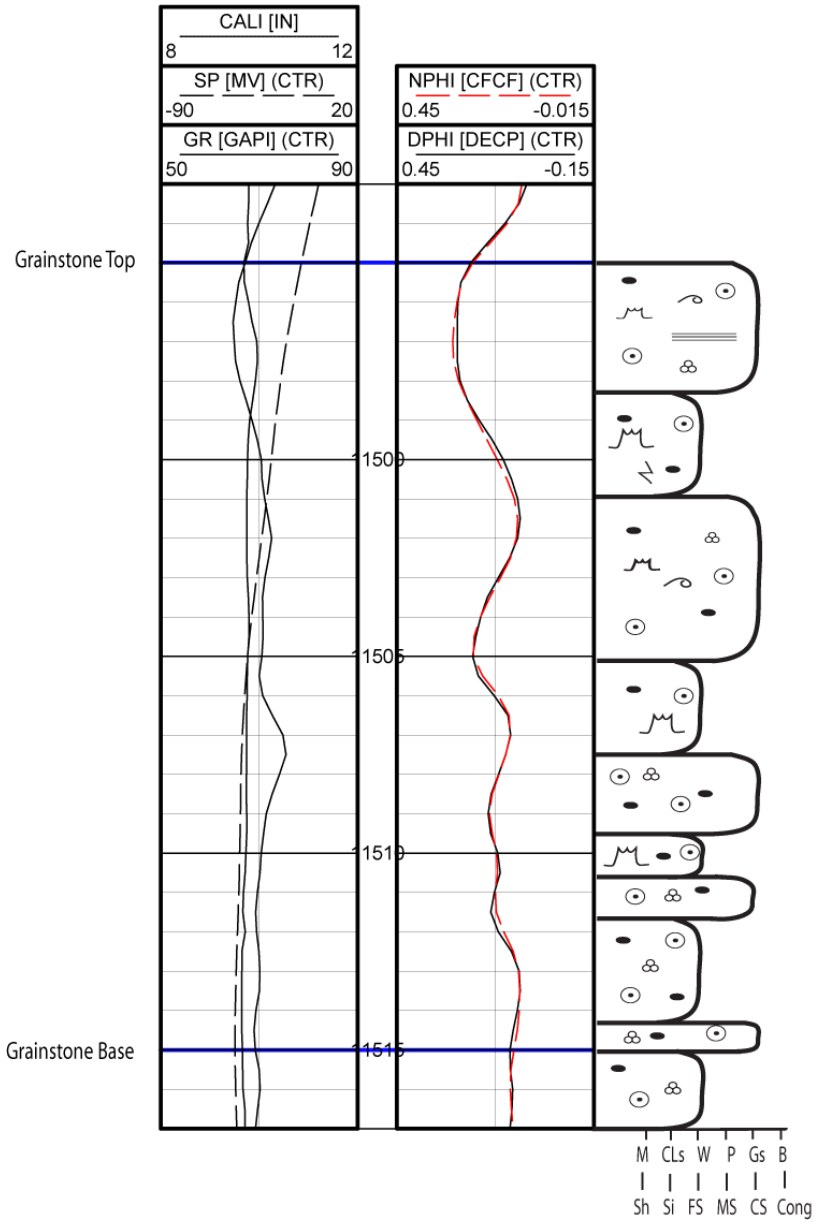


Figure 21. Well logs from 13472 with core description. Although the gamma ray shows more deflection than in well 13510, it does not correlate with the facies changes. The porosity logs do record higher values that initially correspond with upper grainstone facies. However, farther down section where the changes are more rapid, the log responses do not match the facies type.

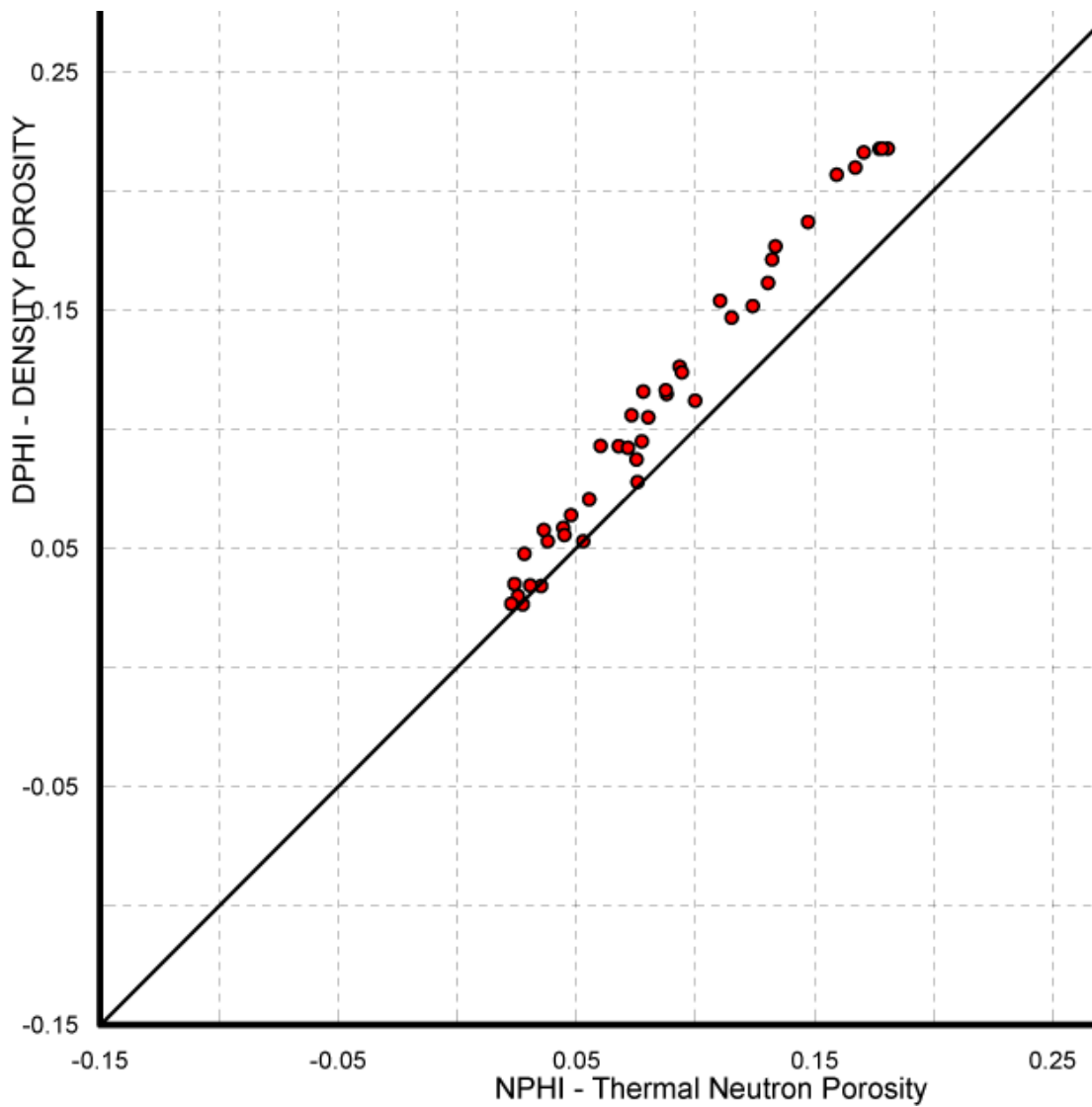


Figure 22. Cross plot of neutron and density porosity log values in the grainstone/packstone unit of Well 11963. The two logs have similar values, varying only slightly. With the addition of a trend line it is apparent that there is a small tendency towards a higher DPHI. This is a common trend in all described wells. The higher DPHI is likely due to the influence of the less dense siliciclastic grains affecting the density readings on a limestone scale. Also, NPHI logs are more accurate at lower porosities, which would account for why the NPHI values are closer the DPHI values as porosity decreases.

14155

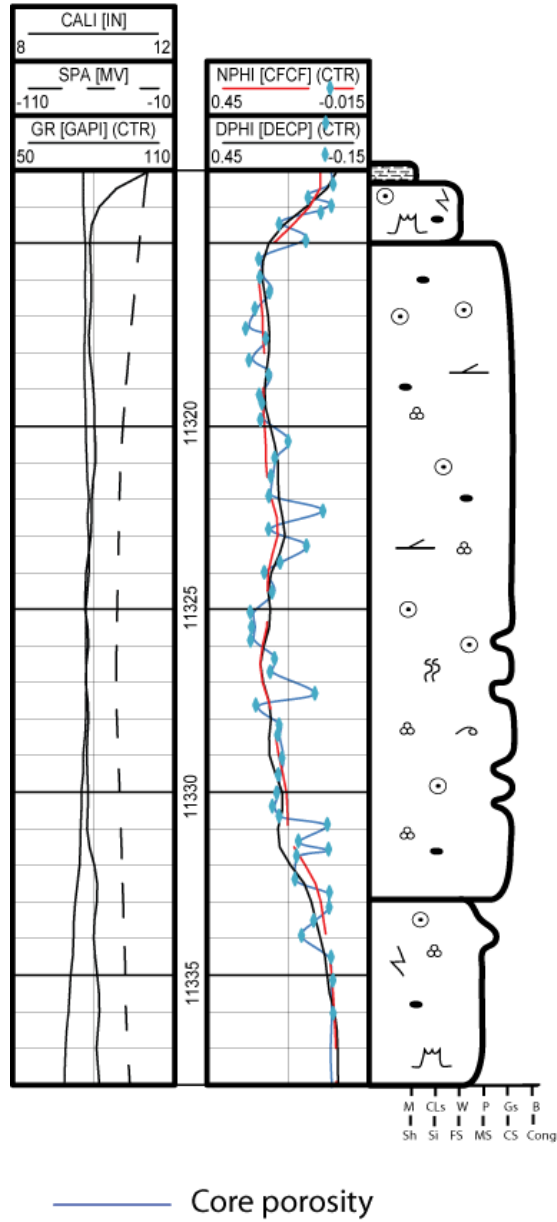


Figure 23. Well 14155 logs with synthetic core porosity trace. The NPHI and DPHI follow core porosity with some variation. The logs commonly overestimate the porosity rather than underestimate porosity. This is likely due to the resolution rather than an effect of lithology.

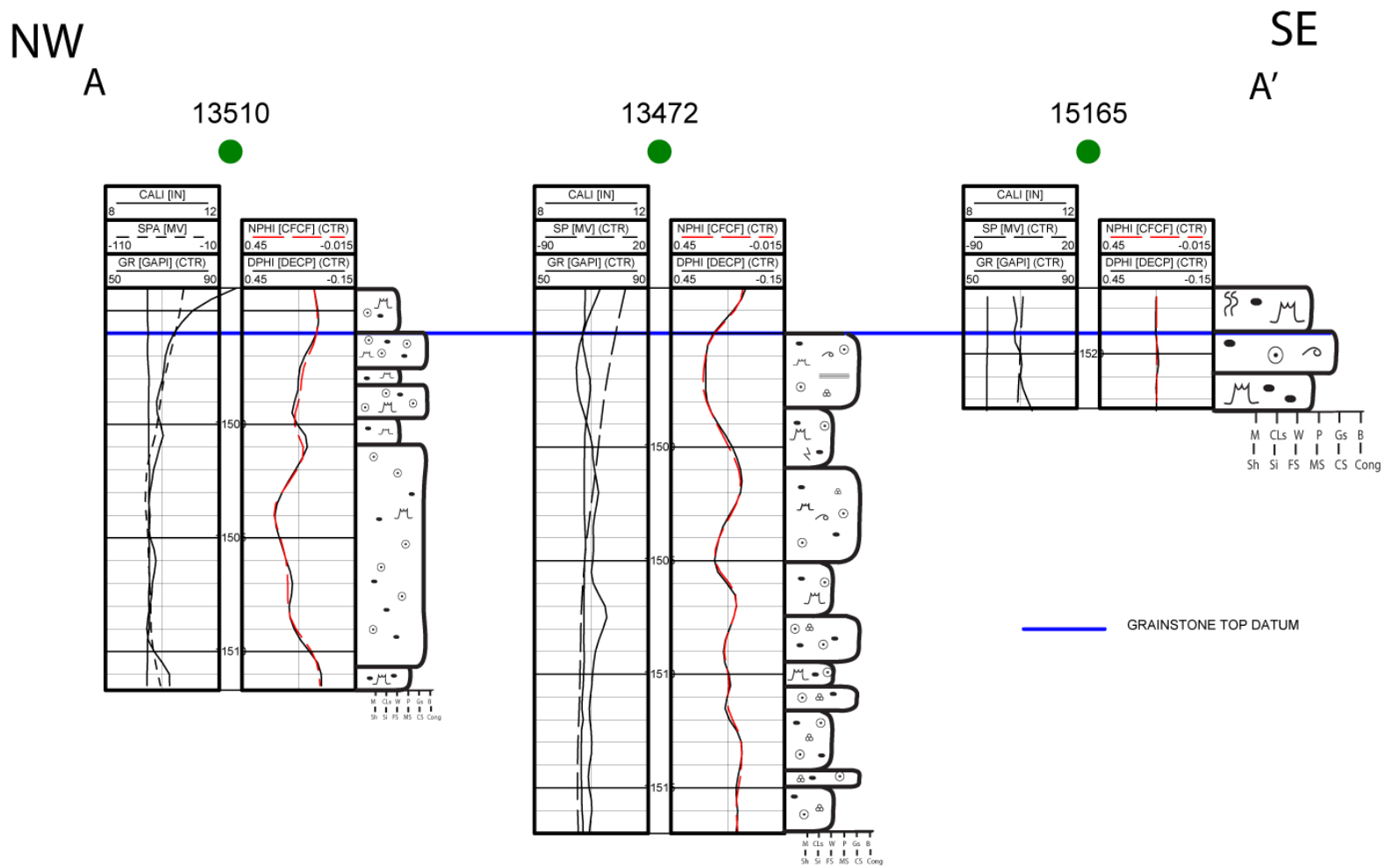


Figure 24. Stratigraphic dip cross-section A-A' (location on Fig. 1) illustrating the difficulty of delineating facies with logs alone.

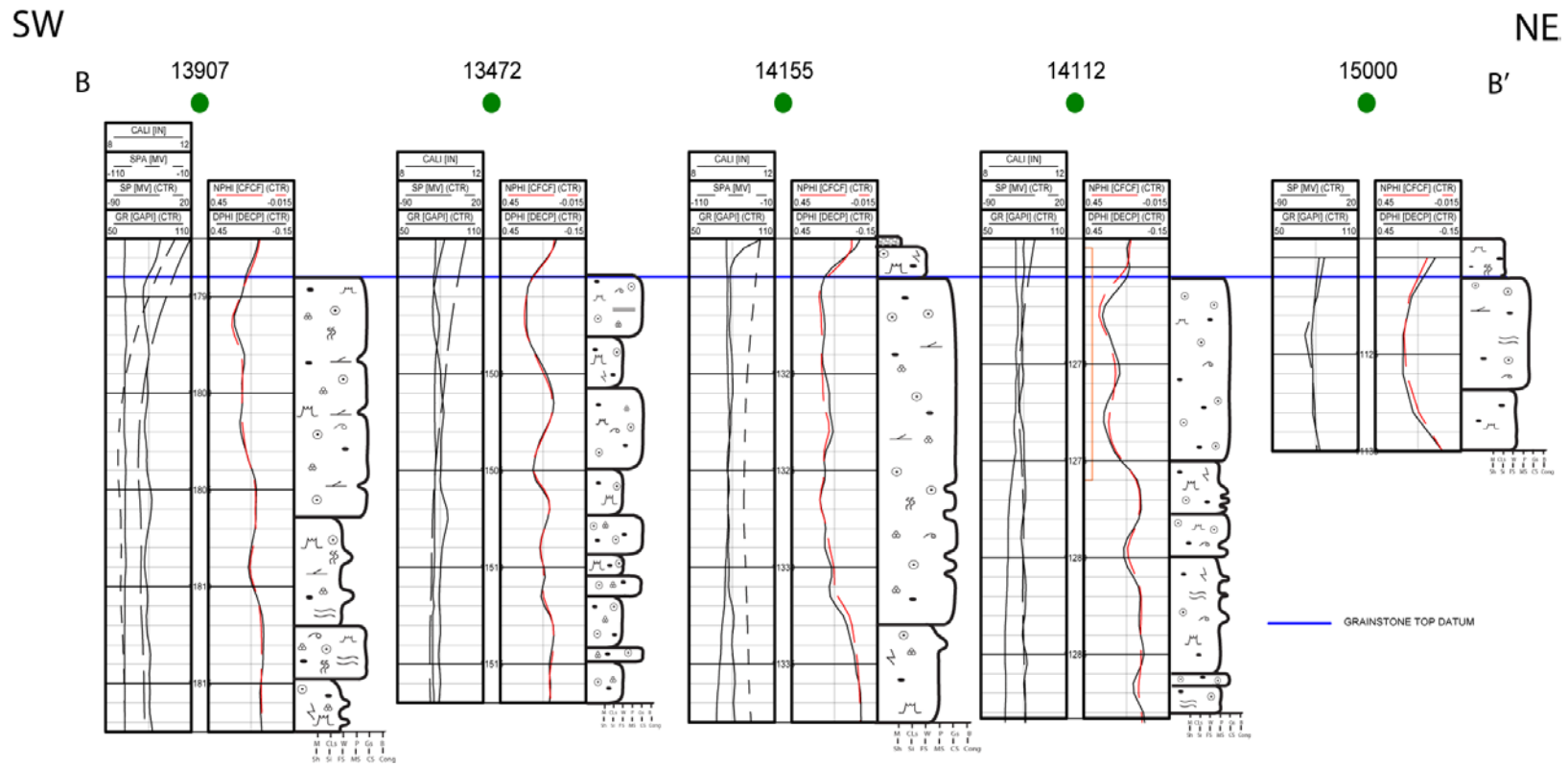


Figure 25. Stratigraphic strike cross-section B-B' (location on Fig. 1) illustrating not only the difficulty of using solely logs to interpret facies, but the number of facies changes throughout the field.

4. DISCUSSION

4.1 Production

Oil production continues to increase in LCCF since the field came on production in November 1994. The field operated with one well until 2000; today there are about 100 producing wells. In 2007, operators began gas injection in two wells in the southwest part of the field with an additional well converted to gas injection in mid 2011 (Fig. 1). The gas injection had a significant impact on the surrounding wells. In well 13907, production went from 14,504 bbls in 2007 to 31,177 bbls in 2009. The field has steadily been increasing oil production, producing over 2.4 million bbls per year for the past four years. Gas production continues to increase as well; in 2011 the field produced over 3.2 million mcf. All production values are from the Alabama Oil and Gas Board online database collected summer 2012.

The last three years of oil production values vary significantly across the field between wells in close proximity (Fig. 26). Since production is commingled in most wells it is difficult to accurately determine which reservoir is contributing the most. A select few wells produce solely from the grainstone reservoir; of the wells described, eight wells (11963, 13472, 13907, 14155, 14646-B, 15000, 15165, and 15614-B-1) report production only from the grainstone. Five additional wells (13176, 13177, 14358, 14270, and 14692) with production only from the grainstone reservoir were also utilized (Fig. 27).

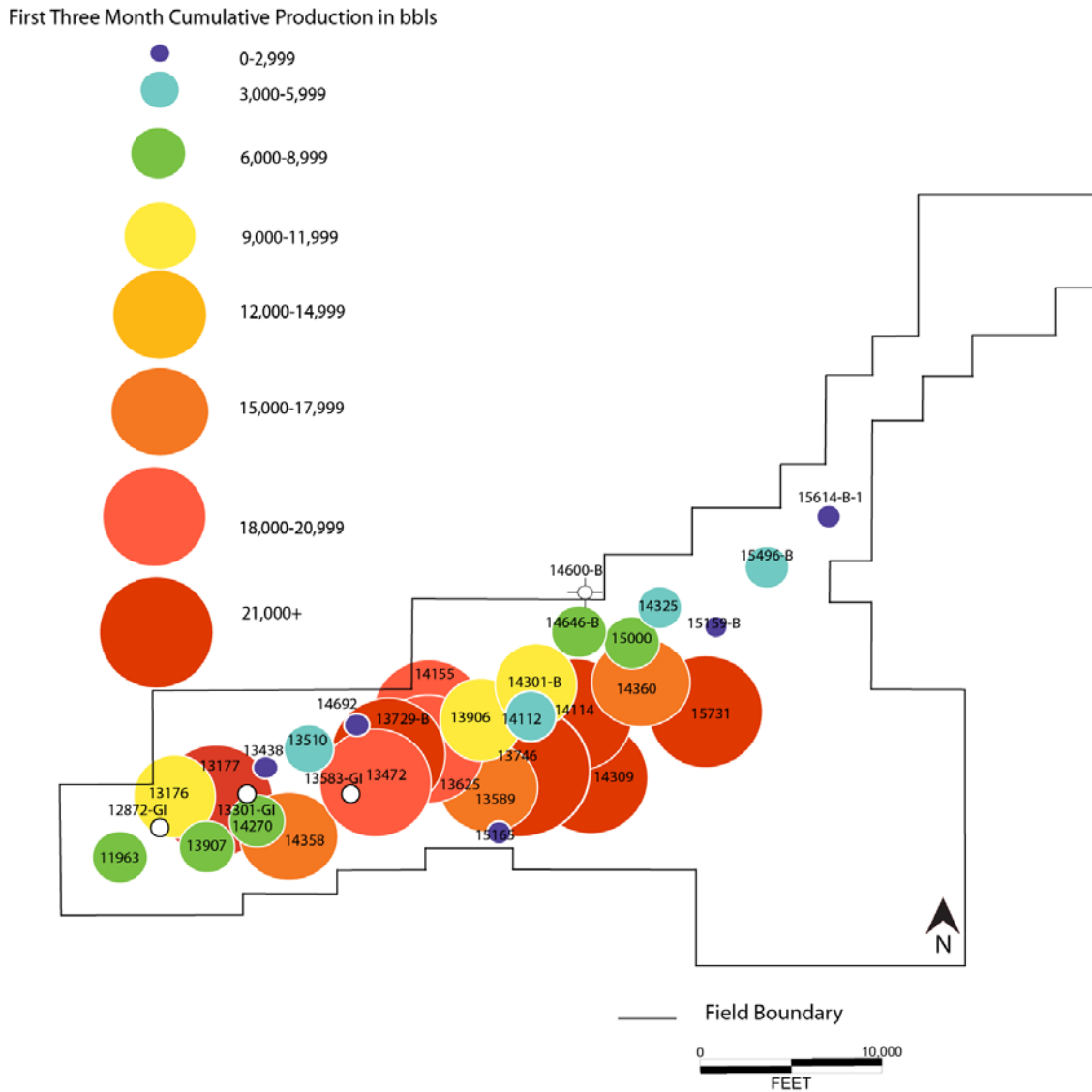


Figure 26. First three month cumulative oil production from selected wells. Production is extremely varied across the field. Production includes commingled wells.

First Three Month Cumulative Production in bbls

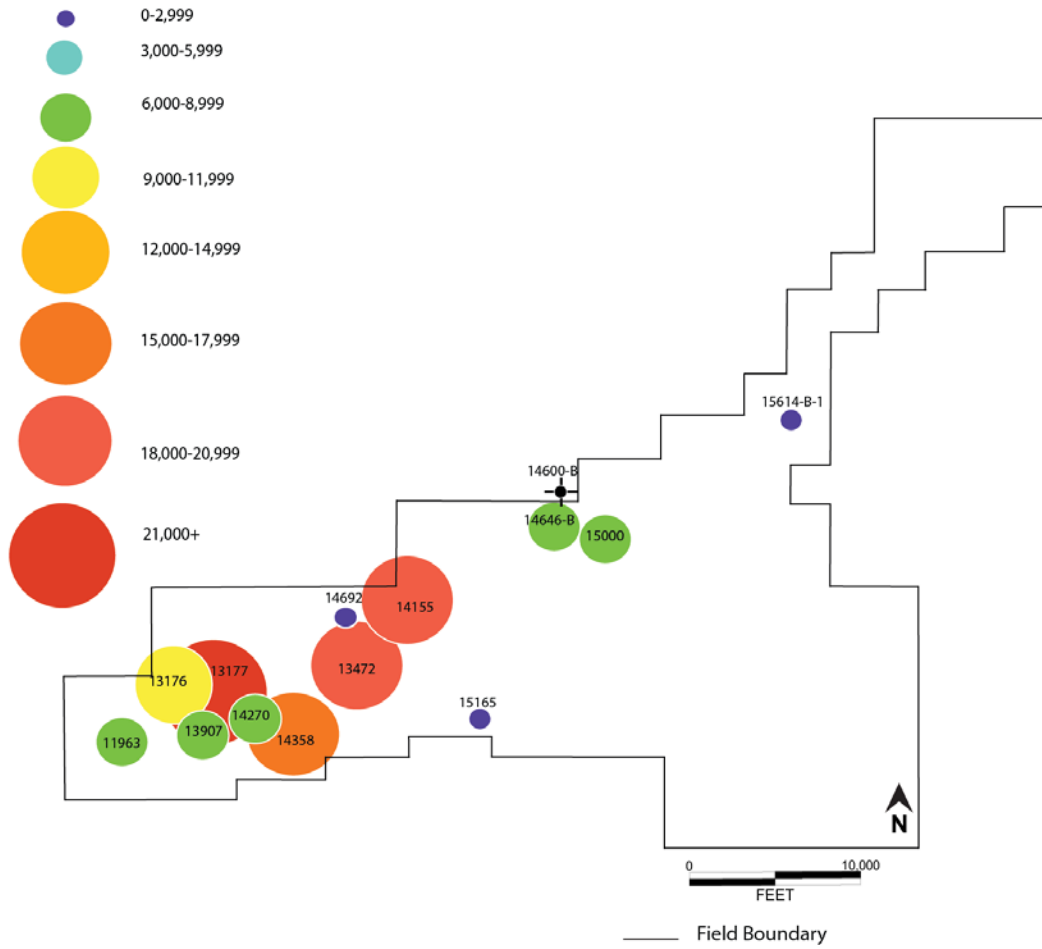


Figure 27. First three month cumulative oil production from wells that only produce from the upper reservoir.

4.1.1 Correlation Between Oil Production and Facies Changes

There is no correlation between the number of facies in core and the production rates of the well (Fig. 28). For example, wells 13472 and 14155 both have similar production values for the first three months of production however well 13472 has five separate grainstone facies, and well 14155 has only a single grainstone facies, both have approximately 20 feet of cumulative grainstone facies thickness. Also, wells with the same number of grainstone facies can have varying production values. For example wells 14155 and 15165 both have a single grainstone facies but produce at very different rates; well 14155 has high production values, whereas well 15165 has much poorer production.

The significant differences between the singular grainstone facies of wells 14155 and 15165 are the porosity characteristics and the thickness of grainstone facies within the grainstone unit. Thin sections and core reports agree that well 14155 has higher grainstone porosity, above 25% in some areas. Well 15165, however, has small vuggy porosity that averages only 5%. Well 14155 also has nearly ten times the amount of grainstone than occurs in well 15165 (Fig. 29).

First Three Month Cumulative Production in bbls

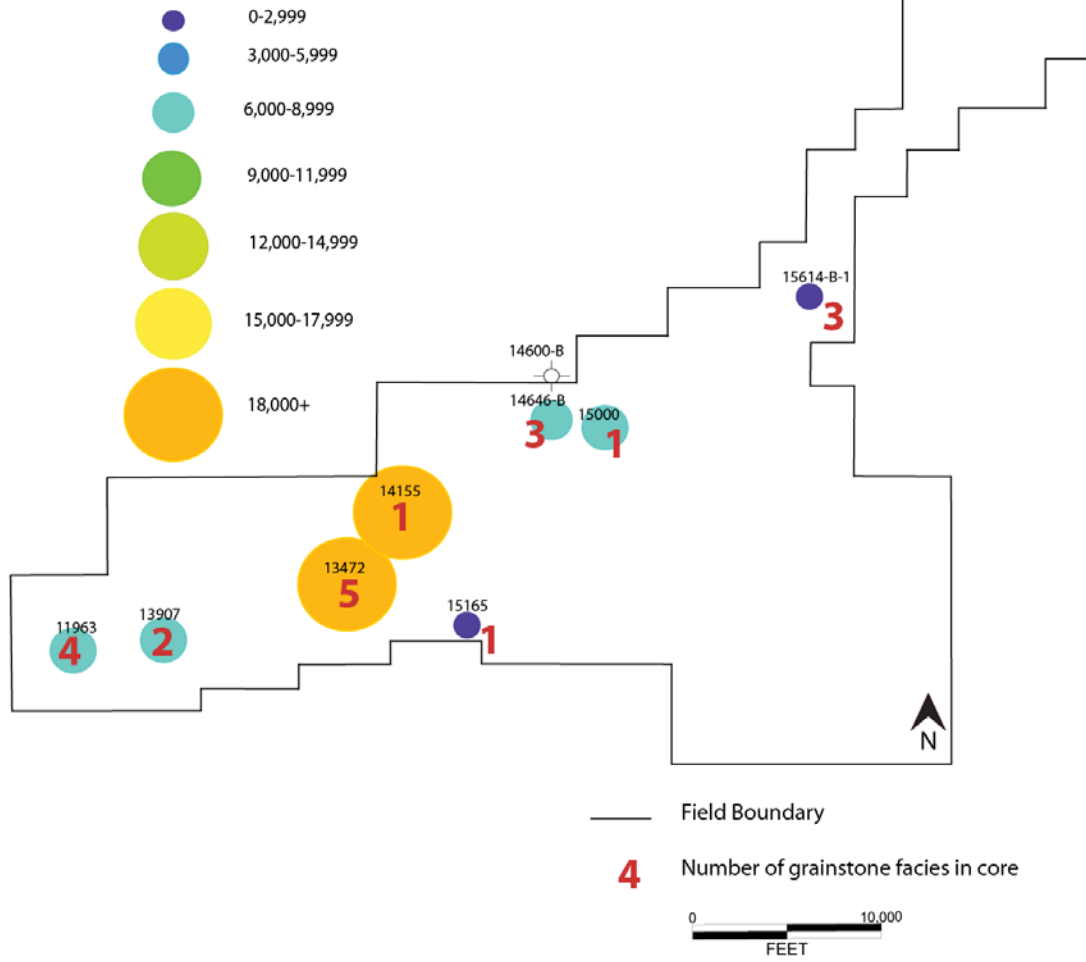


Figure 28. First three month cumulative oil production in wells with described facies changes that are reported to produce only from the upper reservoir. There is no clear trend between the number of facies changes and production values.

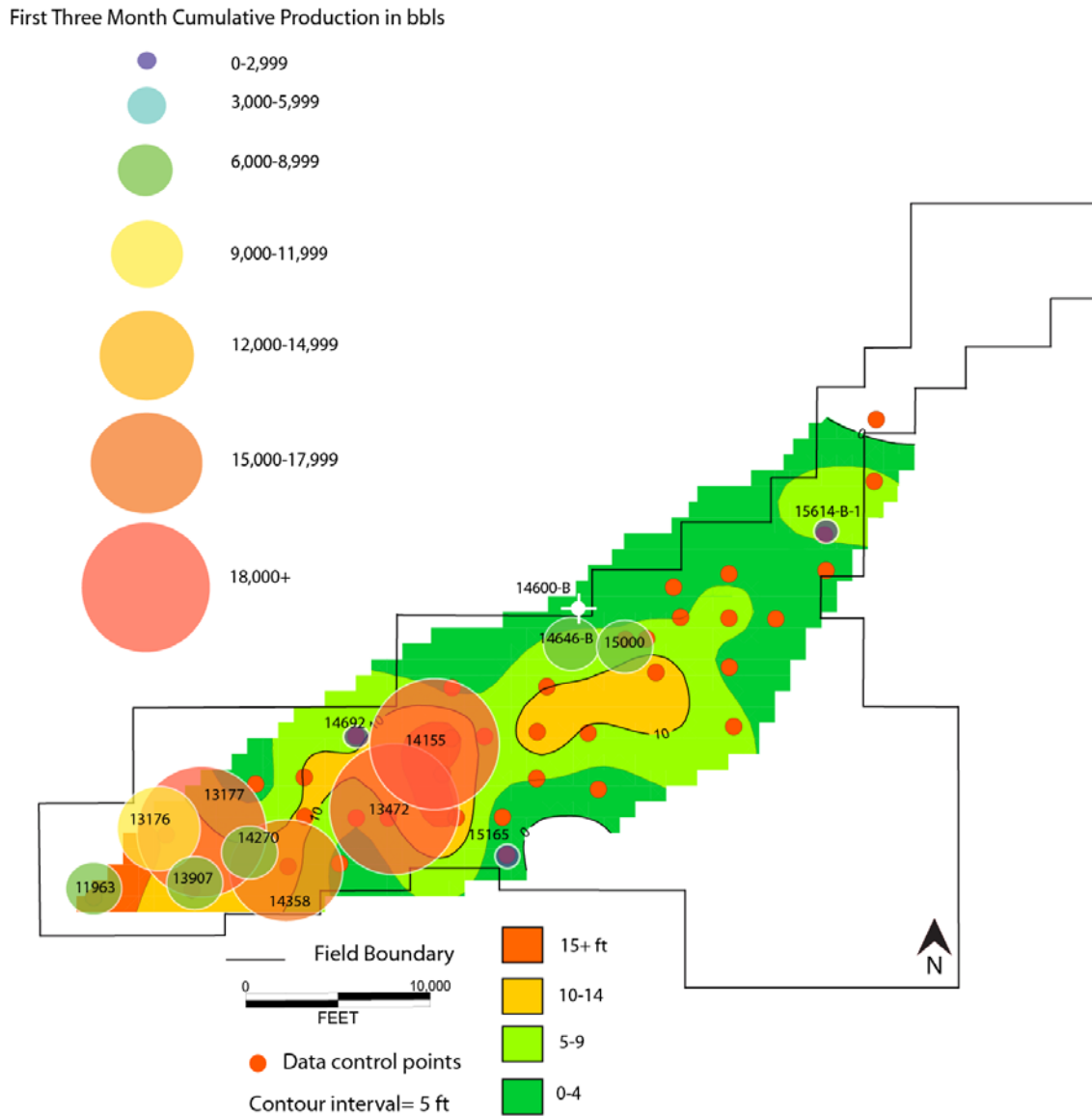


Figure 29. First three month cumulative oil production from wells that produce only from the upper grainstone/packstone reservoir superimposed on the cumulative grainstone facies isopach. Production increases to the southwest where the grainstone facies is thickest. Data control points are wells that have values from cumulative grainstone facies thickness.

4.1.2 Correlation Between Oil Production and Porosity Type

The effect that porosity type has on production is difficult to determine with the wells producing solely from the grainstone reservoir; ten of the twelve wells mainly have vuggy porosity and their first three month cumulative production varies from 1,549 bbls to 22,877 bbls (Fig. 30). The two wells that produce mainly from moldic porosity, 13176 and 13472, produced 9,967 and 18,192 bbls of oil over the first three months on production respectively. Utilizing the porosity and permeability crossplots from core plug analysis and separating porosity type into pore sizes indicates that larger pores have better porosity values and better permeability values (Fig.17). Production may not be significantly affected by distinguishing between moldic and vuggy porosity because by nature they are both voids that may or may not be interconnected and therefore behave very similarly. In a permeability and porosity crossplot it is clear that these types of porosities have similar values. Trend lines are steeper in moldic porosity types indicating that moldic porosity/permeability values are slightly more variable (Fig. 31). The value of average grainstone porosity does not have a strong influence on production (Fig. 32).

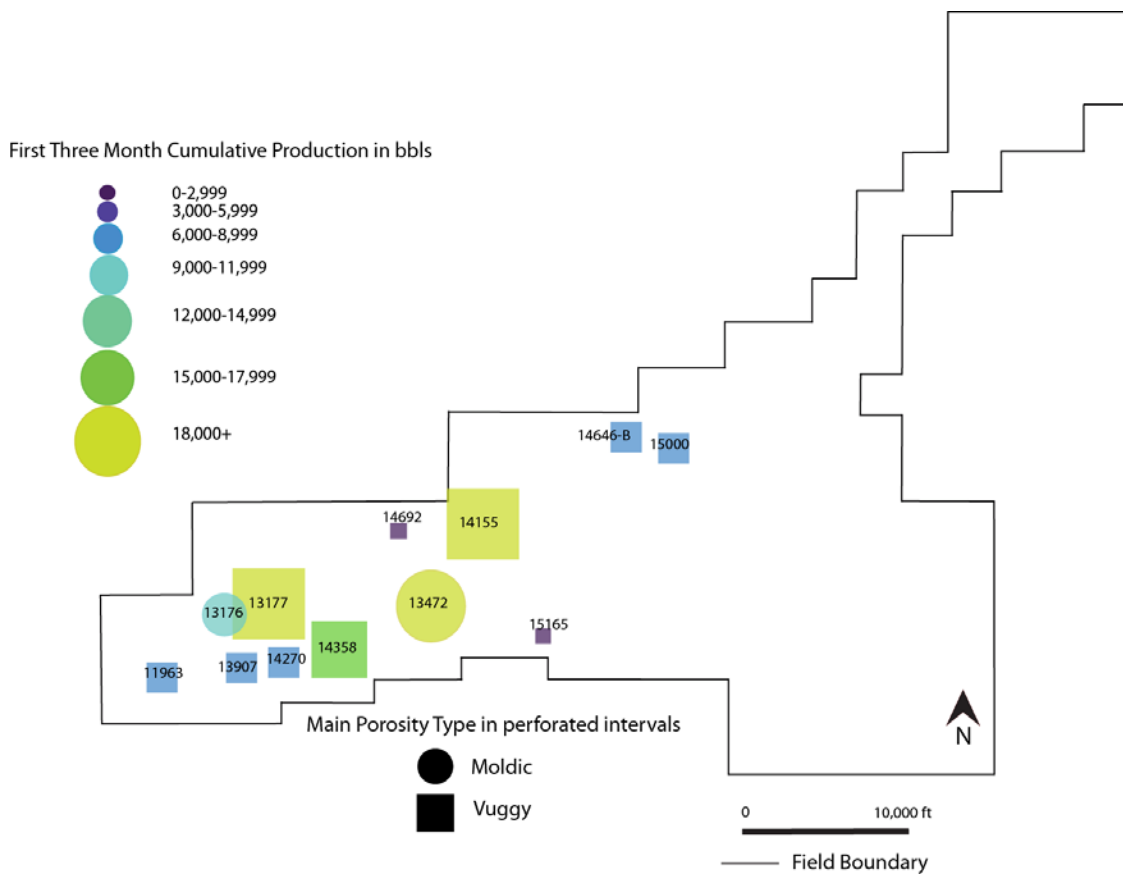


Figure 30. First three month cumulative oil production values from wells that produce only from the upper grainstone/packstone reservoir. The shape of the production bubbles indicates the primary type of porosity. Porosity types from core reports were used in order to consistently define the perforate intervals. The data control points are wells that have values from cumulative grainstone facies thickness.

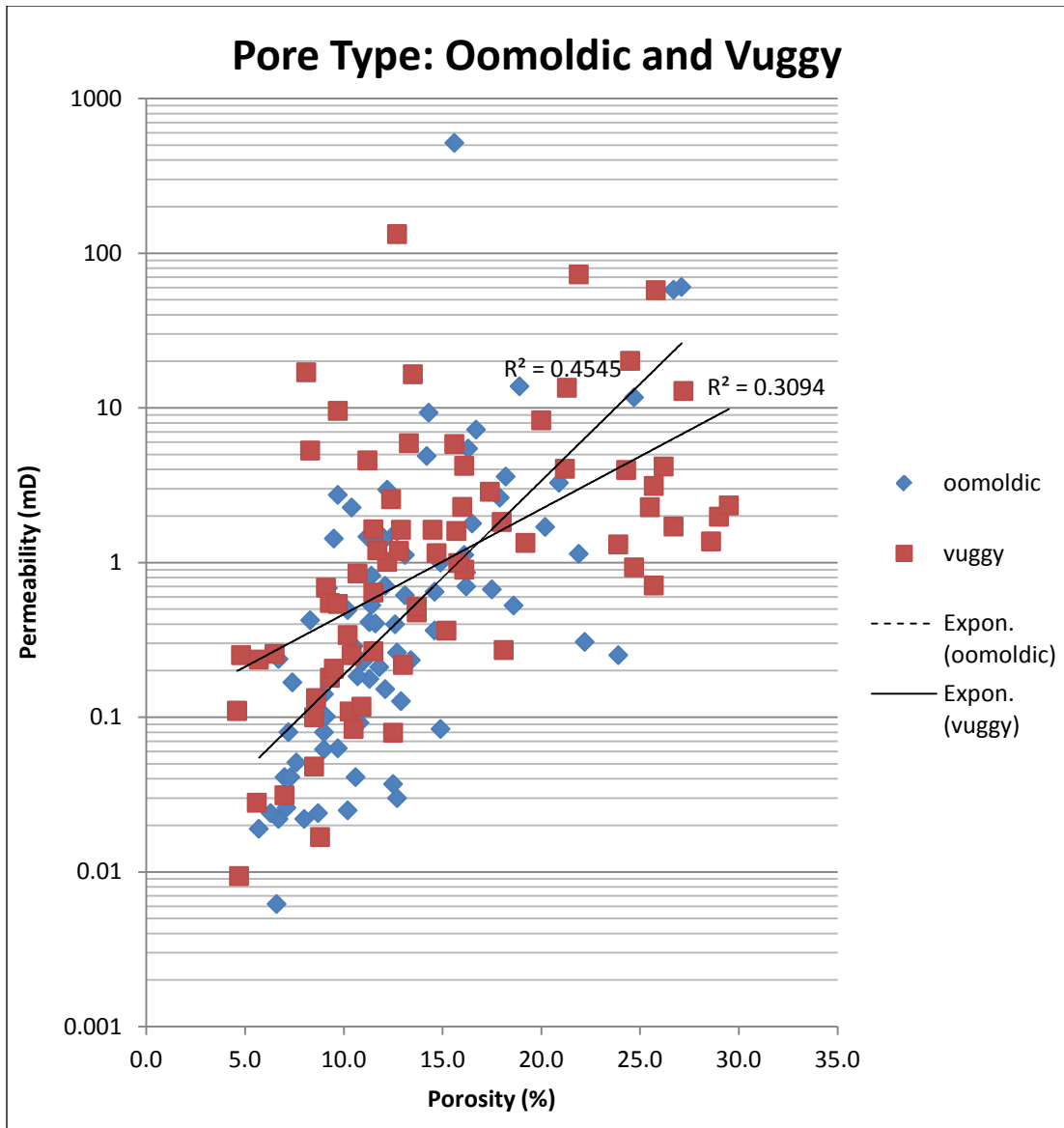


Figure 31. The porosity and permeability crossplot indicates similar ranges for both moldic and vuggy pores. Data points were taken from core analysis reports from a representative selection of wells in the grainstone/packstone unit. Trend lines indicate that moldic pore types are slightly more variable than vuggy pores.

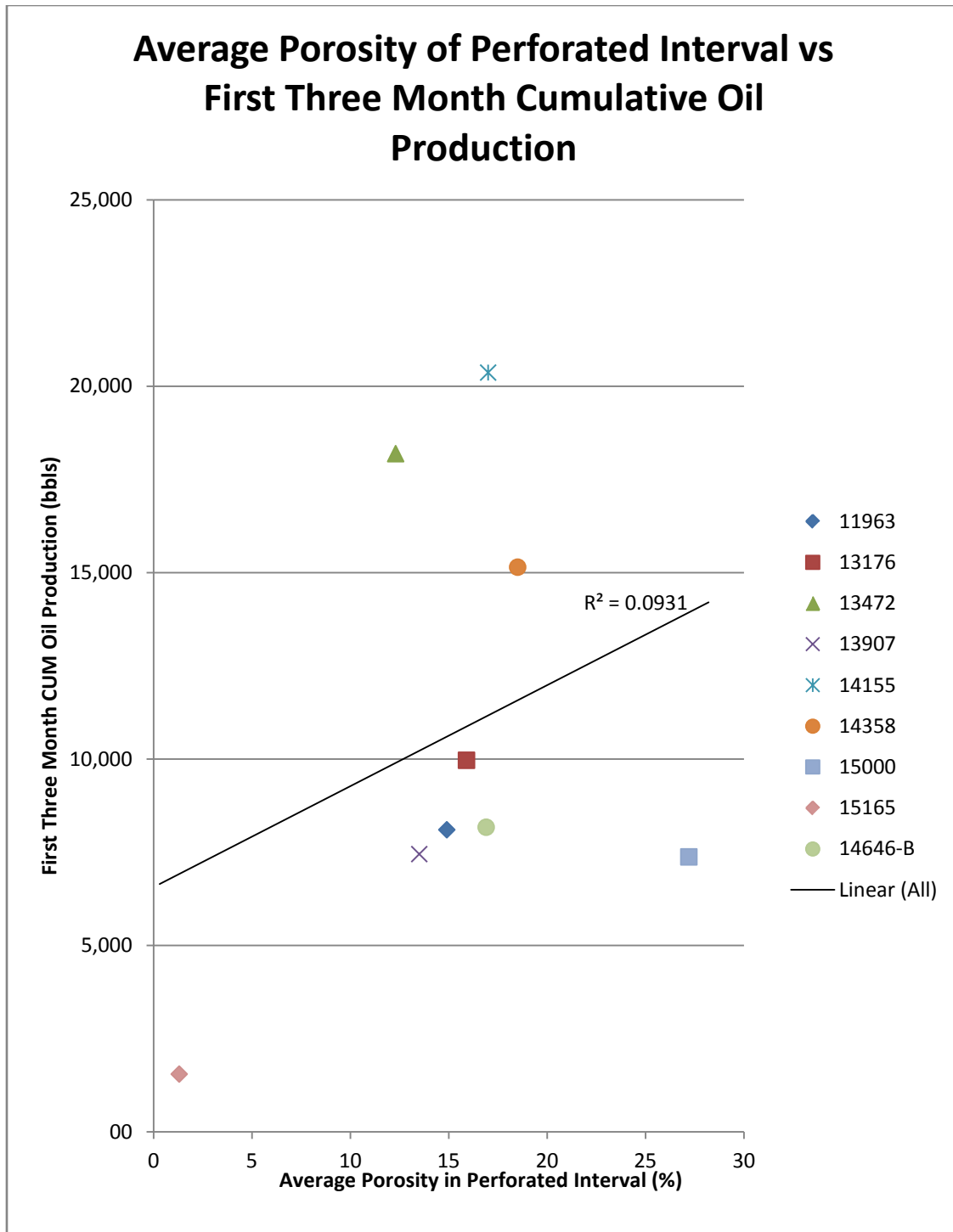


Figure 32. The average porosity of the perforated interval ranges from 1.3% in well 15165 to 27.2 % in well 15000. The average porosity values do not indicate any trend in production.

4.1.3 Correlation Between Oil Production and Grainstone Facies Thickness

There is a strong correlation in wells with thicker intervals of grainstone facies within the grainstone/packstone unit and higher production values (Fig. 33 and 34). This trend is consistent regardless of changing porosity types. The primary oomoldic or vuggy porosity types within the upper reservoir both behave similarly and do not appear to affect production independently, the most important factor in predicting production is cumulative grainstone facies thickness. Packstone/wackestone facies within the grainstone unit were subtracted from the unit thickness to obtain the cumulative grainstone thickness. The wells with the thicker cumulative grainstone facies are located in the southwest part of the field and follow an elongate trend, which extends into the south central portion of the field. The farthest southwest wells have the highest production values. This elongate trend is consistent with a shoal environment in which the thicker build ups are exposed to higher energy waters, the higher energy waters deter microbial growth and increase ooid content allowing for the accumulation of well sorted ooid grainstones (Mancini, personal correspondence). The grainstones have consistently higher porosity and permeability (Fig. 35).

Although the ooid grainstone/packstone unit isopach map indicates that the unit thickens to the southwest, multiple dry holes were drilled outside of the field along the strike of the trend (Fig. 36). No data were available to estimate the thickness of their grainstone/packstone units. The peloid-ooid grainstones were deposited in a formed in a relatively lower energy shoal environment (Benson, 1988). A discontinuous elongate

shoal form could mean that the grainstone shoals terminated at the edge of the current field boundary due to natural depositional controls such as an energy deficient restricted environment (Ridgway, 2010). Since extending the field along trend has proven unsuccessful, secondary recovery has become necessary.

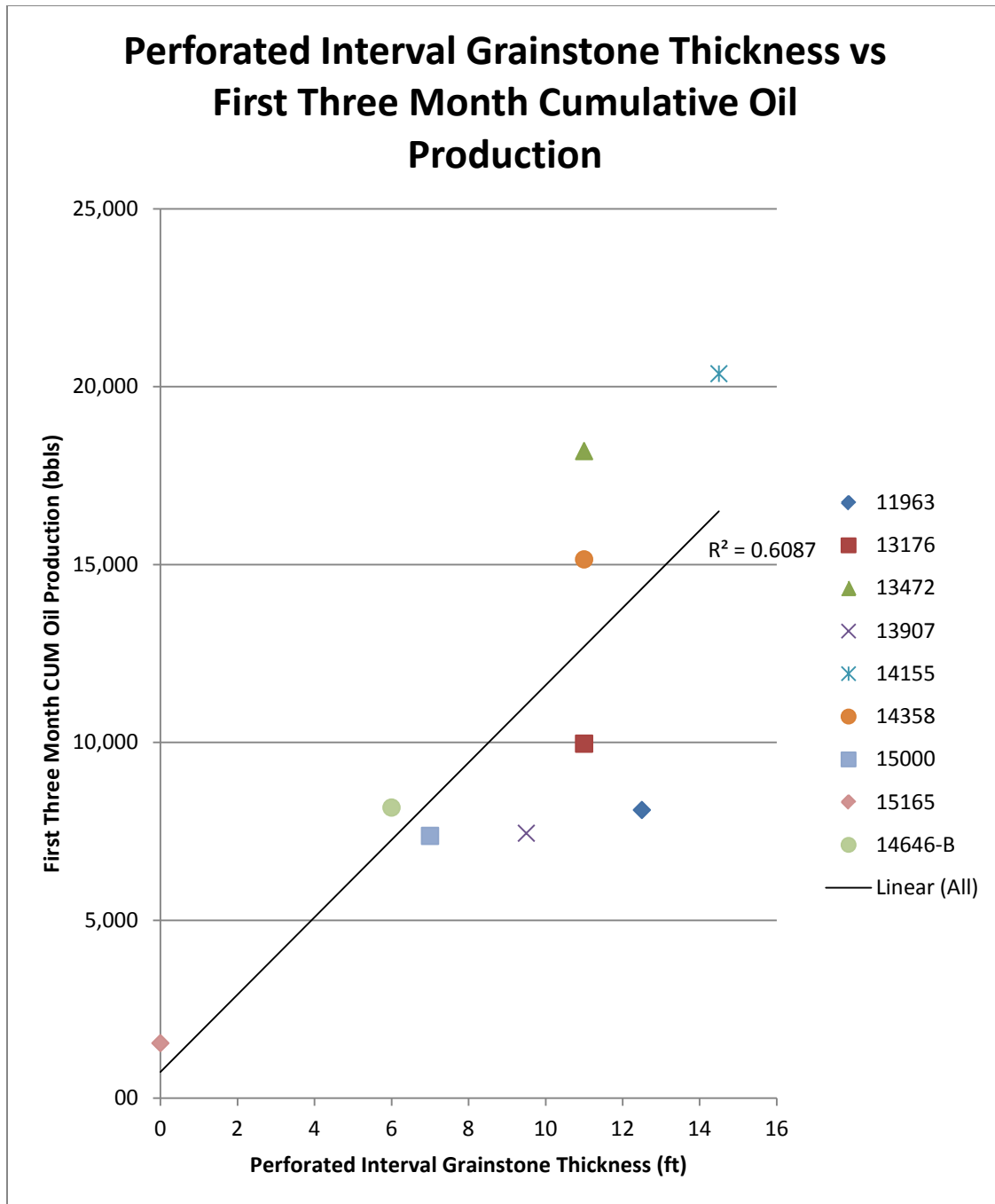


Figure 33. There is a direct correlation between three year cumulative oil production and perforated grainstone facies thickness. Wells used to create this chart were described from this study with the addition of wells 13176 and 14358 from Ridgway (2010).

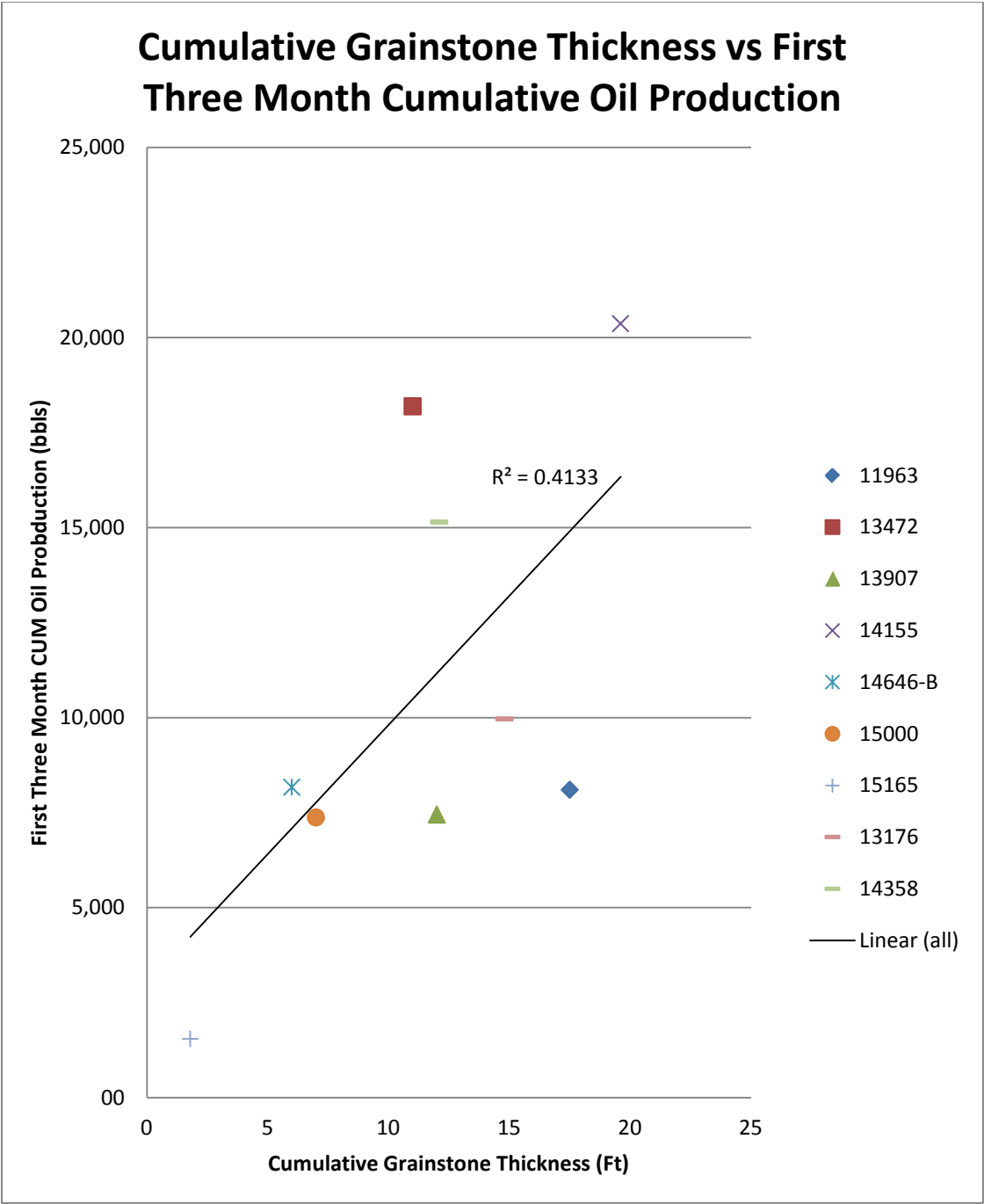


Figure 34. An even closer correlation is seen with the cumulative amount of grainstone facies and the production values from wells that produce from the upper reservoir. Wells used to create this chart were described from this study with the addition of wells 13176 and 14358 from Ridgway (2010).

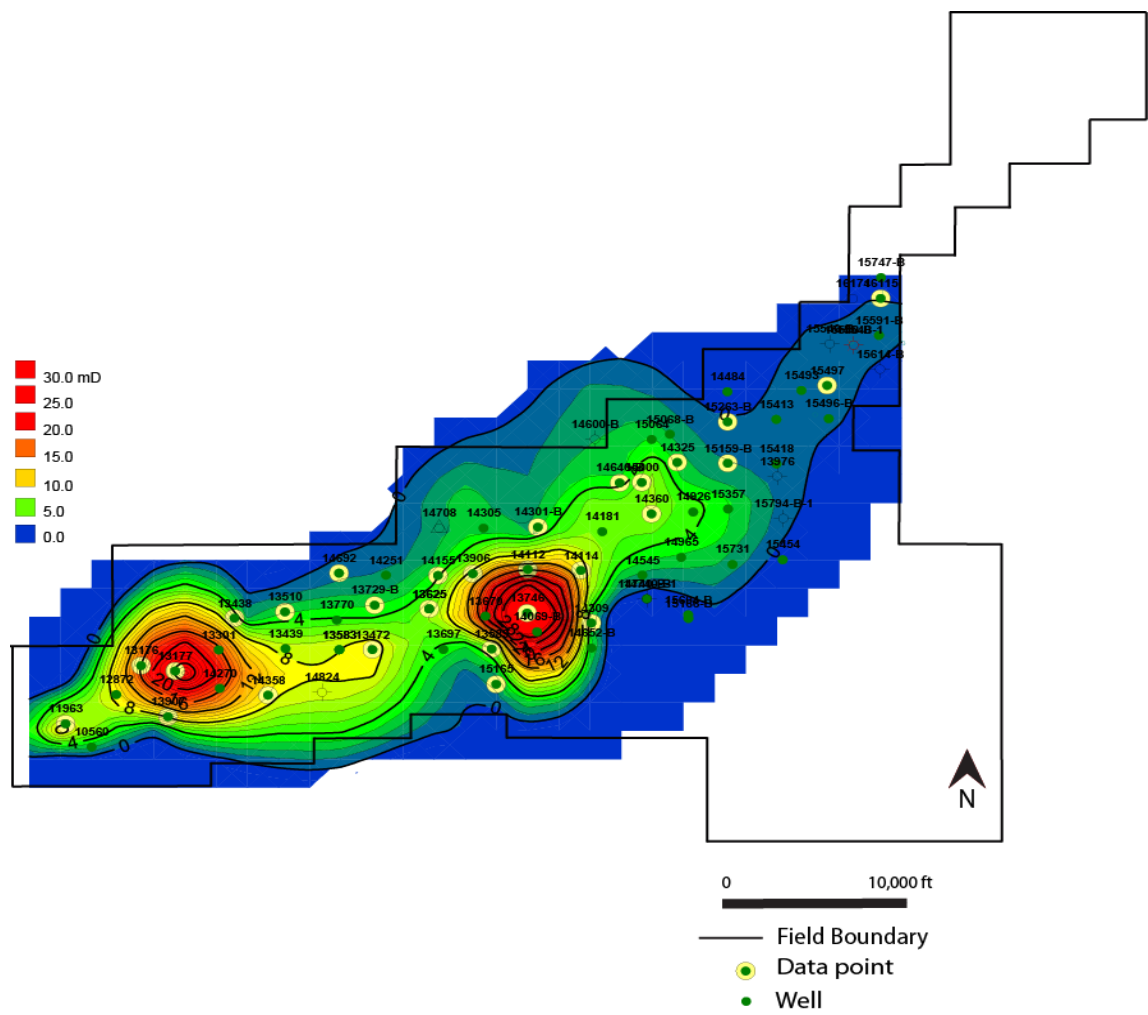


Figure 35. Map of average grainstone unit permeability from core analysis. Areas of higher permeability are in areas of greater grainstone facies accumulation (Fig. 29).

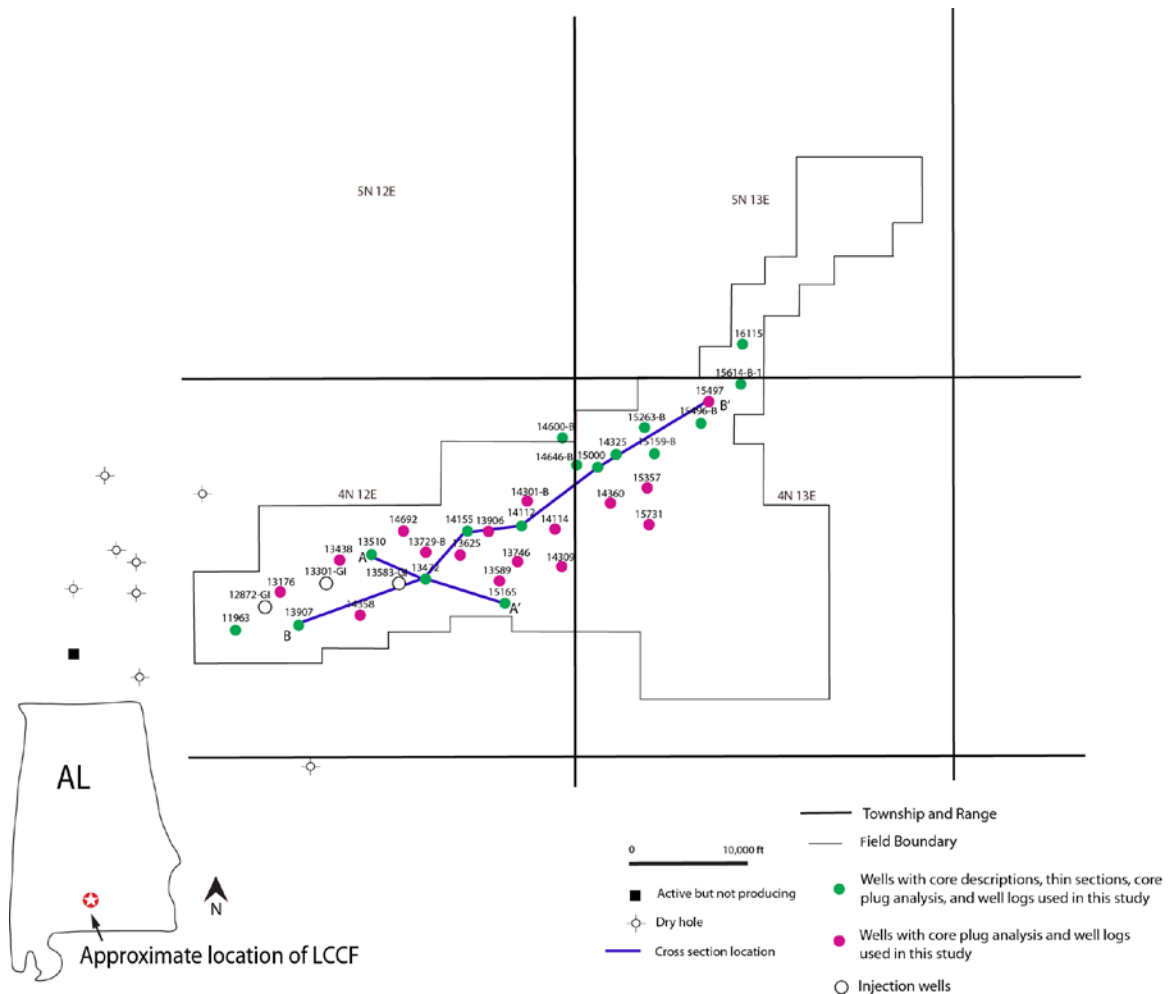


Figure 36. Location of dry wells with respect to Little Cedar Creek Field. It is possible that the thick grainstone facies trend within the grainstone/packstone unit did not extend far past the last producing grainstone well (11963) due to the termination of the ooid shoals at the field boundary leading to the dry holes past the boundary.

4.1.4 Implications of Gas Injection for Oil Recovery

Currently there are three natural gas injection wells located in the southwestern part of the field (Fig. 1). The first two were converted from production in September 2007. At that time, well 12872 was producing approximately 20,000 bbls annually and well 13301 was producing more than 30,000 bbls annually. Both were producing the month before they were converted in September 2007. These wells were initially converted for pressure maintenance. In mid-2012 well 13583 also was converted to gas injection. Production in this well was declining and it was producing approximately 3,200-3,400 bbls a year for the three years prior to being converted to injection. It contains less than 6 ft of grainstone facies.

The effects of the injections are apparent in the surrounding wells with thicker grainstone facies. In well 13176 production had been steadily decreasing, then five months after injection began oil production picked up and in the first year production doubled and had more than quadrupled the pre-injection production by 2009. This well likely saw such a strong effect because it is situated between the two injectors. This is similar of well 13177, also located between the two injecting wells. Other nearby wells like 11963 and 13907 have seen a strong positive effect as well. However, nearby well 13438 contains only 2 ft of grainstone facies and has been following a steady decline in production regardless of its proximity to the injecting wells. While it appears that grainstone facies thickness does affect the efficacy of injection, it remains difficult to

predict the radius of influence that an injection well will have in these vuggy and moldic carbonate reservoirs.

Since LCCF is a petrophysically heterogeneous field due to the multiple facies and differential diagenesis, efforts of secondary recovery would likely be maximized by injecting gas into the thicker, generally more porous and permeable grainstones in the southwest sweeping the oil towards the northern portion of field where the grainstone is thin or non-existent. This not only would maximize overall reservoir recovery since this strategy begins at one end of the field and moves laterally, it would allow for increased oil production from current wells without having to drill new injectors or producers.

4.2 Modified Ahr Porosity Type

As a tool for mapping by porosity type, each thin section was classified (Fig. 37) using the modified Ahr porosity classification; (Ahr, 2008). The pore type in each sample was classified as a hybrid 1-B. Hybrid 1-B porosity occurs when the diagenetic features such as dissolution or recrystallization predominantly affect porosity but the original depositional texture is preserved. All samples have mainly moldic and vuggy porosity with interparticle porosity and a range of cementation, from none to complete. Molds range from less than 0.1 mm to slightly larger than 1 mm. Vugs range from approximately 0.1 mm to about 1 cm across. Primarily moldic porosity is specific to the thicker accumulations of grainstone because molds formed preferentially in the ooids and there are more ooids in the wells with thicker accumulations of grainstone

(Appendix A). All samples have well preserved depositional textures; in most samples of the ooid grainstone unit, the internal radial and concentric structure of the ooids can still be identified even when most of ooid is dissolved. The depositional intergranular porosity commonly is not well preserved being filled by rim cement, or recrystallized microsparry calcite. Larger pores are preferable to maintain good porosity, regardless of moldic, vuggy, or interparticle pore type. The progression of significant diagenesis with preserved original depositional texture is what distinguishes hybrid 1-B porosity. The goal of this genetic pore typing is to map areas of a field that have different pore types to aid in predicting other characteristics such as oil production. While this may be helpful in fields with a range of porosity types, all samples from across LCCF have similar porosity types and therefore would not benefit from mapping according to genetic pore type.

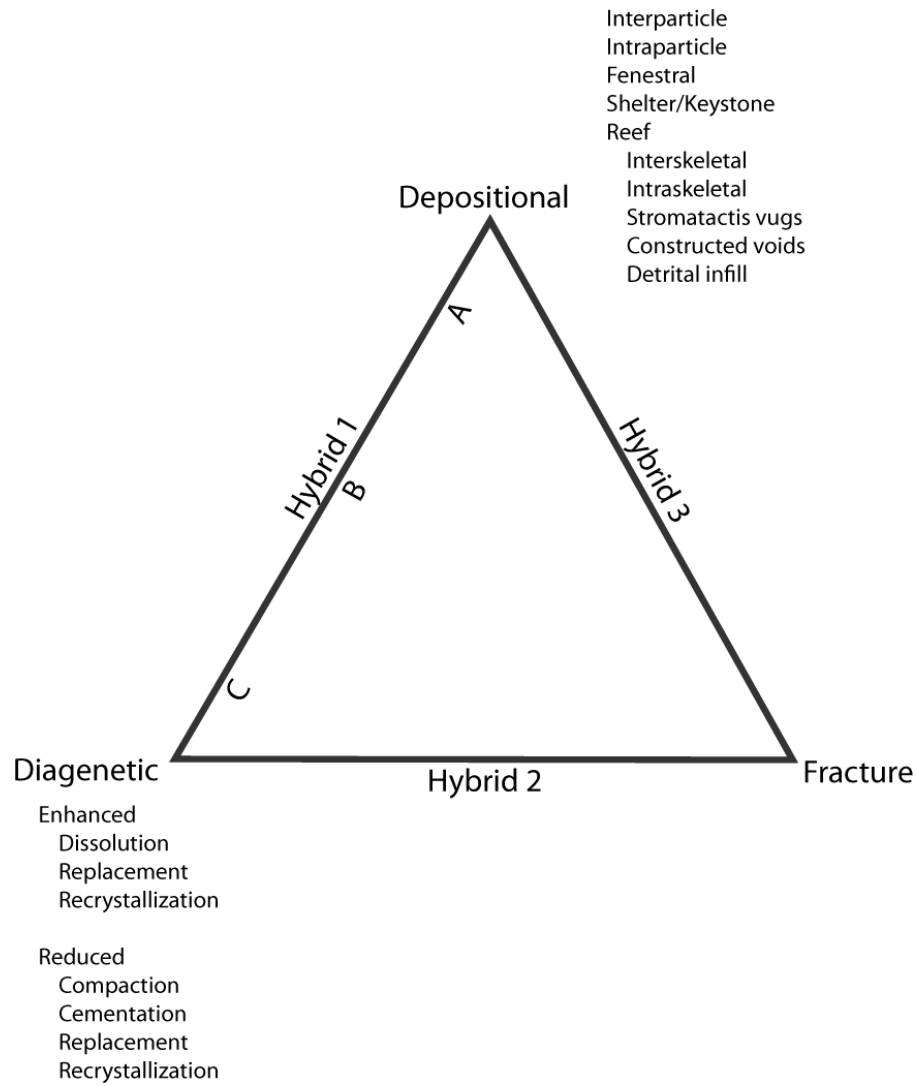


Figure 37. The modified Ahr (2008) porosity classification simplifies porosity types into three main categories, depositional, diagenetic, and fracture. Rocks can further be classified by hybrid type depending on the degree of influence the end members have on the main porosity characteristics. All thin section samples from the upper grainstone reservoir are classified as hybrid 1-B.

5. CONCLUSIONS

Petrophysical characteristics of the Smackover Formation peloid-oid grainstone/packstone unit at Little Cedar Creek Field, Conecuh County, Alabama, are highly variable and complex. The peloid-oid grainstone/packstone unit often consists of multiple rapid facies changes that cannot be laterally correlated. The lack of continuity does not allow for the prediction of flow paths in the grainstone/packstone unit utilizing these separate rock types. However, oil production shows that the most significant control on production is cumulative grainstone facies thickness and that it is not affected by the number of facies changes. Porosity is higher in the grainstone facies, averaging 17%, while the wackestone facies averages 5.6% porosity. In areas with thicker accumulations of grainstone facies both permeability and porosity values are higher. Thicker accumulations of grainstone formed shoals that were exposed to higher energies, this decreased microbial influence and enabled the formation of more ooid grains.

The two most common porosity types in the peloid-oid grainstone/packstone unit of the Smackover Formation are oomoldic and vuggy. Production does not favor one type of porosity over the other. Early rim cement formed in the phreatic zone creating a framework that preserved depositional porosity. Diagenesis occurred over six stages and included two significant dissolution events which created moldic and vuggy pores and four cementation stages, the most porosity reducing stage being the formation of microsparry calcite.

Thicker grainstones facies within the grainstone/packstone unit lead to better production because the grainstone facies has higher porosity and permeability. In order to maximize secondary recovery efforts, it would be beneficial to focus gas injection in the southwestern part of the field. The injected gas will be able to propagate through the higher porosity and permeability of the thicker grainstone units, sweeping the hydrocarbons up dip into nearby wells.

REFERENCES





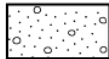

















- Ahr, W. M., 2008, *Geology of Carbonate Reservoirs the Identification, Description, and Characterization of Hydrocarbon Carbonate Rocks*, Wiley Publishing, Hoboken, N.J., p. 1-277
- Benson, D. J., 1988, Depositional History of the Smackover Formation in Southwest Alabama, *Gulf Coast Association of Geological Societies Transactions*, v. 38, p. 197-204.
- Geological Survey of Alabama State Oil and Gas Board, 2009, An Overview of the Little Cedar Creek Field Development, p. 1-2.
- Heydari, E., and Baria, L. R., 2005, A Microbial Smackover Formation and the Dual Reservoir-Seal System at the Little Cedar Creek Field in Conecuh County of Alabama, *Gulf Coast Association of Geological Societies Transactions*, v. 56, p. 294-320.
- Heydari, E., and Baria, L. R., 2006, Reservoir Characteristics of the Smackover Formation at the Little Cedar Creek Field, Conecuh County, Alabama, *Gulf Coast Association of Geological Societies Transactions*, v. 56, p. 238-289.
- Heydari, E., and Moore, C.H., 1993, Zonation and Geochemical Pattern of Burial Calcite Cements: Upper Smackover Formation, Clarke County, Mississippi, *Journal of Sedimentary Petrology*, v. 63, n. 1, p. 44-60
- Mancini, E. A., 2010, Jurassic Depositional Systems, Facies, and Reservoirs of the Northern Gulf of Mexico: *Gulf Coast Association of Geological Societies Transactions*, v. 60, p. 481-486.
- Mancini, E. A., Mink, R. M., Bearden, B. L., 1985, Upper Jurassic Norphlet Hydrocarbon Potential Along the Regional Peripheral Fault Trend in Mississippi, Alabama, and the Florida Panhandle, *Gulf Coast Association of Geological Societies Transactions*, v. 35, p. 225-232.

- Mancini, E. A., Puckett, T. M., Parcell, W. C., Panetta, B. J., 1999, Basin Analysis of the Mississippi Interior Salt Basin and Petroleum System Modeling of the Jurassic Smackover Formation, Eastern Gulf Coastal Plain, U.S. Department of Energy, Reports 1 & 2, p. 1-344.
- Mancini, E. A., Badali, M., Puckett, T. M., Llinas, J. C., Parcell, W. C., 2001, Mesozoic Carbonate Petroleum Systems in the Northeastern Gulf of Mexico Area, GCSSEPM Foundation 21st Annual Research Conference, Petroleum System of Deep-Water Basins, p. 423-451.
- Mancini, E.A., and Puckett, T. M., 2002, Jurassic and Cretaceous Transgressive -Regressive (T-R) Cycles, Northern Gulf of Mexico, USA, Stratigraphy, v. 2, n. 1, p. 31-48
- Mancini, E. A., Parcell, W. C., Puckett, T. M., Benson, D. J., 2003, Upper Jurassic (Oxfordian) Smackover Carbonate Petroleum System Characterization and Modeling, Mississippi Interior Salt Basin Area, Northeastern Gulf of Mexico, USA, Carbonates and Evaporites, v. 18, p. 125-150.
- Mancini, E. A., W. C. Parcell, W. M. Ahr, 2006, Upper Jurassic Smackover Thrombolite Buildups and Associated Nearshore Facies, Southwest Alabama: Gulf Coast Association of Geological Transactions, v. 56, p. 551–563.
- Mancini, E. A., Parcell, W. C., Ahr, W. M., Ramirez, V. O., Llinas, J. C., Cameron, M., 2008, Upper Jurassic Updip Stratigraphic Trap and Associated Smackover Microbial and Near Shore Carbonate Facies, Eastern Gulf Coastal Plain, American Association of Petroleum Geologists Bulletin, v. 92, p. 417-442.
- Meyers, W. J., 1974, Carbonate Cement Stratigraphy of the Lake Valley Formation (Mississippian) Sacramento Mountains, New Mexico, Journal of Sedimentology, v. 25 p. 371-400.
- Meyers, W. J., and Lohmann, K. C., 1985, Isotope Geochemistry of Regionally Extensive Calcite Cement Zones and Marine Components in Mississippi Limestones, New Mexico, The Society of Economic Paleontologists and Mineralogists, Carbonate Cements SP36, p. 223–239.

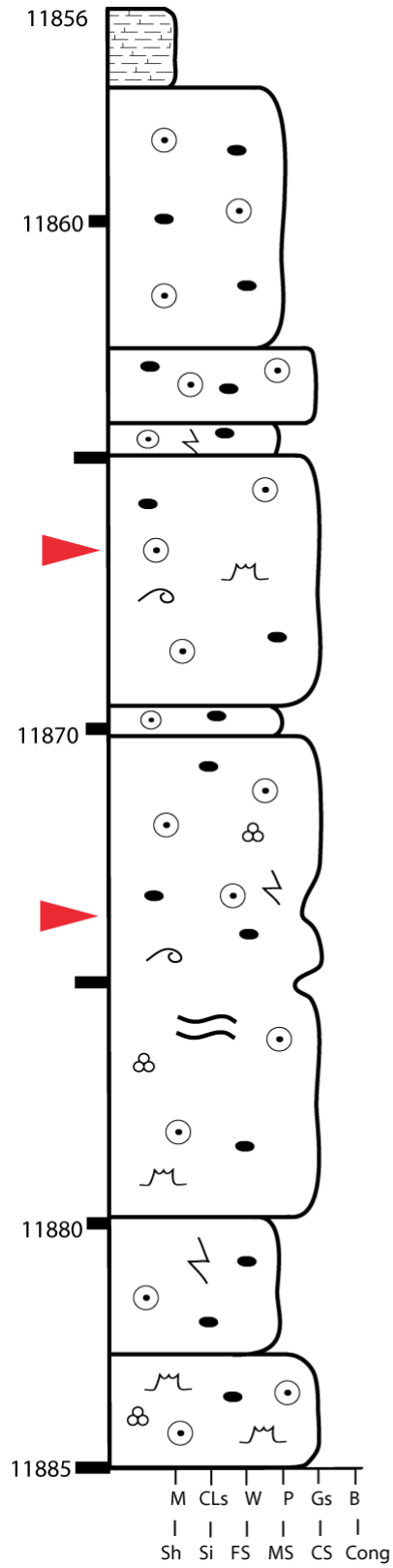
- Murray, R. C., 1964, Origin and Diagenesis of Gypsum and Anhydrite, *Journal of Sedimentary Petrology*, v. 34 .n. 3, p. 512-523
- Pindell, J., 2010, History of Tectonic Modeling and Implications for Depositional Architecture in the Gulf of Mexico: Where We Should Go From Here, *Gulf Coast Association of Geological Societies Transactions*, v. 60, p. 917-929.
- Ridgway, J. G., 2010, Upper Jurassic (Oxfordian) Smackover Facies Characterization at Little Cedar Creek Field, Conecuh County, Alabama, University of Alabama, 84 p.
- Scott, R. W., 2010, Cretaceous Stratigraphy, Depositional Systems, and Reservoir Facies of the Northern Gulf of Mexico: *Gulf Coast Association of Geological Societies Transactions*, v. 60, p. 597-609.
- Winland H. D. and Matthews R.K., 1974, Origin and Significance of Grapestone, Bahama Islands, *Journal of Sedimentary Petrology*, v. 44, p. 921-927.

APPENDIX A- CORE DESCRIPTIONS

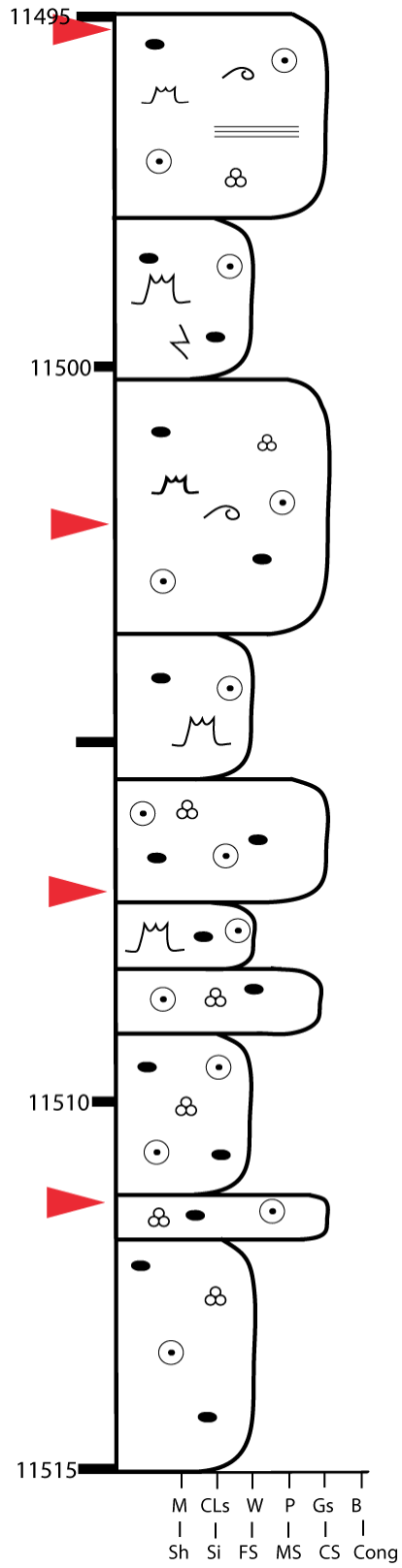
Legend

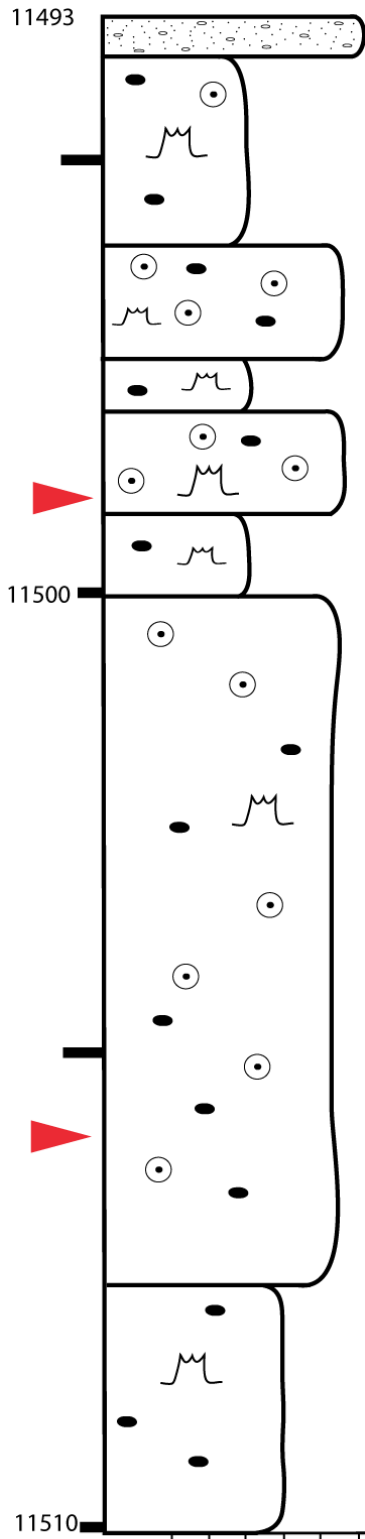
	Calcareous Shale		Forams
	Anhydrite		Miliolids
	Conglomerate		Bioturbation
	Algal Structures		Skeletal Grains
	Laminations		Ooid
	Subhorizontal Laminations		Peloid
	Stylolite		Grapestone
	Microstylolite		Anhydrite nodules
	Crossbedding		Fractures
	Missing Core		Thin sections taken from this depth
	Shale		5 ft

Permit #11963
Grainstone Unit



Permit #13472
Grainstone Unit



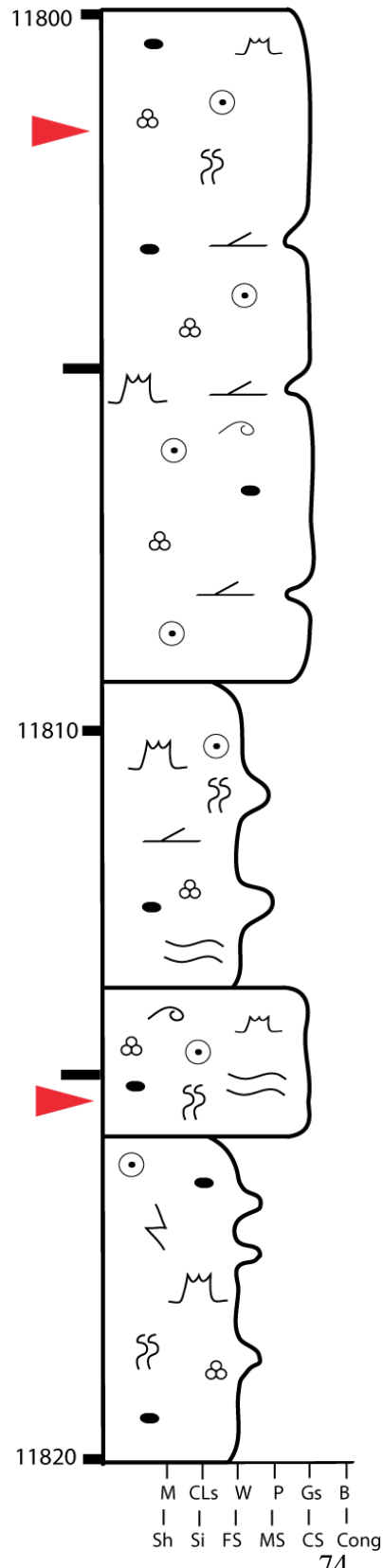


Permit #13510
Grainstone Unit

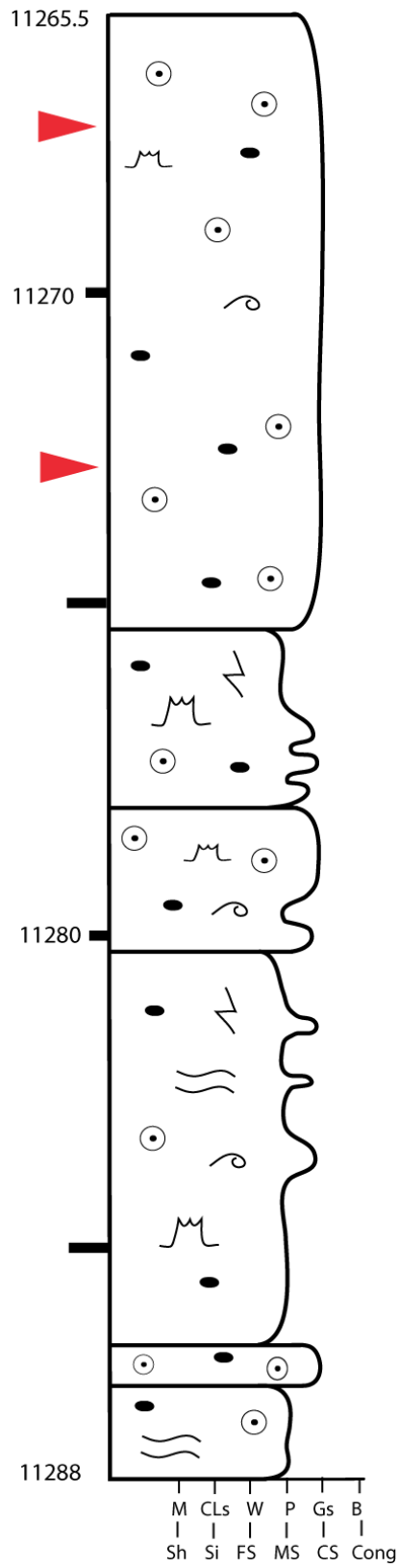
M	CLs	W	P	Gs	B
Sh	Si	FS	MS	CS	Cong

Permit #13907

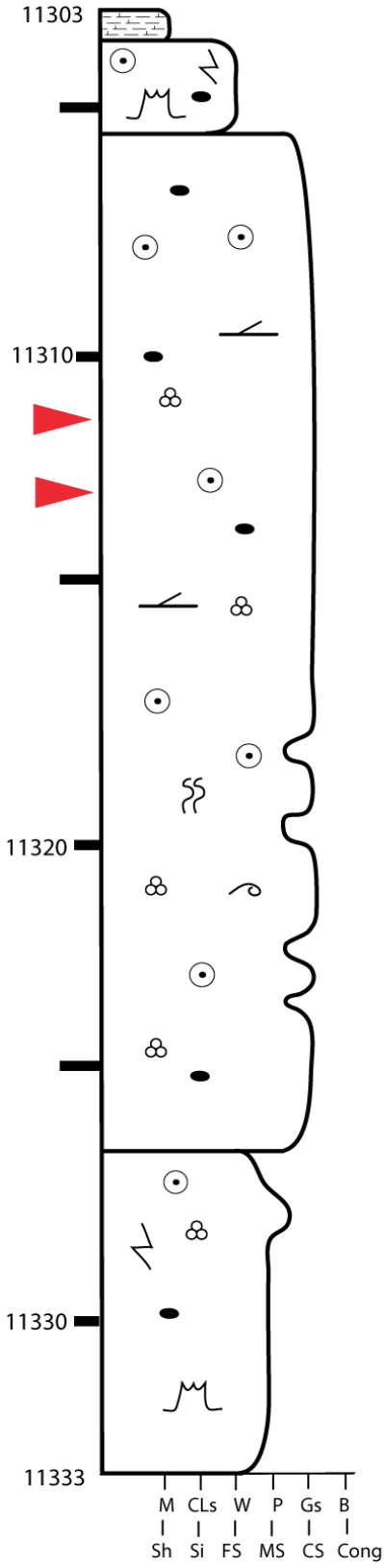
Grainstone Unit

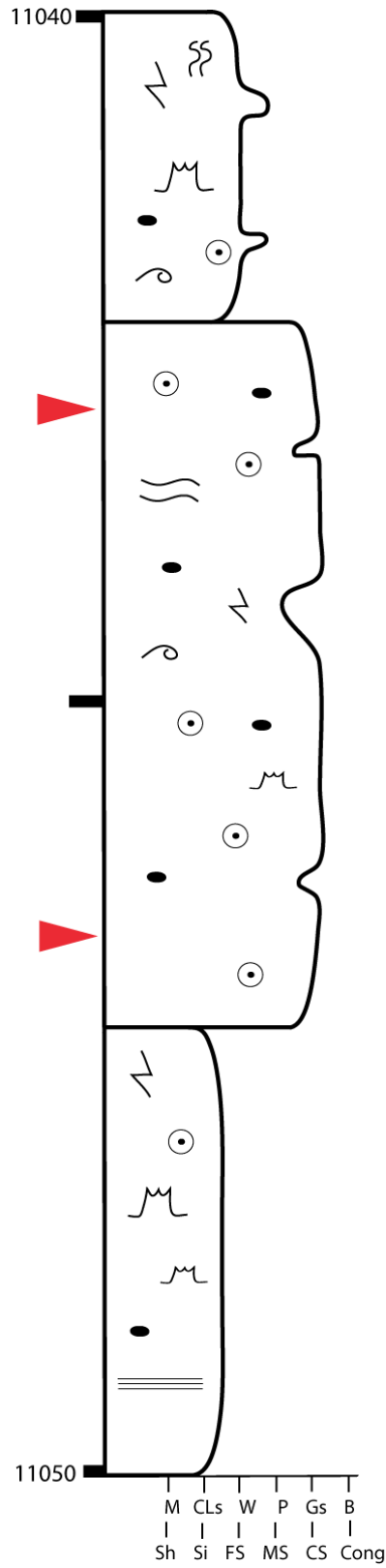


Permit #14112
Grainstone Unit



Permit #14155
 Grainstone Unit

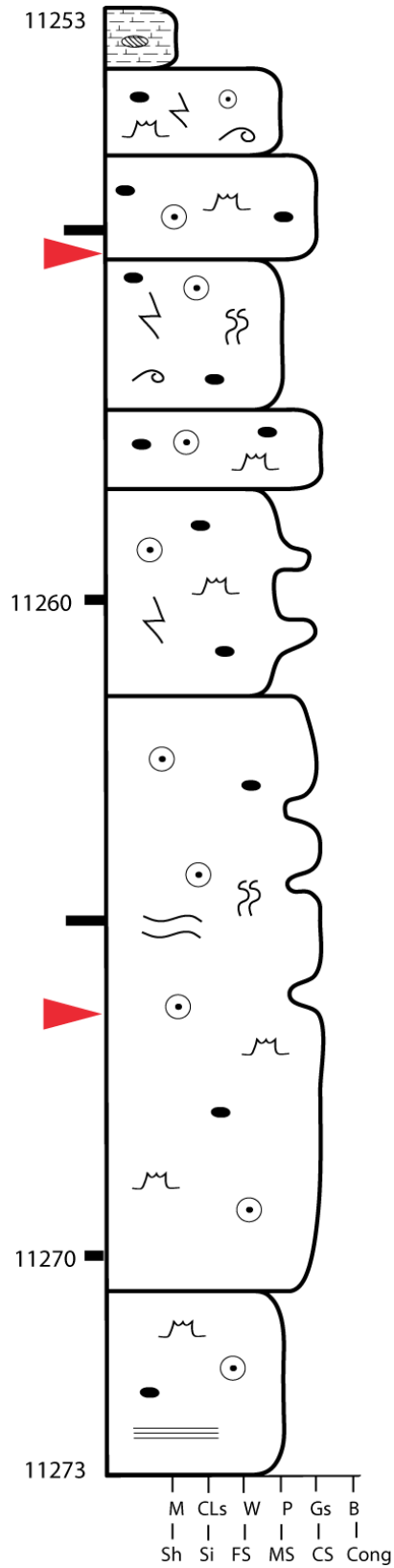




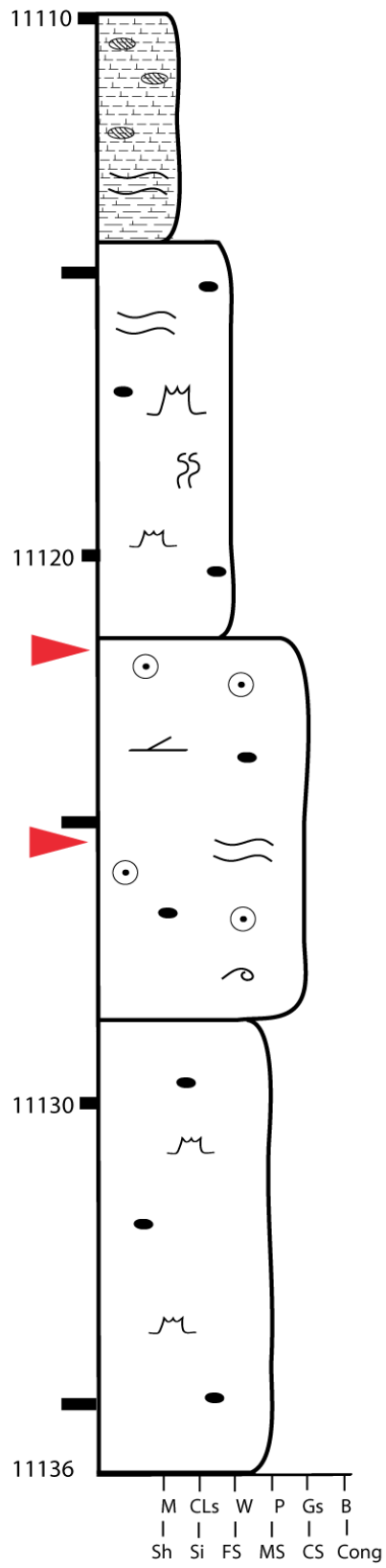
Permit #14325
 Grainstone Unit

Permit #14646-B

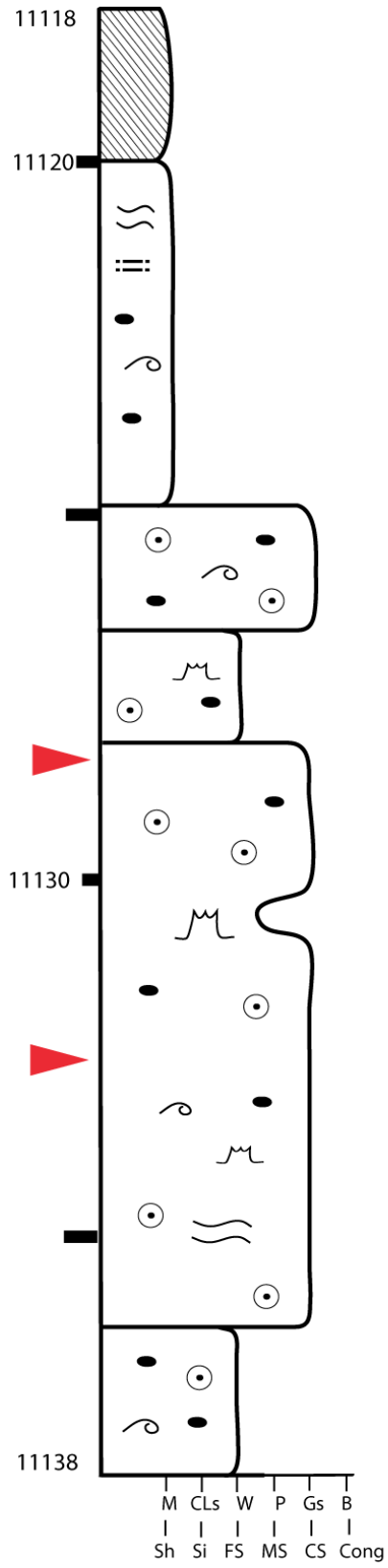
Grainstone Unit



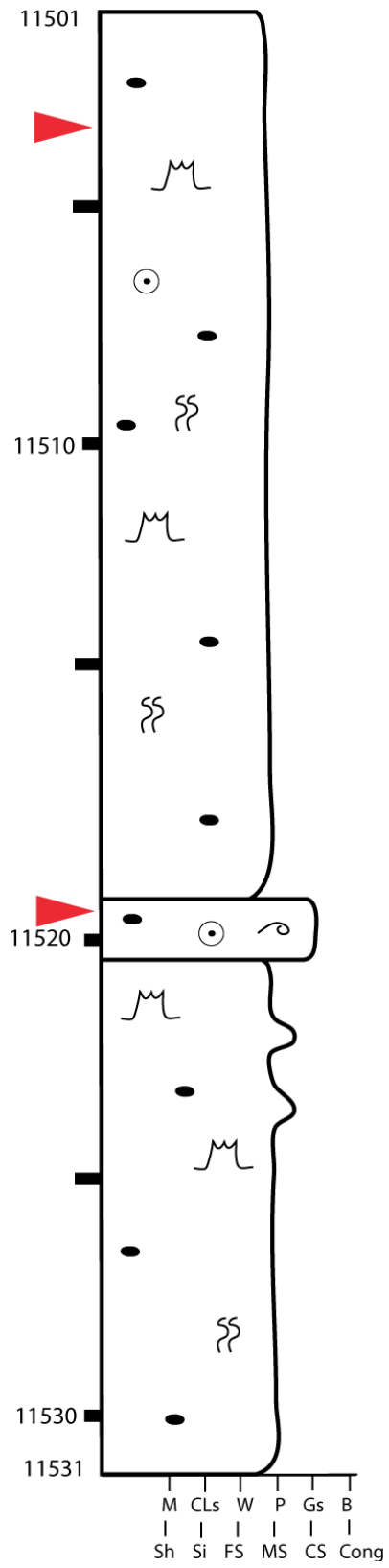
Permit #15000
Grainstone Unit



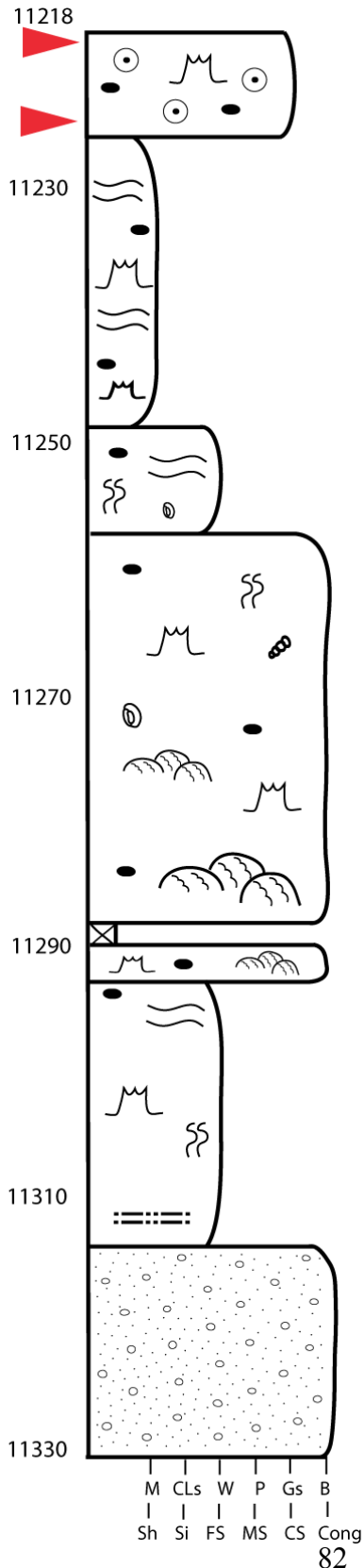
Permit #15159-B
 Grainstone Unit



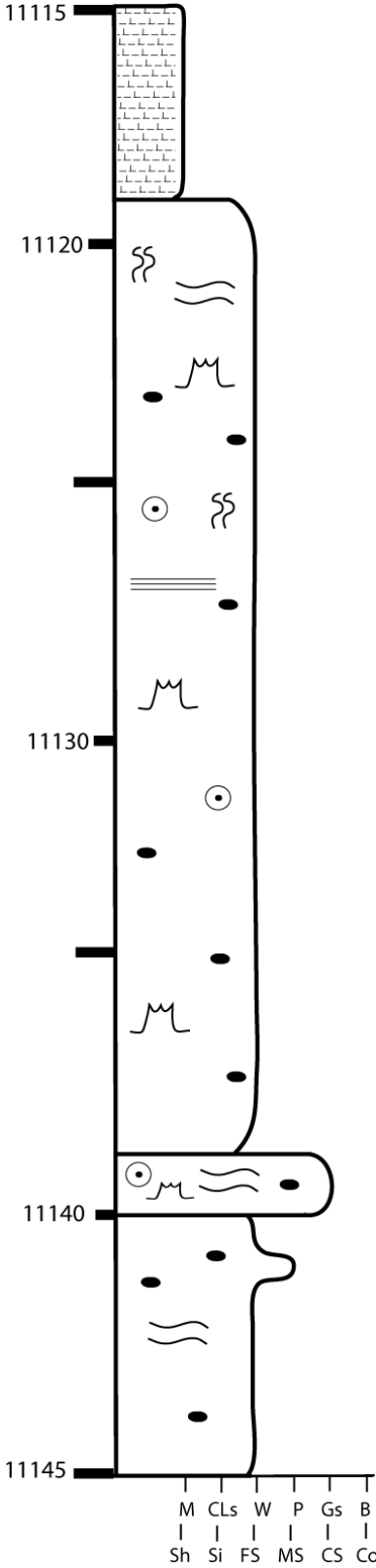
Permit #15165
Grainstone Unit



Permit #15263-B
Smackover

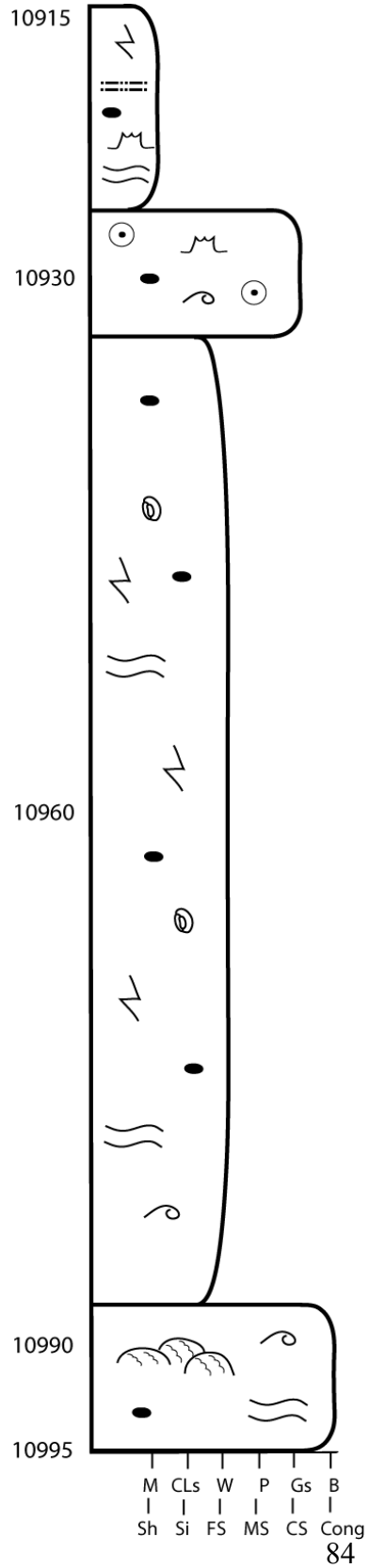


Permit #15496-B
 Grainstone Unit

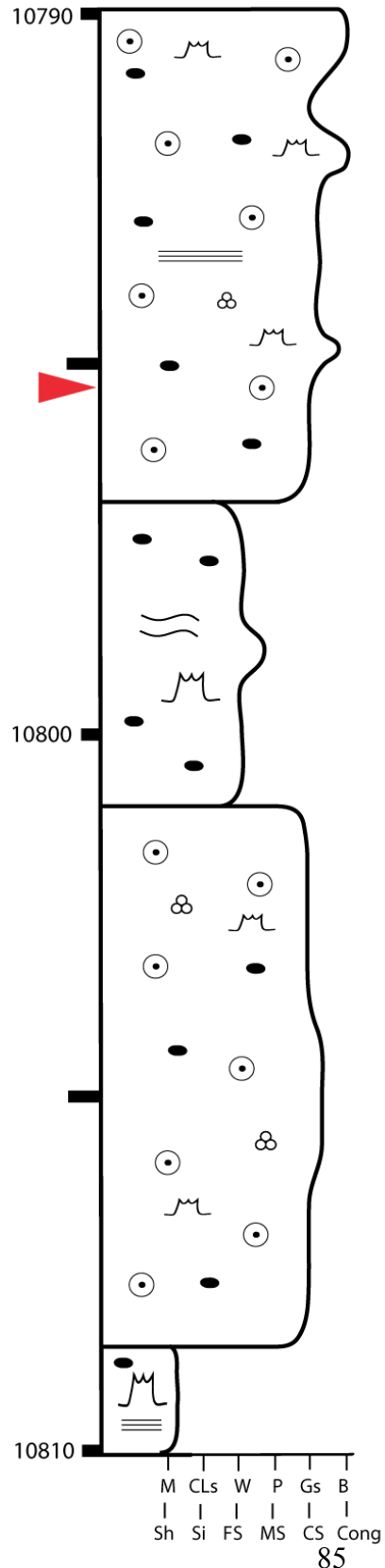


▶ Core depths and thin section depths are inconsistent. However, the samples were taken in the grainstone facies of this well.

Permit #15614-B-1
Smackover

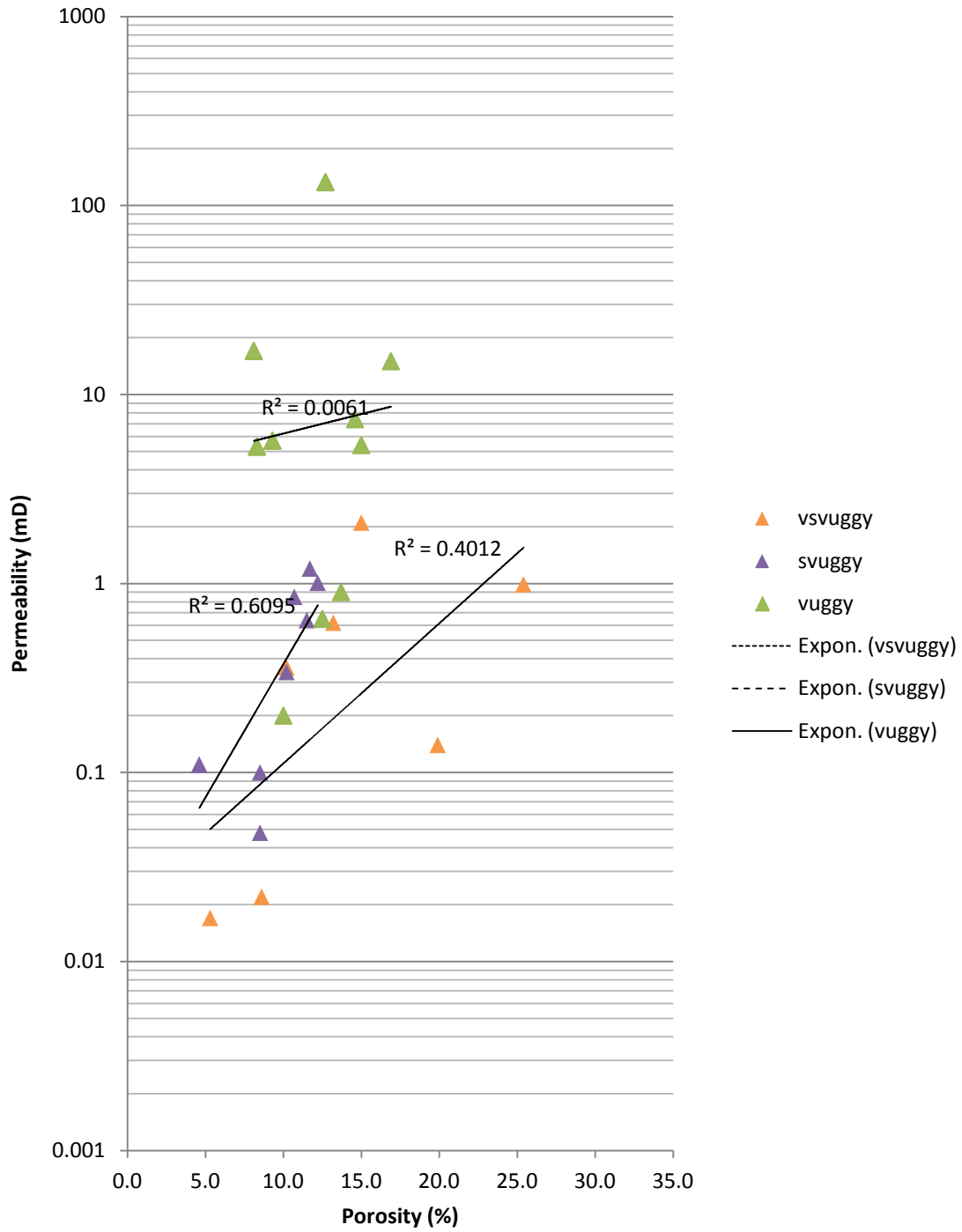


Permit #16115
Grainstone Unit

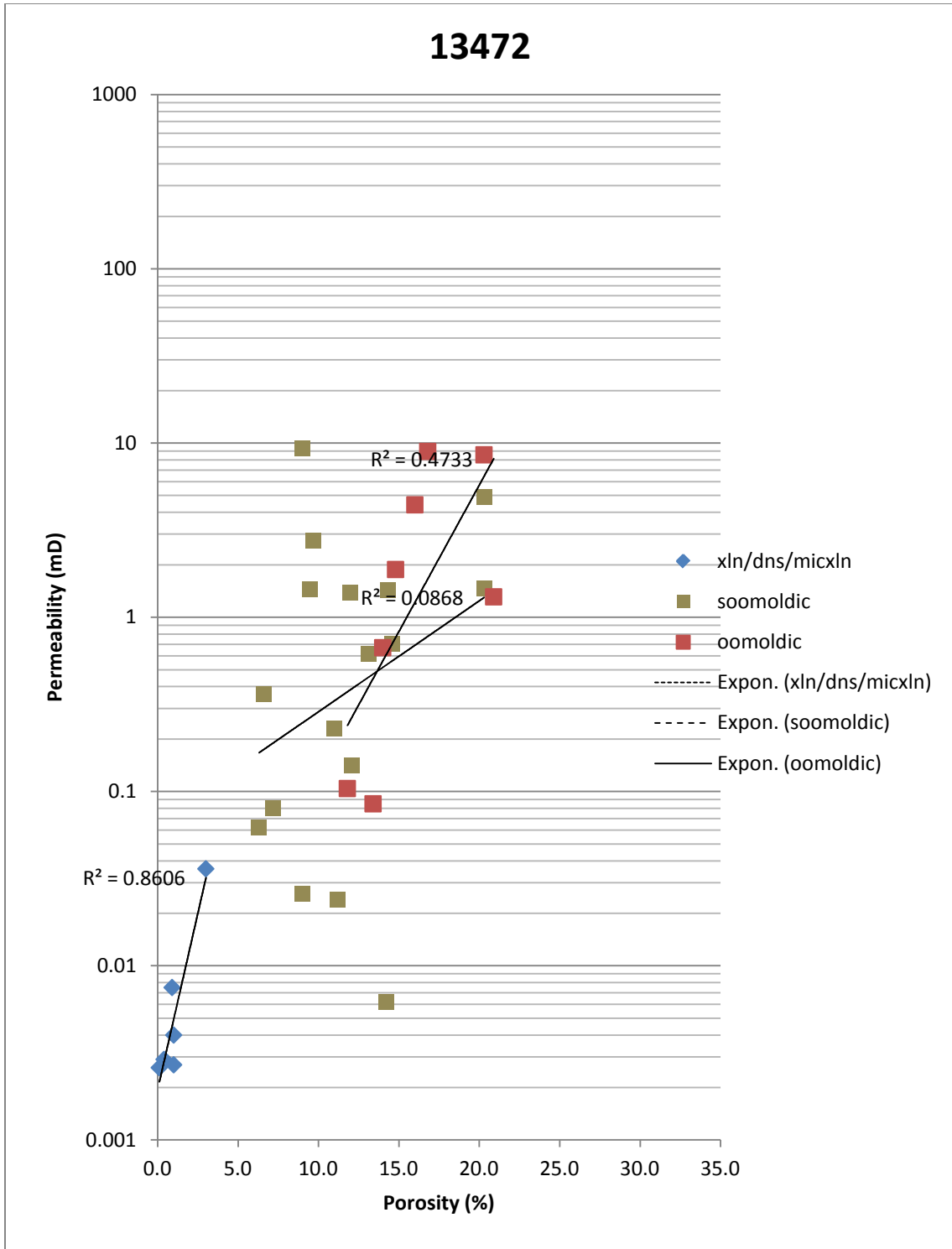


APPENDIX B- POROSITY AND PERMEABILITY CROSSPLOTS

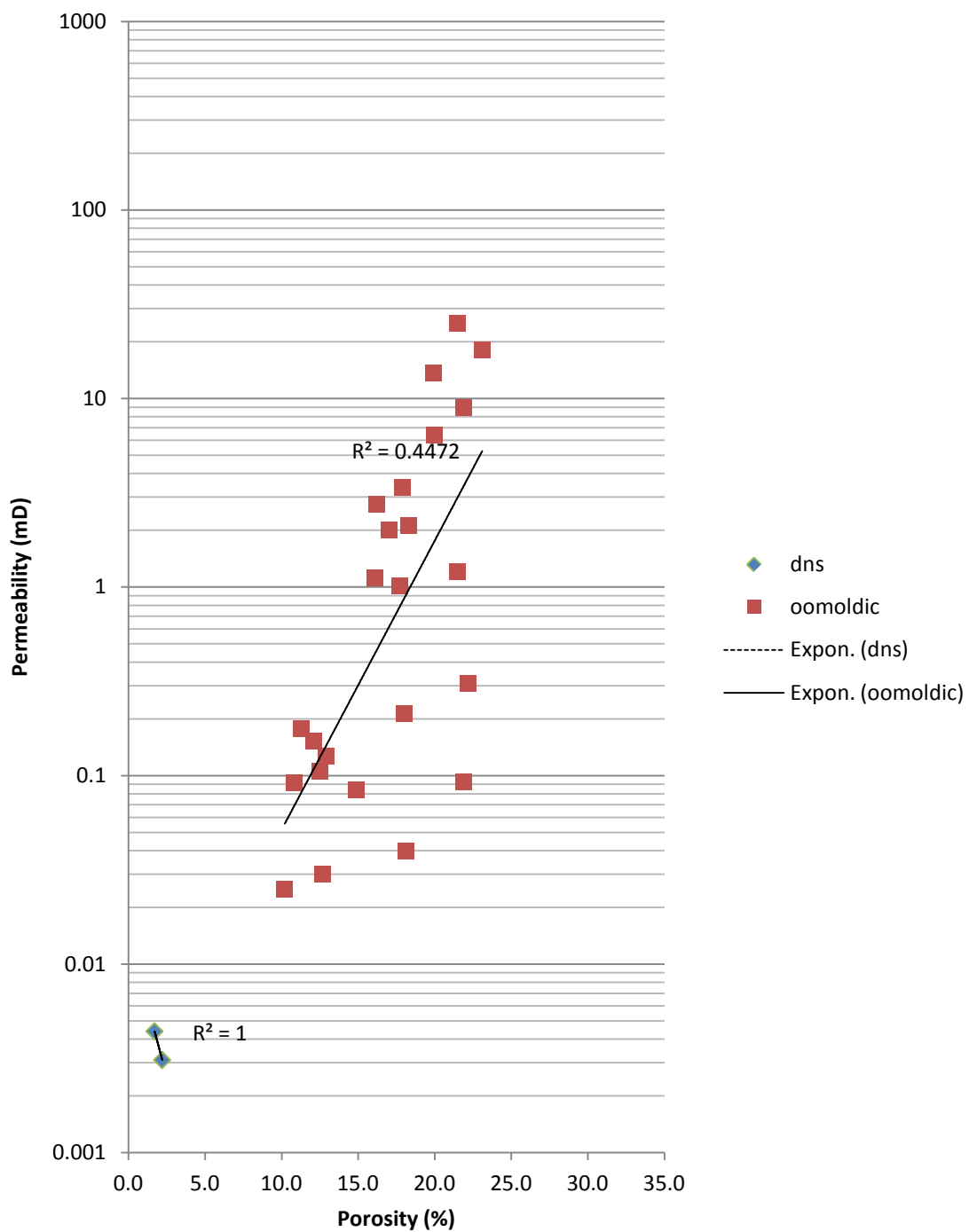
11963



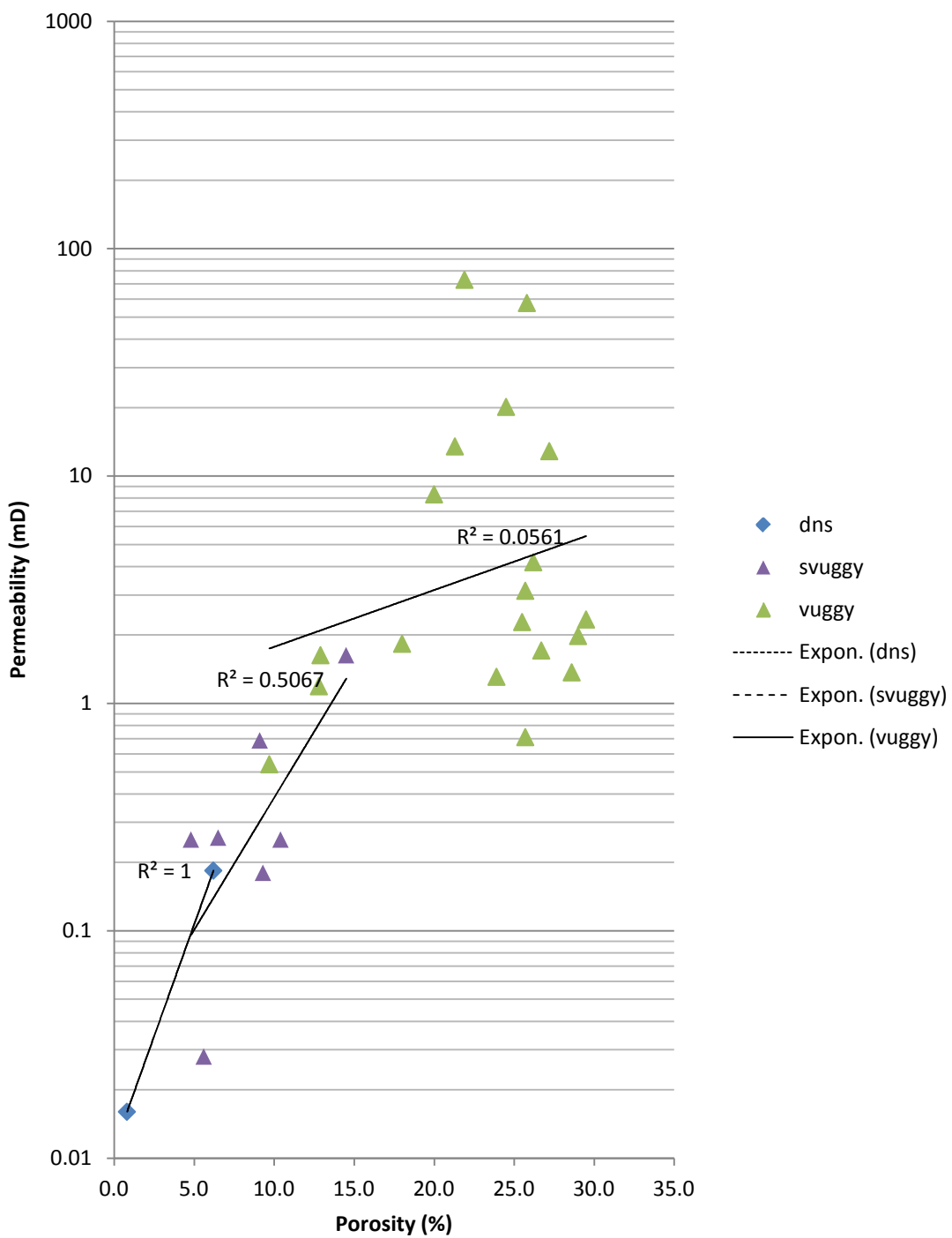
13472



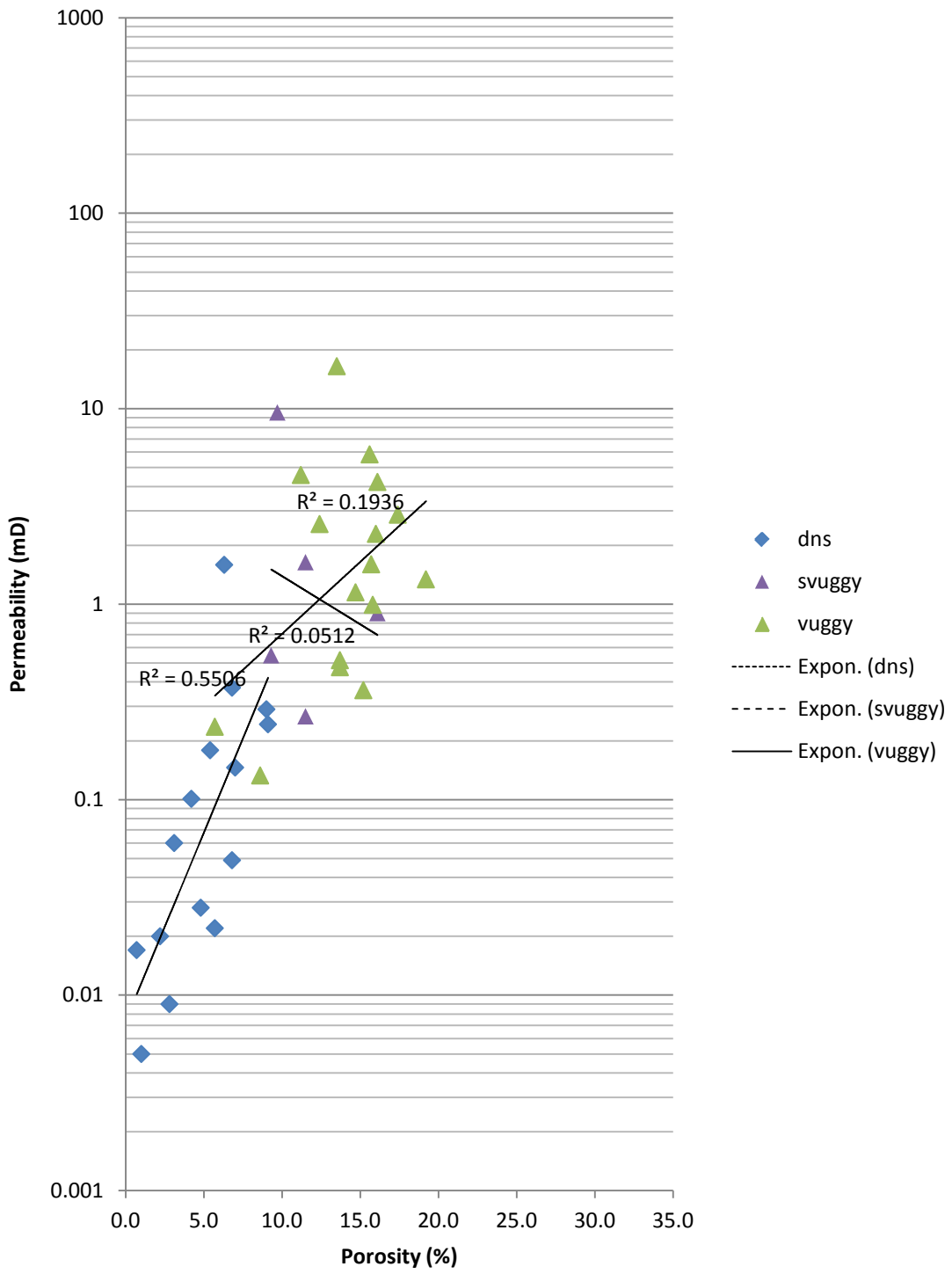
13510



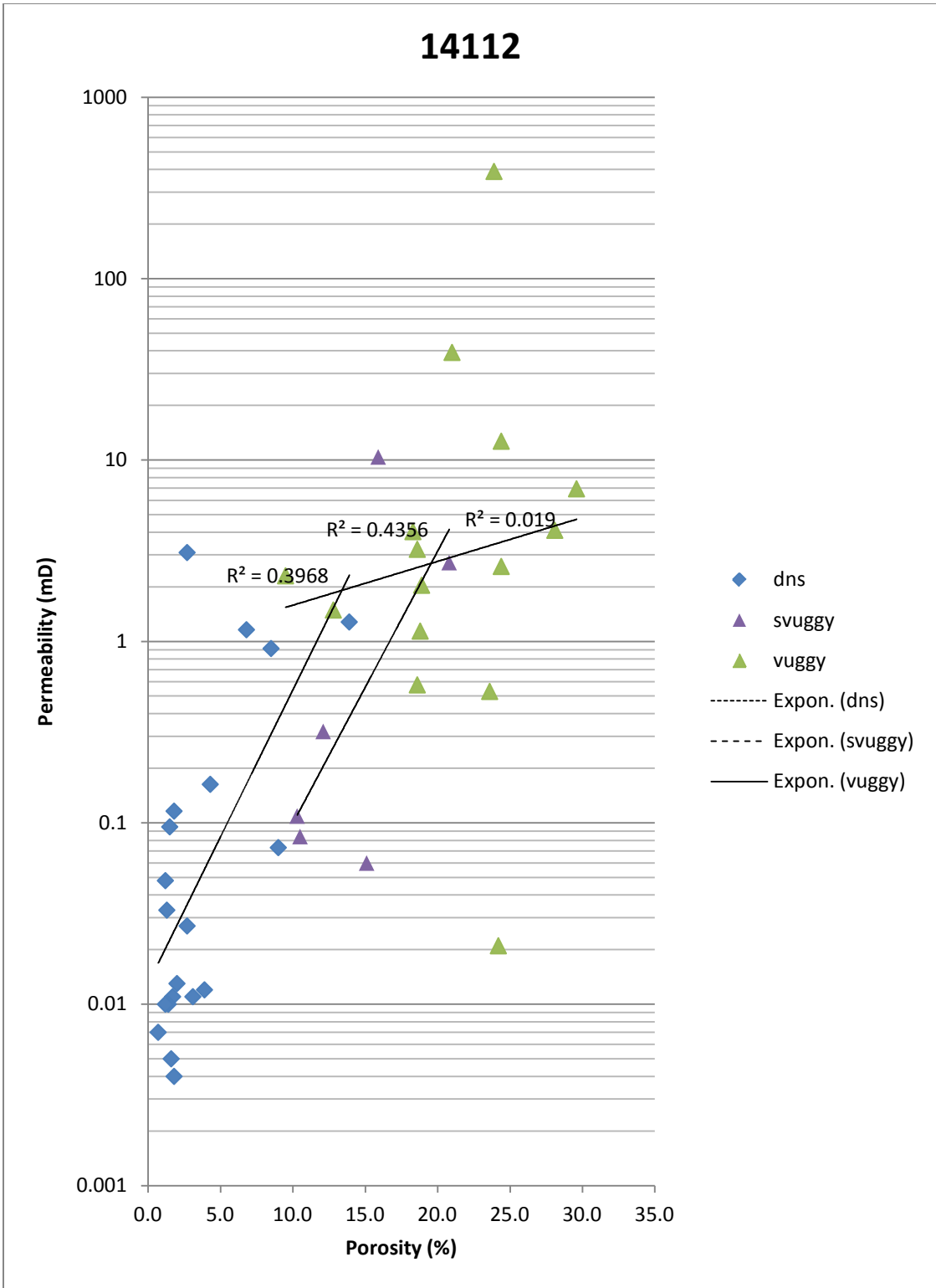
13906



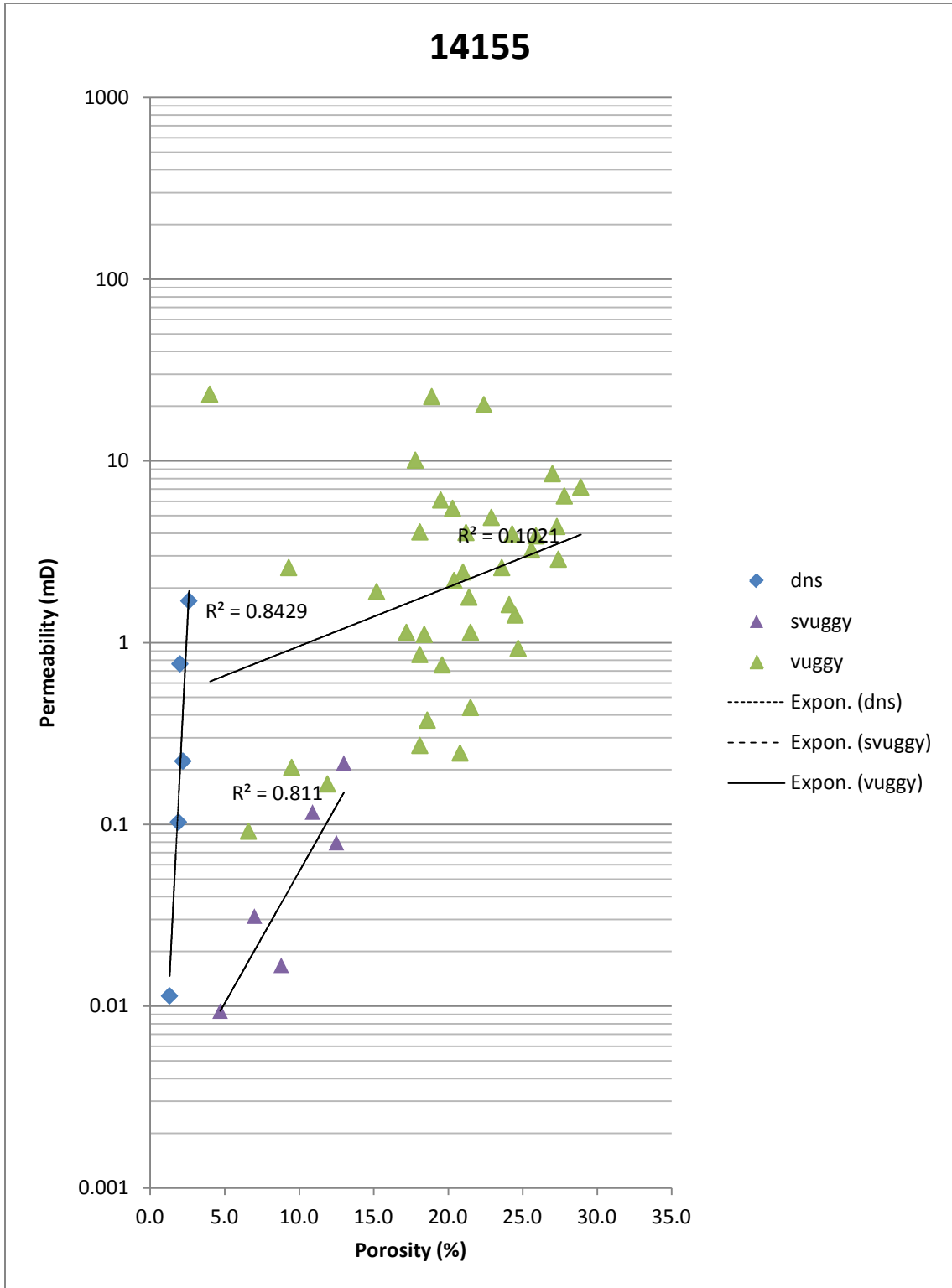
13907



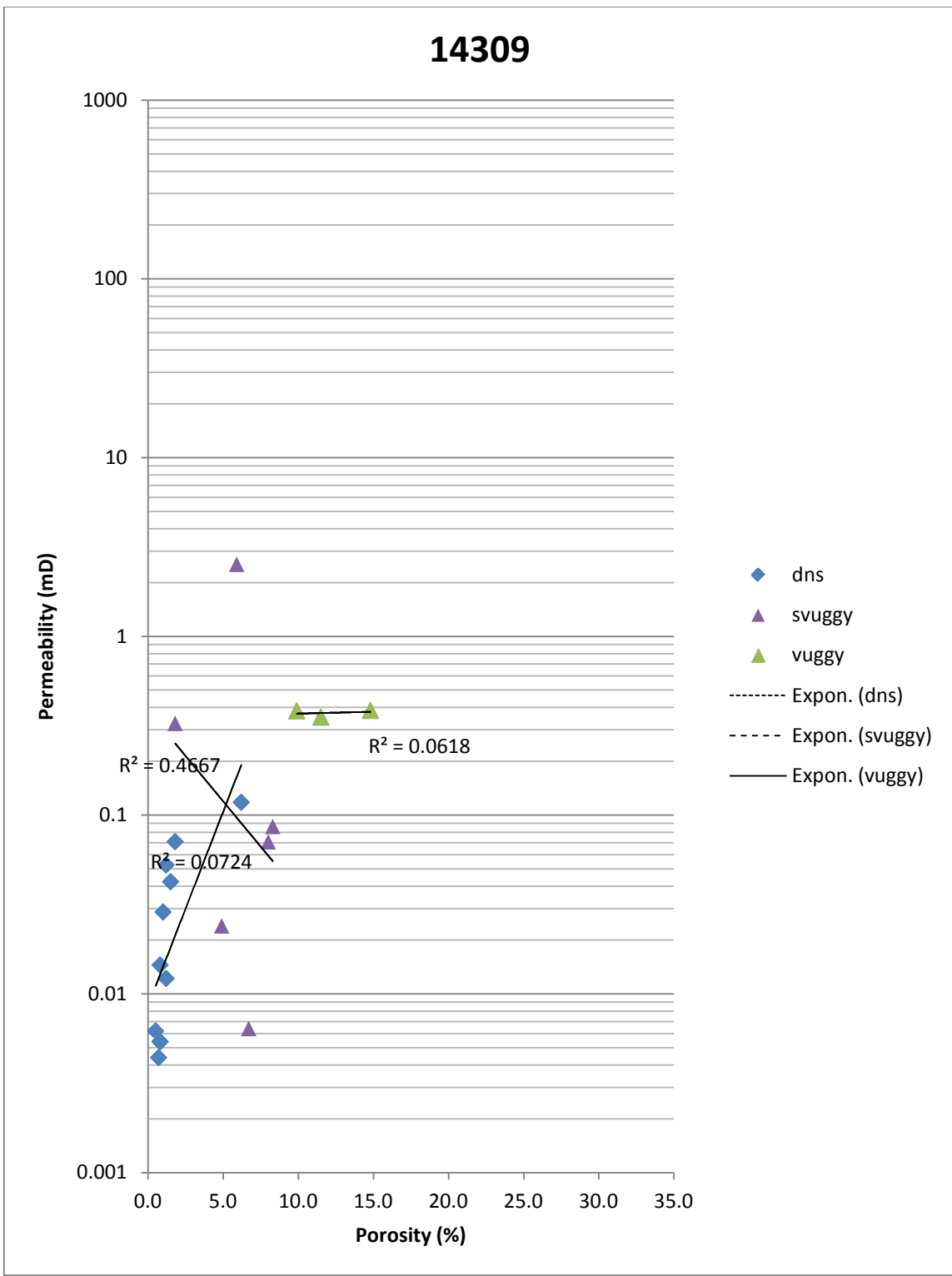
14112



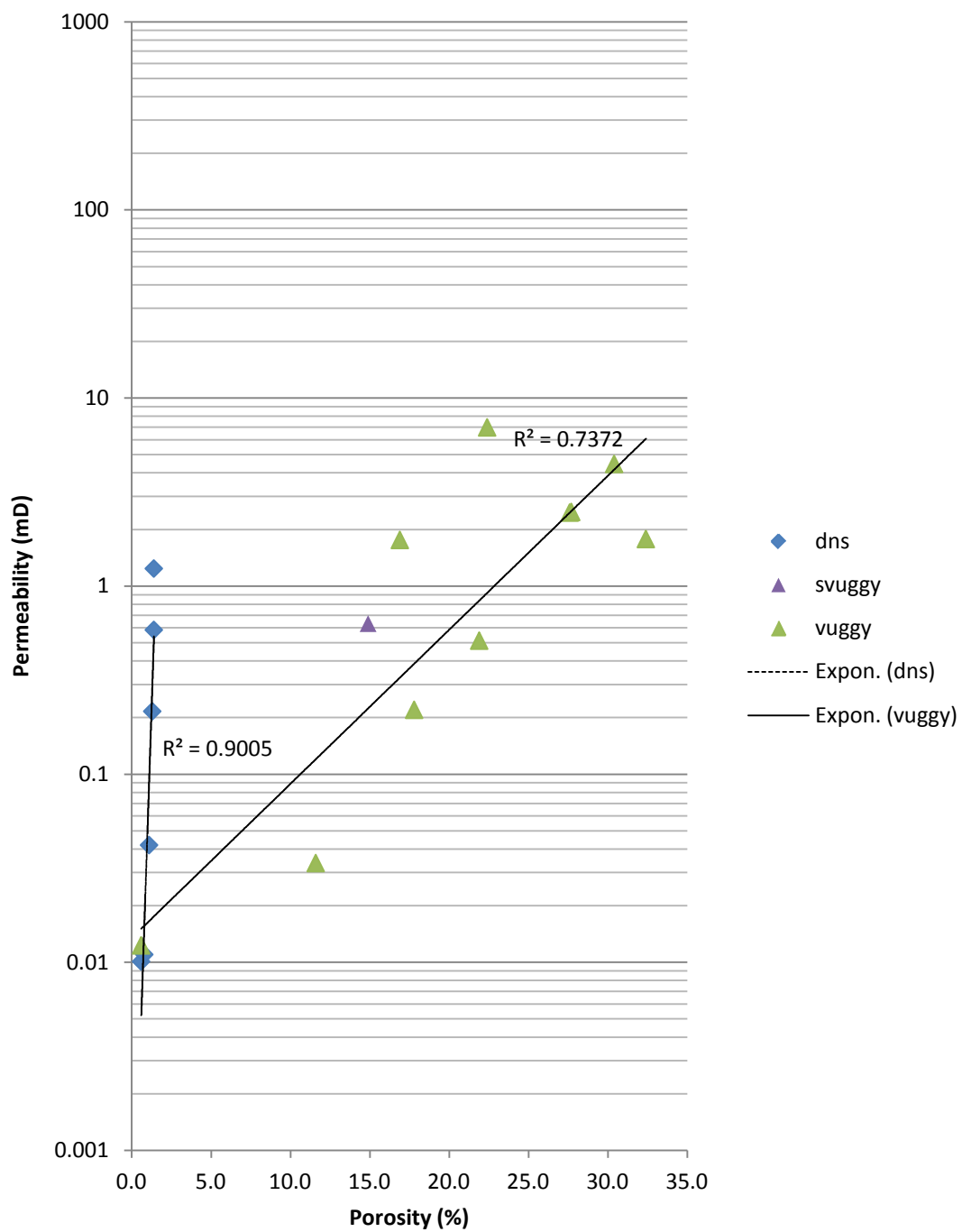
14155



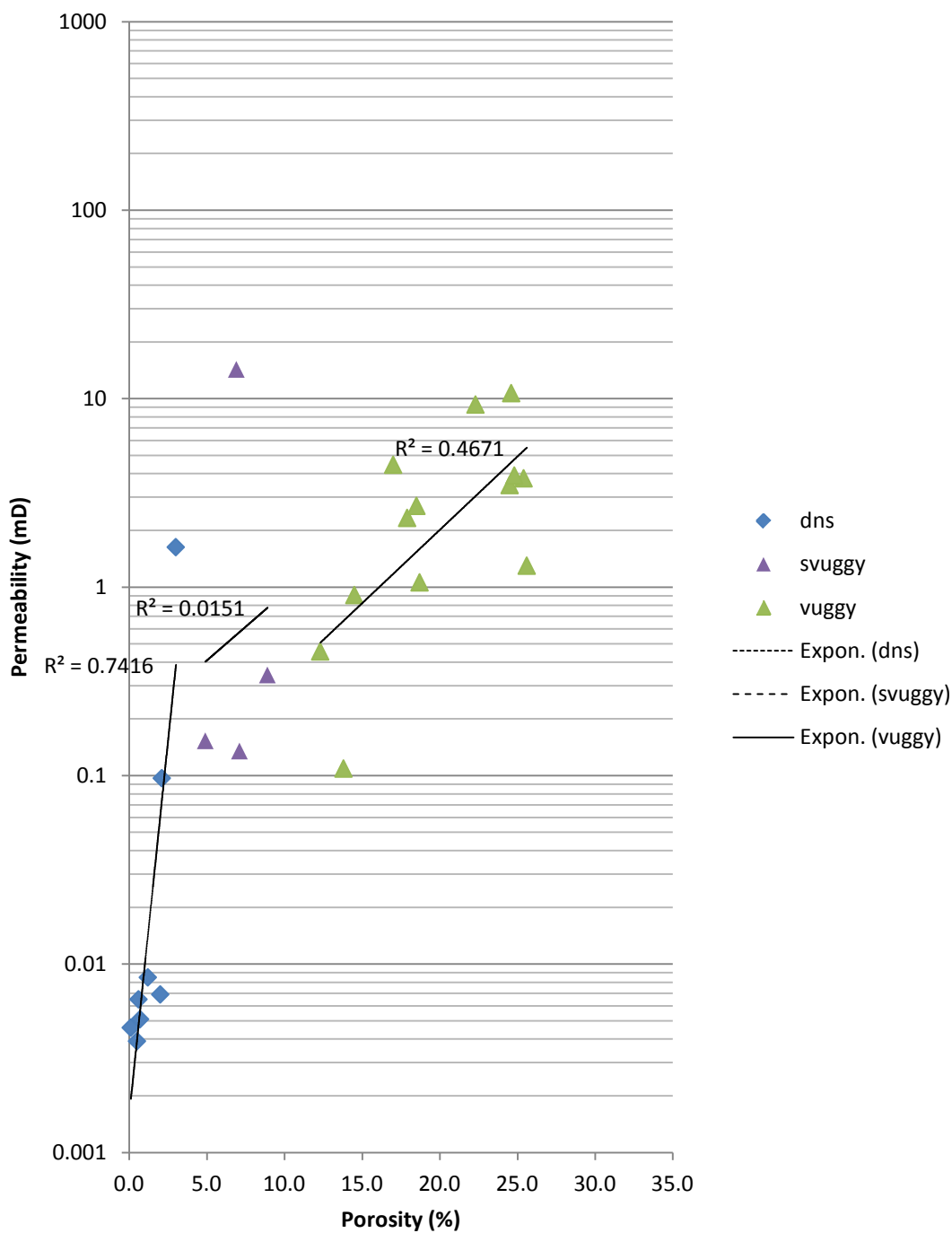
14309



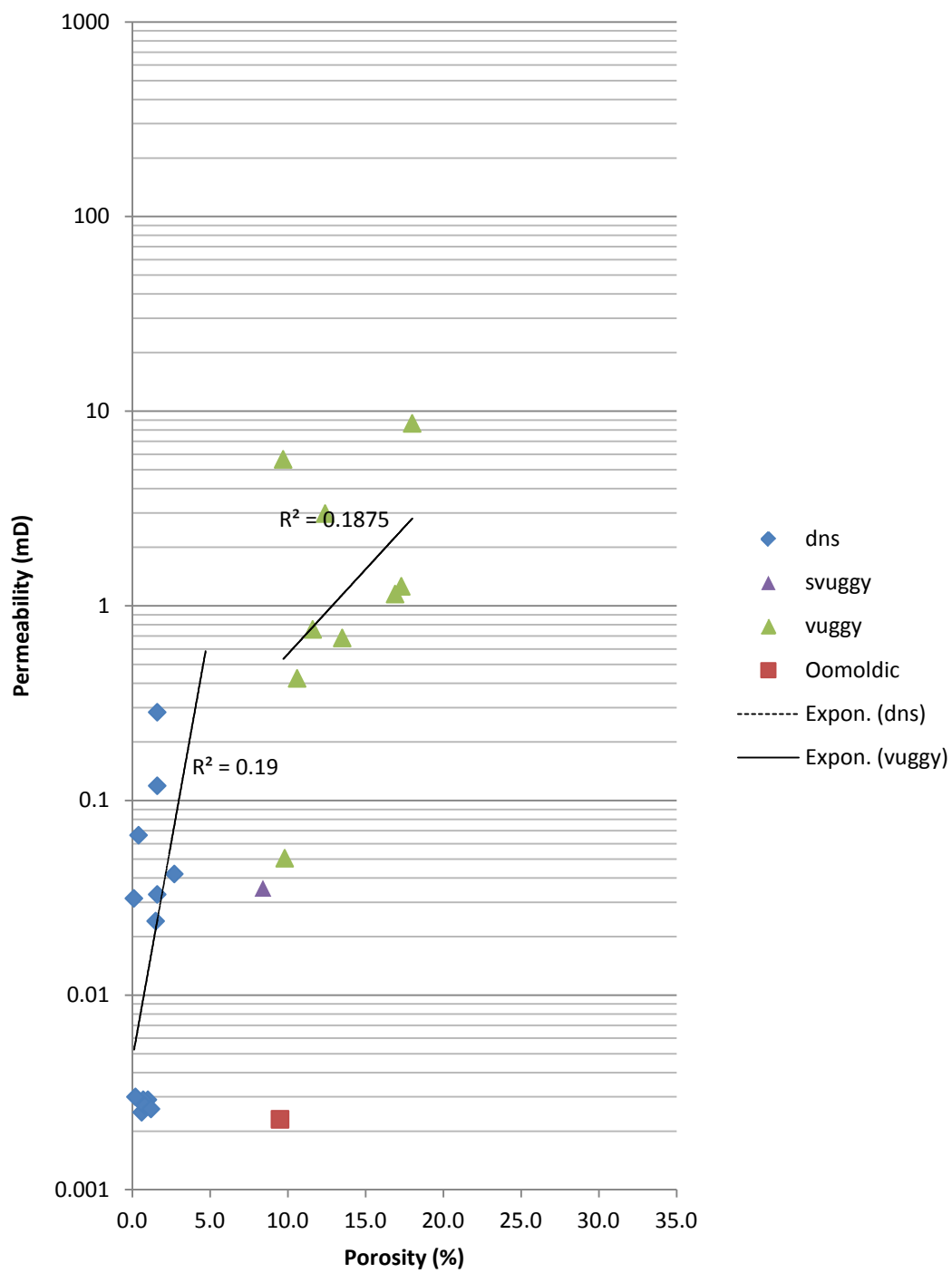
14325



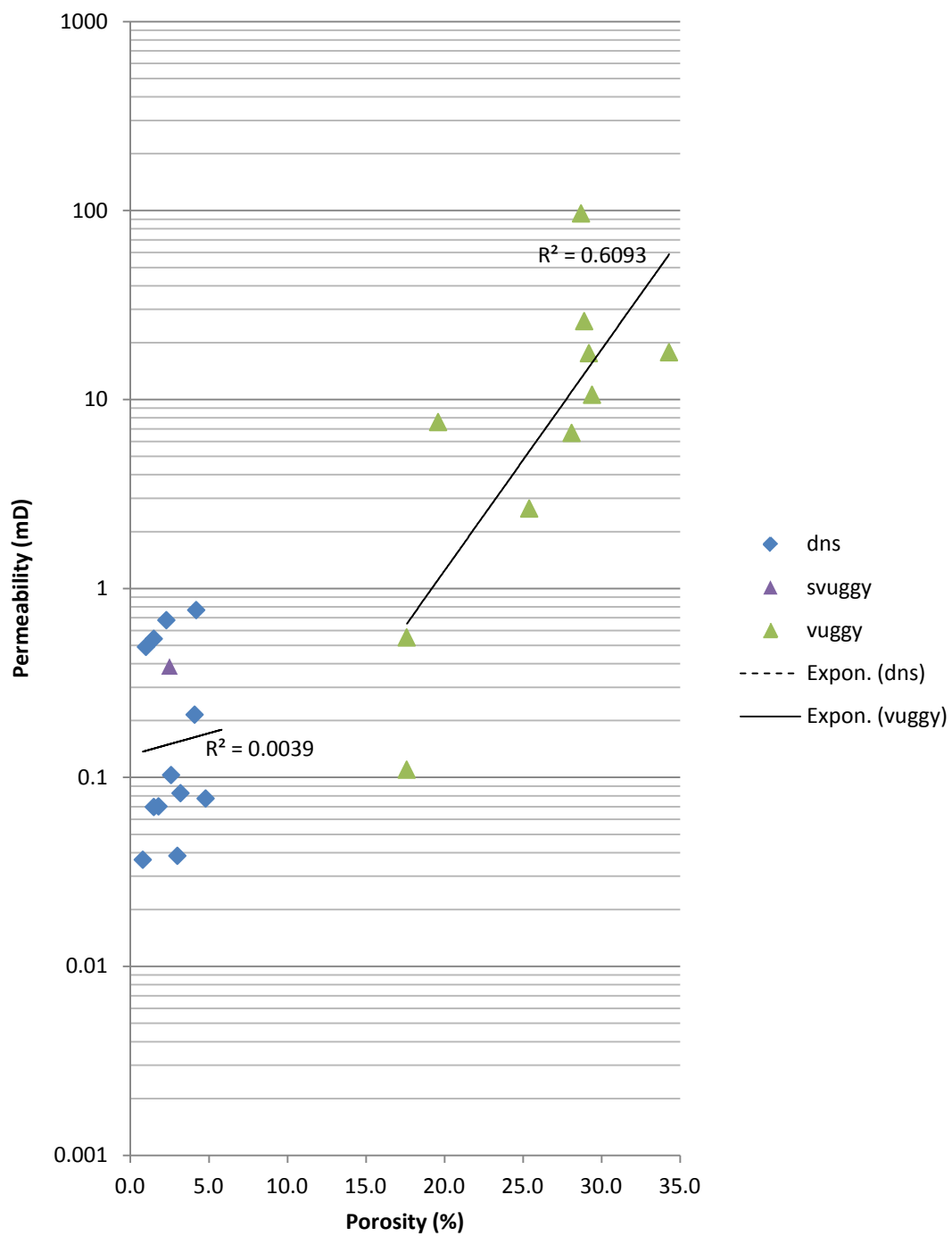
14646-B



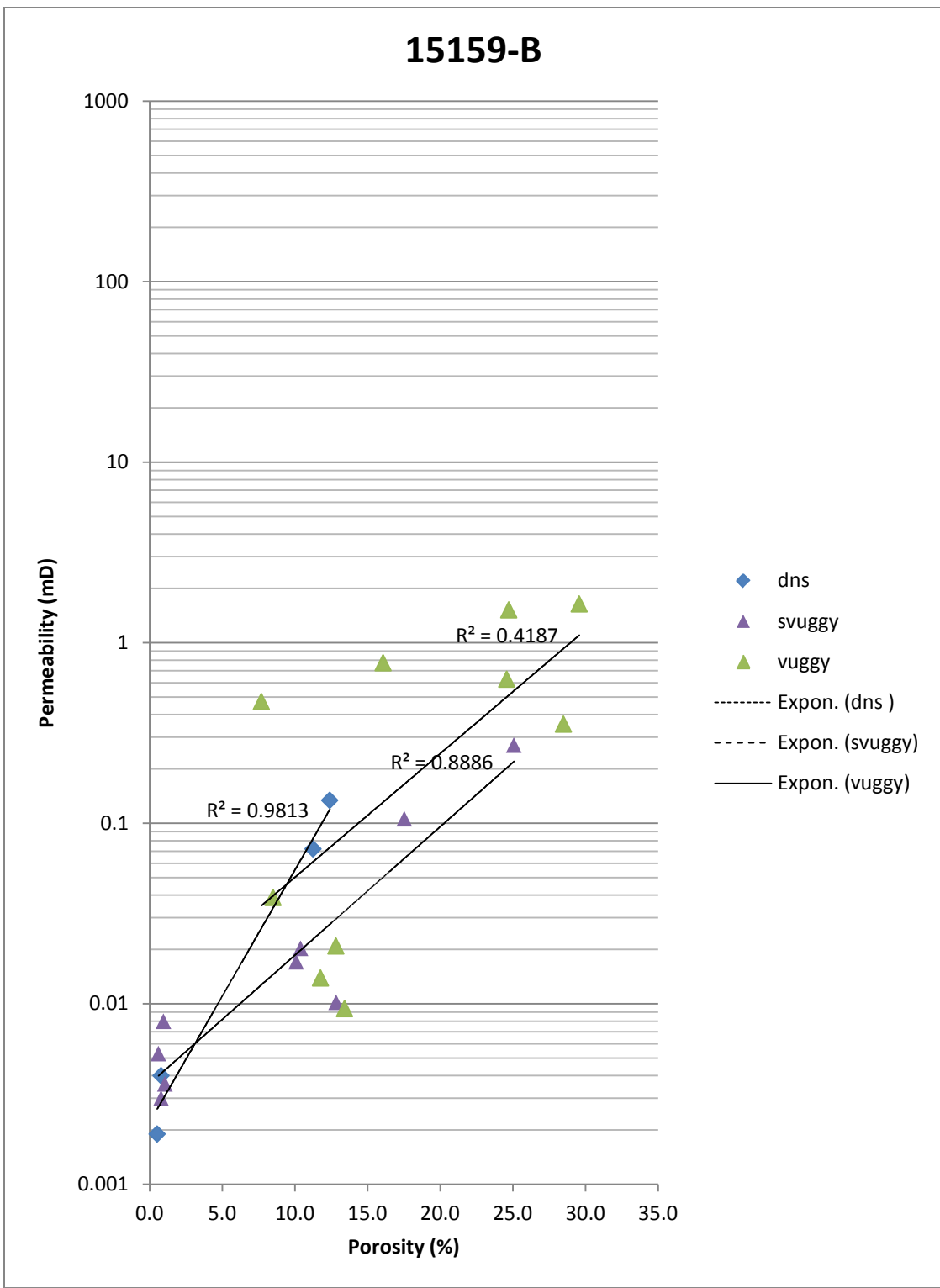
14692



15000



15159-B



15165

